

000 001 002 003 004 005 006 007 008 009 010 011 012 WHY HAS PREDICTING DOWNSTREAM CAPABILITIES OF FRONTIER AI MODELS WITH SCALE REMAINED ELUSIVE?

013
014
015
016
017
018
019
020
021
022
023
024
025
026
027
028
029
030
031
032
Anonymous authors
Paper under double-blind review

033 034 035 ABSTRACT

036
037 Predictable behavior from scaling advanced AI systems is an extremely desirable
038 property for engineers, industry, economists and governments alike, and, while
039 a well-established literature exists on how pretraining performance scales, pre-
040 dictable scaling behavior on downstream capabilities remains elusive. While many
041 factors are certainly responsible, this paper identifies a significant factor that makes
042 predicting scaling behavior on widely used multiple-choice question answering
043 benchmarks challenging and illuminates a path towards making such downstream
044 evaluations predictable with scale. Using five model families and twelve well-
045 established multiple-choice benchmarks, we show that downstream performance
046 is computed from negative log likelihoods via a sequence of transformations that
047 progressively degrades the statistical relationship between performance and scale.
048 We then pinpoint the mechanism causing this degradation: downstream metrics
049 require comparing the correct choice against a small number of specific incorrect
050 choices, meaning accurately predicting downstream capabilities requires predict-
051 ing not just how probability mass concentrates on the correct choice with scale,
052 but also how probability mass fluctuates on specific incorrect choices with scale.
053 We empirically study how probability mass on the correct choice co-varies with
054 probability mass on incorrect choices with increasing compute, suggesting that
055 scaling laws for *incorrect* choices might be achievable. Our work also explains
056 why pretraining scaling laws are commonly regarded as more predictable than
057 downstream capabilities and contributes towards establishing scaling-predictable
058 evaluations of frontier AI models.

059 060 1 THE IMPORTANCE OF PREDICTING CAPABILITIES WITH SCALE

061
062 Predictable scaling behavior of frontier AI systems such as GPT-4 (OpenAI, 2024; OpenAI et al.,
063 2024), Claude (Anthropic, 2024) and Gemini (Team et al., 2023; Reid et al., 2024) is crucial for
064 anticipating capabilities and informing key decisions regarding model development and deployment
065 (Anthropic, 2023; OpenAI, 2023; Dragan et al., 2024). Predictable scaling behaviors enable engineers
066 to make informed decisions about optimal model design choices and to de-risk investment in exceed-
067 ingly expensive pretraining runs by determining the payoff from scaling up compute. For instance,
068 OpenAI noted in the GPT-4 Technical Report (Achiam et al., 2023) that “A large focus of the GPT-4
069 project was building a deep learning stack that scales predictably” and that “[OpenAI] developed
070 infrastructure and optimization methods that have very predictable behavior across multiple scales”;
071 OpenAI noted that this ideally goes beyond predicting loss values, and that “Having a sense of the
072 capabilities of a model before training can improve decisions around alignment, safety, and deploy-
073 ment”. Meta’s Llama Team similarly conducted experiments aimed at predicting the downstream
074 performance of models, used to inform the design of their 405 billion parameter model (Dubey et al.,
075 2024). Additionally, predicting capabilities is of interest beyond AI practitioners: economists and
076 governments also have a significant interest in predicting the capabilities of current and future frontier
077 AI systems for better decision-making (regulation, taxation, and safety) and forecasting of economic
078 impacts (Council of Economic Advisers, 2024). Downstream capabilities are especially of interest
079 because quantities like pretraining loss are difficult to translate into quantities more meaningful to
080 society, such as the impact on economic labor or societal harms.

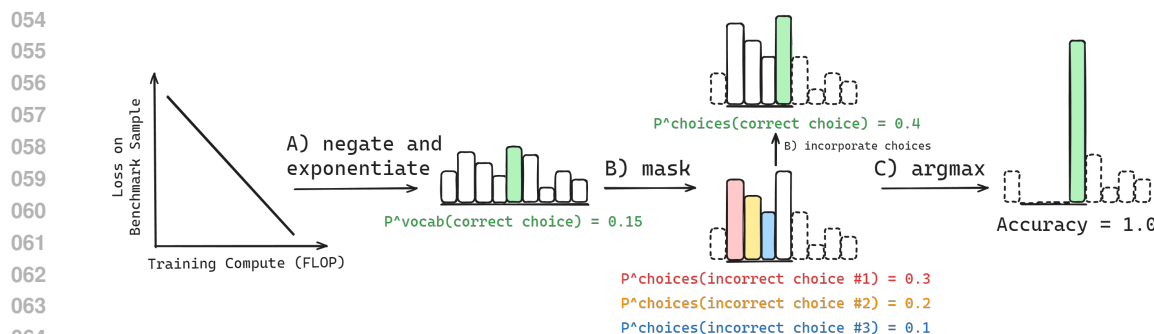


Figure 1: **Multiple-choice benchmark accuracy is computed from negative log likelihoods via a sequence of transformations that degrades predictability.** Computing Accuracy begins with computing the negative log likelihoods of each choice, then negating and exponentiating each to obtain the probability of each choice (**A**). Choices are then restricted to a set of available choices by **masking** invalid continuations, and renormalizing to obtain relative probability mass on each choice (**B**). Lastly, the model’s choice is defined as $\arg \max_i \{p^{\text{Choices}}(\text{Available Choice}_i)\}$, and Accuracy is 1 if and only if the model’s choice is the correct choice (**C**).

However, while scaling laws describing relationships amongst parameters, data, compute, and pretraining loss are well-established (Hestness et al., 2017; Rosenfeld et al., 2019; Henighan et al., 2020; Kaplan et al., 2020; Gordon et al., 2021; Hernandez et al., 2021; Jones, 2021; Zhai et al., 2022; Hoffmann et al., 2022; Clark et al., 2022; Neumann & Gros, 2022; Hernandez et al., 2022; Maloney et al., 2022; Sardana & Frankle, 2023; Muennighoff et al., 2024; Besiroglu et al., 2024), the literature is less conclusive regarding predicting specific downstream capabilities with scale. For instance, prior work has observed that performance on standard natural language processing (NLP) benchmarks can exhibit *emergent abilities* (Brown et al., 2020; Ganguli et al., 2022; Srivastava et al., 2022; Wei et al., 2022) where performance changes unpredictably with scale, but further work demonstrated that such unpredictable changes might at times be artifacts of researchers’ analyses, i.e., choices of metrics and lack of sufficient resolution from too few samples (Srivastava et al., 2022; Schaeffer et al., 2023; Hu et al., 2024). More recently, Du et al. (2024) claim that downstream capabilities *can* be predicted, but *only* after the pretraining cross-entropy loss falls below a certain threshold, and Gadre et al. (2024) claim that while performance on individual tasks can be difficult to predict, aggregating results across dozens of diverse benchmarks yields clearer scaling trends. In this work, we ask: in contrast with strongly-predictable pretraining losses, *why has predicting specific downstream capabilities with scale remained elusive?*

2 CONTRIBUTION: EXPLAINING WHY PREDICTING DOWNSTREAM CAPABILITIES WITH SCALE HAS REMAINED ELUSIVE

Our goal is to understand what breaks down between the predictability of pretraining losses and the unpredictability of downstream evaluations. To do this, we investigated the relative predictability of different evaluation methodologies and setups, focusing on popular and comparatively simple (yet still highly difficult to predict) multiple-choice question answering benchmarks. We began with scaling-predictable pretraining log likelihoods and tracked how these log likelihoods are transformed in the process of calculating downstream evaluation metrics that are notoriously difficult to predict, such as Accuracy or Brier Score (See Fig. 1 and Sec. 4 for further detail):

$$\underbrace{\log p_{\theta}^{\text{Vocab}}(\text{Correct Choice})}_{\text{Scaling-Predictable}} \rightarrow p_{\theta}^{\text{Vocab}}(\text{Correct Choice}) \rightarrow p_{\theta}^{\text{Choices}}(\text{Correct Choice}) \rightarrow \underbrace{\text{Accuracy}}_{\text{Scaling-Unpredictable}}$$

This paper will demonstrate the following summary of our findings:

1. **Calculating downstream metrics requires a sequence of transformations applied to the original scaling-predictable quantities. These transformations progressively de-**

- 108 **priorate the statistical relationship between those metrics and the scaling parameters**
 109 **(parameters, data, and compute).** This formalizes an intuition that “more complex”
 110 metrics might be less easily predictable.
 111
 112 **2. Accurately predicting downstream multiple-choice performance requires modeling**
 113 **not only the probability mass assigned to the correct choice with scale, but also the**
 114 **probability mass assigned to the incorrect alternatives.** This explains the cause of
 115 comparative unpredictability of multiple-choice benchmarks, and also suggests a potential
 116 path forward for successful predictive models of downstream performance in the area of
 117 multiple-choice question answering, and in general the need to model *external information*
 118 not related to scaling-predictable log likelihoods needed for downstream metric computation.
 119
 120 **3. Continuous metrics such as Brier Score are insufficient for recovering predictabil-**
 121 **ity.** We observe that, contrary to prior work showing that metrics such as Brier Score
 122 can hide *emergent behavior* at times, Brier Score is insufficient to improve the statistical
 123 relationship degraded by incorporating incorrect choices’ probability mass.
 124
 125

Our findings explain that the apparent unpredictability of individual downstream evaluations is due to specific incorrect choices, which the strongly predictable pretraining losses do not depend upon. More broadly, we argue that a precise understanding of the factors affecting downstream performance is essential for designing evaluations to reliably track the progression of frontier AI models’ capabilities.

3 METHODOLOGY: DATA FOR STUDYING SCALING OF DOWNSTREAM CAPABILITIES

To study how downstream capabilities on specific tasks change with scale for different model families, we generated per-sample scores from a large number of model families and multiple-choice NLP benchmarks. To ensure the computed scores were consistent with prior work, we used EleutherAI’s Language Model Evaluation Harness (Gao et al., 2023).

Model Families Because our goal is to explore the scaling behavior of evaluations with increasing compute, we chose to evaluate model families with dense combinations of parameter counts and token counts. The following families were evaluated (additional details in App. D):

1. **Pythia** (Biderman et al., 2023b): The Pythia family contains 8 models from 70M to 12B parameters trained on the Pile (Gao et al., 2020) for 300B tokens. We used 8 checkpoints per size of the non-deduplicated variants.
2. **Cerebras-GPT** (Dey et al., 2023): The Cerebras-GPT family contains 7 models ranging from 111M to 13B parameters. The models were trained on the Pile (Gao et al., 2020) for different durations as part of a scaling study with a ratio of $\sim 20\times$ tokens to parameters in a “Chinchilla”-optimal manner (Hoffmann et al., 2022).
3. **OLMo** (Groeneveld et al., 2024): The OLMo family contains a 1B parameter model trained for 3T tokens and two 7B parameter models trained for 2T-2.5T tokens. We selected 7 checkpoints for 1B (spanning 84B¹ to 3T tokens) and 7 checkpoints for 7B (spanning 4B to 2.4T tokens).
4. **INCITE** (AI, 2023): The INCITE family contains 3B and 7B parameter models, trained on 0.8T and 1T tokens of RedPajama-v1(Computer, 2023). The 3B model has only a single checkpoint, so we excluded it. We found this family to be a slight outlier from other families, which we speculate is because its pretraining data were contaminated by benchmarks (Elazar et al., 2023).
5. **LLM360** (Liu et al., 2023): LLM360 includes two 7B parameter LLMs trained on 1.3T and 1.4T tokens. We selected 13 checkpoints of Amber spaced approximately logarithmically.

NLP Benchmarks We evaluated the above model families on widely-used multiple-choice benchmarks for assessing comprehension, reasoning, and world knowledge: AI2 Reasoning Challenge (ARC) Easy and Hard (Clark et al., 2018), HellaSwag (Zellers et al., 2019), MathQA (Amini et al.,

¹OLMo 1B checkpoints below 84B tokens were unfortunately accidentally lost by their creators.

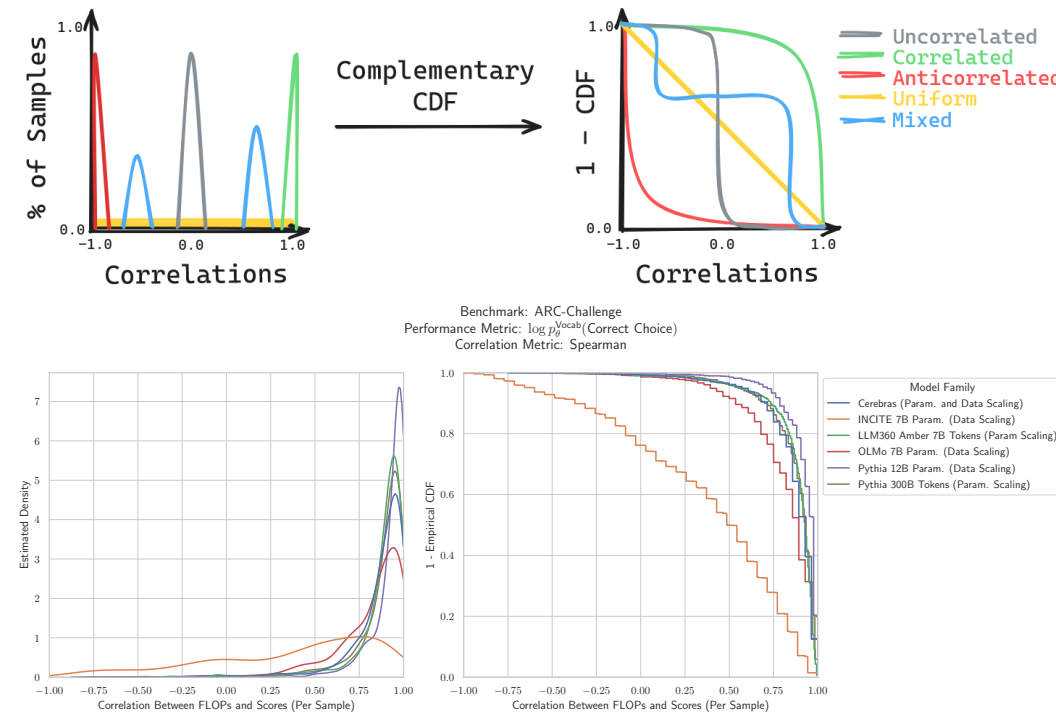


Figure 2: **Distributions of score-compute correlations and their corresponding complementary cumulative distribution functions.** **Left:** For each benchmark, model family, performance metric, and correlation metric, we computed how scores correlate with compute. This yields a distribution (over samples) of score-compute correlations. Note: the uniform distribution is small but non-zero everywhere. **Right:** To easily extract what fraction of samples in a benchmark has score-compute correlations above any given threshold, we converted the probability distributions to *complementary cumulative distribution functions*, i.e., 1 minus the empirical cumulative distribution function (CDF). **Top:** Idealized distributions. **Bottom:** Actual data on ARC Challenge.

2019), MCTACO (Zhou et al., 2019), MMLU (Hendrycks et al., 2020), OpenbookQA (Mihaylov et al., 2018), PIQA (Bisk et al., 2020), RACE (Lai et al., 2017), SciQ (Welbl et al., 2017), SIQA (Sap et al., 2019a), WinoGrande (Keisuke et al., 2019) and XWinoGrad En (Muennighoff et al., 2023). For MMLU, we analyzed each of the 57 subjects (e.g., Abstract Algebra) independently. For each benchmark, we used default evaluation settings from the LM Evaluation Harness (Gao et al., 2023).

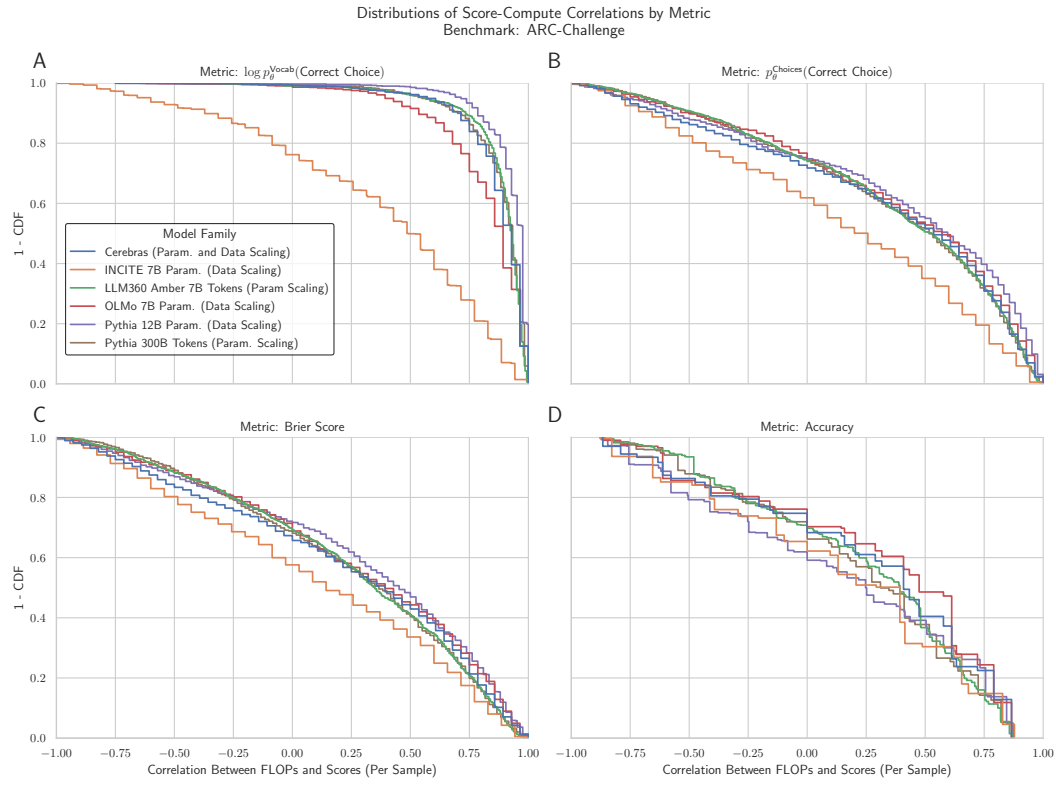
Performance Metrics We used three common multiple-choice metrics (Srivastava et al., 2022; Schaeffer et al., 2023; Du et al., 2024): Accuracy, Brier Score (Brier, 1950), and probability mass on the correct choice relative to the available choices $p_{\theta}^{\text{Choices}}(\text{Correct Choice})$.

Compute Budget Calculations Following prior work (Kaplan et al., 2020), we approximated² the pretraining compute C (in terms of training FLOP) of a given model checkpoint as a function of the parameter count (excluding embeddings) N and the amount of training data seen in tokens D : $C = C(N, D) \approx 6ND$.

4 WHAT MAKES PREDICTING DOWNSTREAM PERFORMANCE DIFFICULT?

Performance on multiple choice benchmarks is commonly published as Accuracy, Brier Score, or probability mass on the correct choice out of the available choices $p_{\theta}^{\text{Choices}}(\text{Correct Choice})$. These

²This approximation neglects FLOP costs associated with attention calculations over sequence length; however, such operations are negligible so long as $d_{\text{model}} \gg n_{\text{ctx}}/12$, and this approximation is therefore standard in most language model scaling law analyses.



242 **Figure 3: Multiple-choice metrics like Accuracy and Brier Score are computed via a**
 243 **sequence of transformations that degrades correlations between performance scores and pre-**
 244 **training compute.** (A) Initially, scores under $\log p_\theta^{\text{Vocab}}(\text{Correct Choice})$ and compute are highly
 245 correlated. Transforming $\log p_\theta^{\text{Vocab}}(\text{Correct Choice}) \rightarrow p_\theta^{\text{Vocab}}(\text{Correct Choice})$ has no effect for
 246 rank correlations. (B) Transforming $p_\theta^{\text{Vocab}}(\text{Correct Choice}) \rightarrow p_\theta^{\text{Choices}}(\text{Correct Choice})$ decorrelates
 247 scores from compute. (C) Transforming $p_\theta^{\text{Choices}}(\text{Correct Choice}) \rightarrow \text{Brier Score}$ minorly de-
 248 creases score-compute correlations. (D) Transforming $p_\theta^{\text{Choices}}(\text{Correct Choice}) \rightarrow \text{Accuracy}$ more
 249 substantially decorrelates scores from compute. Correlation: Spearman. Results are consistent across
 250 benchmarks and all three correlation metrics (App. G).

251
252 quantities are computed via a sequence of transformations that begins with the negative log likelihood
 253 of the correct choice on this particular benchmark sample as some function $f(\cdot, \cdot)$ of compute:

$$\mathcal{L}_\theta^{\text{Vocab}}(\text{Correct Choice}) = f(\text{Compute}, \text{Benchmark Datum}) \quad (1)$$

254
255 Two details are critical. Firstly, this negative log likelihood is not computed in expectation over a
 256 corpus; it is specific to this particular singular datum in the benchmark. *All the scores we discuss are*
 257 *per-datum.* Secondly, this negative log likelihood is computed over the vocabulary of the model. One
 258 can then compute the probability mass of the correct choice, again with respect to the vocabulary:

$$p_\theta^{\text{Vocab}}(\text{Correct Choice}) = \exp(-\mathcal{L}_\theta^{\text{Vocab}}(\text{Correct Choice})) \quad (2)$$

259 Next, probabilities are restricted to the set of available choices $\{\text{Available Choice}_i\}_i^{|\text{Available Choices}|}$ by
 260 masking invalid continuations and normalizing again with respect to this set:

$$p_\theta^{\text{Choices}}(\text{Correct Choice}) \stackrel{\text{def}}{=} \frac{p_\theta^{\text{Vocab}}(\text{Correct Choice})}{\sum_i p_\theta^{\text{Vocab}}(\text{Available Choice}_i)} \quad (3)$$

We distinguish the support over the token space of the model versus over the set of available choices in the benchmark’s question because, as we will show, the support crucially affects predictability. Finally, the choices-normalized probability masses become standard downstream metrics:

$$\text{Accuracy}_\theta \stackrel{\text{def}}{=} \mathbb{1}\left(\text{Correct Choice} == \arg \max_i \left\{ p_\theta^{\text{Choices}}(\text{Available Choice}_i) \right\}\right) \quad (4)$$

$$\text{Brier Score}_\theta \stackrel{\text{def}}{=} \sum_i \left(\mathbb{1}(\text{Available Choice}_i == \text{Correct Choice}) - p_\theta^{\text{Choices}}(\text{Available Choice}_i) \right)^2 \quad (5)$$

where $\mathbb{1}(\cdot)$ is an indicator variable. To quantify how this sequence of transformations affects predictability of performance, we measured how per-sample scores correlate with pretraining compute, and then studied how the distribution (over samples) of correlation values shifts from log likelihoods to $p_\theta^{\text{Vocab}}(\text{Correct Choice})$ to $p_\theta^{\text{Choices}}(\text{Correct Choice})$ to Accuracy or Brier Score. Specifically, for each combination of (*model family*, *benchmark*, *performance metric*, *correlation metric*), we computed a correlation value for each sample in the benchmark between pretraining compute and scores. This yielded a distribution (over samples) of correlation values for the combination (Fig. 2 Left). Visualizing the distribution of correlations for the combination told us what fraction of samples in the benchmark yielded scores that are correlated, uncorrelated or anticorrelated with compute (Fig. 2 Right). We found consistent results using all three standard correlation metrics: Pearson (1895), Kendall (1938) and Spearman (1961).

We demonstrate how the sequence of transformations affects the distribution of score-compute correlations using ARC Challenge (Clark et al., 2018) as an illustrative benchmark; we note that all other benchmarks exhibited similar patterns as well (App. G). We visualized the distributions via their complementary (empirical) cumulative distribution functions (complementary CDFs) (App. B):

$$\hat{S}(c) \stackrel{\text{def}}{=} \frac{1}{S} \sum_{s=1}^S \mathbb{1}\{C_s > c\}, \quad (6)$$

where S is the number of samples in the benchmark and C_s is the correlation (over the models in the model family) between compute and scores on the s -th sample in the benchmark. For a given threshold c , the complementary CDF $\hat{S}(c)$ returns the fraction of the benchmark’s samples with score-compute correlations greater than the threshold c (Fig. 3A). Beginning with log likelihoods, approximately 90% of samples exhibit score-compute correlations > 0.75 , regardless of the model family (Fig. 3A). Transforming negative log likelihoods into probability masses $p_\theta^{\text{Vocab}}(\text{Correct Choice})$ does not affect the distribution of score-compute correlations for Spearman and Kendall. However, transforming $p_\theta^{\text{Vocab}}(\text{Correct Choice})$ into $p_\theta^{\text{Choices}}(\text{Correct Choice})$ decreases the distribution of score-compute correlations (Fig. 3B), with only 40% of samples having score-compute correlations > 0.75 . Transforming $p_\theta^{\text{Choices}}(\text{Correct Choice})$ into Brier Score has little-to-no effect (Fig. 3C), but transforming into Accuracy (Fig. 3D) furthers decreases score-compute correlations. To quantitatively test whether these transformations indeed decrease the correlation between scores and compute, we measured four statistics of these score-compute correlation distributions: (1) the mean, (2) the median, (3) the area under the complementary CDF and (4) the negative³ of the minimum of two Wasserstein distances: between the empirical correlation distribution and an ideal distribution of all correlations = 1, and between the empirical distribution and an ideal distribution of all correlations = -1. Across the four summary statistics, for most benchmarks and for most model families, we discovered a consistent ordering of metrics of the score-compute correlation distributions (Fig. 4):

$$\begin{aligned} & \text{Corr}(\text{Compute}, \log p_\theta^{\text{Vocab}}(\text{Correct Choice})) \\ & \geq \text{Corr}(\text{Compute}, p_\theta^{\text{Vocab}}(\text{Correct Choice})) \\ & > \text{Corr}(\text{Compute}, p_\theta^{\text{Choices}}(\text{Correct Choice})) \\ & \geq \text{Corr}(\text{Compute}, \text{Brier Score}) \\ & > \text{Corr}(\text{Compute}, \text{Accuracy}) \end{aligned}$$

³We chose the *negative* Wasserstein distance for consistency with the other statistics: higher values correspond to higher correlations between scores and compute.



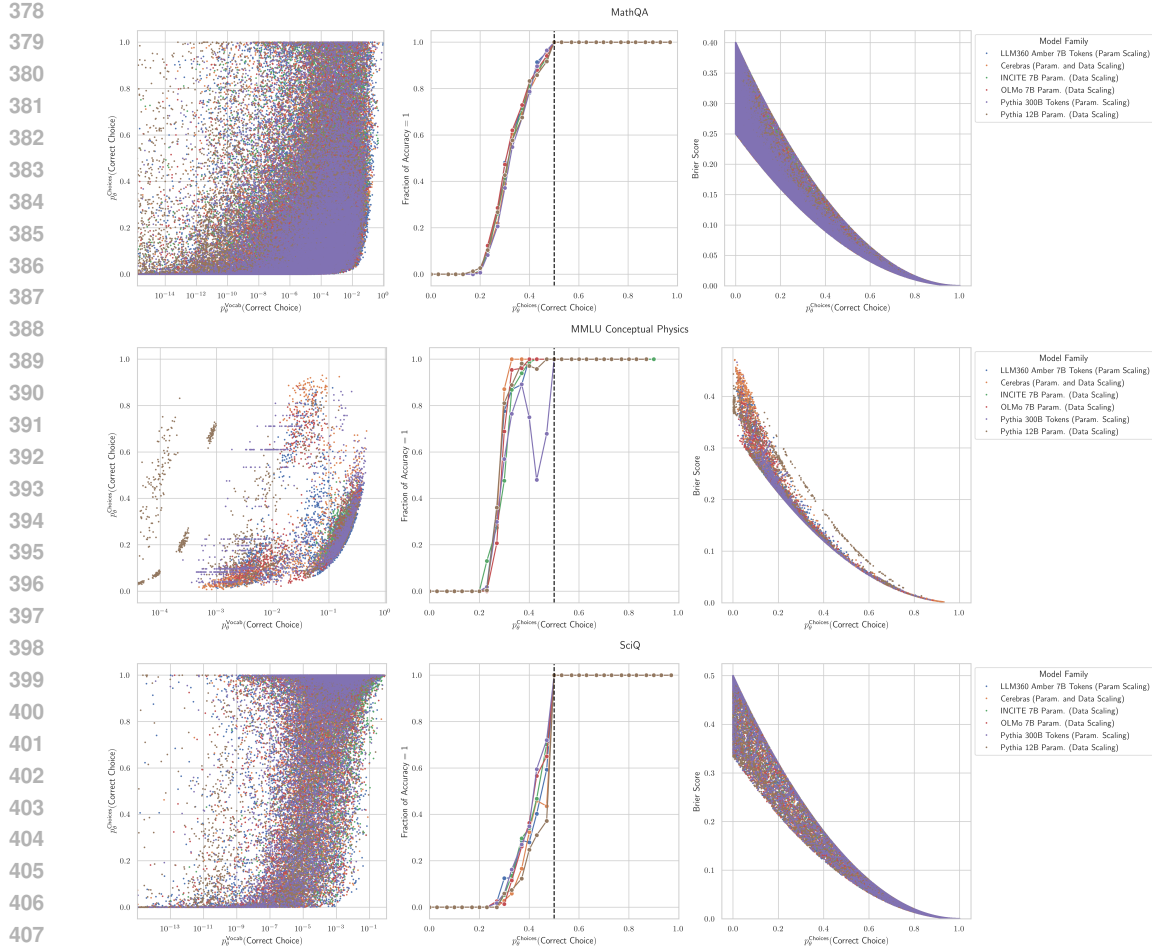
Figure 4: **All four statistics of score-compute correlation distributions demonstrate that transforming $\log p_\theta^{\text{vocab}}(\text{Correct Choice})$ into Accuracy causes score-compute correlations to deteriorate.** We find a consistent trend that the sequence of transformations degrades score-compute correlations, as shown by the right-to-left $\log p_\theta^{\text{vocab}}(\text{Correct Choice})$ -to- $p_\theta^{\text{vocab}}(\text{Correct Choice})$ -to- $p_\theta^{\text{vocab}}(\text{Correct Choice})$ -or-Brier Score-to-Accuracy vertical stripes. This trend holds across benchmarks and model families for three correlation metrics (Spearman, Pearson and Kendall) and for four statistics of correlation distributions (mean, median, the area under the survival function, and negative Wasserstein distance from perfect correlation or perfect anti-correlation). See App. Figs. 7, 8, 9 for other correlation metrics and other score-compute correlation distribution statistics.

To quantitatively confirm that the correlation scores indeed follow this ordering, we computed what fraction of (benchmark, correlation metric, model family, correlation distribution statistic) tuples obey the ordering. To be maximally conservative, we checked for strict inequalities only. We found that across benchmarks, model families, and the 4 correlation distribution statistics, the claimed ordering of metrics held at least 82.4% of the time for Pearson, 85.6% for Spearman and 90.4% for Kendall.

5 PROBABILITY MASS ON INCORRECT CHOICES CAUSES UNPREDICTABILITY

What is the mechanism that degrades how correlated scores are with compute? All three metrics with degraded correlations - $p_\theta^{\text{Choices}}(\text{Correct Choice})$, Accuracy, and Brier Score - depend not just on how the model's probability mass $p_\theta^{\text{vocab}}(\text{Correct Choice})$ concentrates on the correct choice as compute increases, but also depend on how the model's probability mass fluctuates on *incorrect* available choices $\{p_\theta^{\text{vocab}}(\text{Incorrect Choice})\}_{\text{Incorrect Choices}}$ as compute increases. As an example, suppose $p_\theta^{\text{vocab}}(\text{Correct Choice}) = 0.4$ on a 4-way multiple-choice question; what is the accuracy? Spreading the remaining mass uniformly on the incorrect choices will make Accuracy = 1, whereas concentrating mass on a single incorrect choice will make Accuracy = 0.

To demonstrate how drastically the probability mass placed on incorrect choices can alter performance, we visualized the relationships between pairs of metrics immediately preceding and following a given transformation (Fig. 5). For negative log likelihood of the correct choice and $p_\theta^{\text{vocab}}(\text{Correct Choice})$ (not pictured), we observed a clean correspondence between performance under the metric and compute: one can reliably map a given value of these metrics to compute, and vice versa. In contrast, once performance is evaluated using a metric that is a function of the incorrect choices



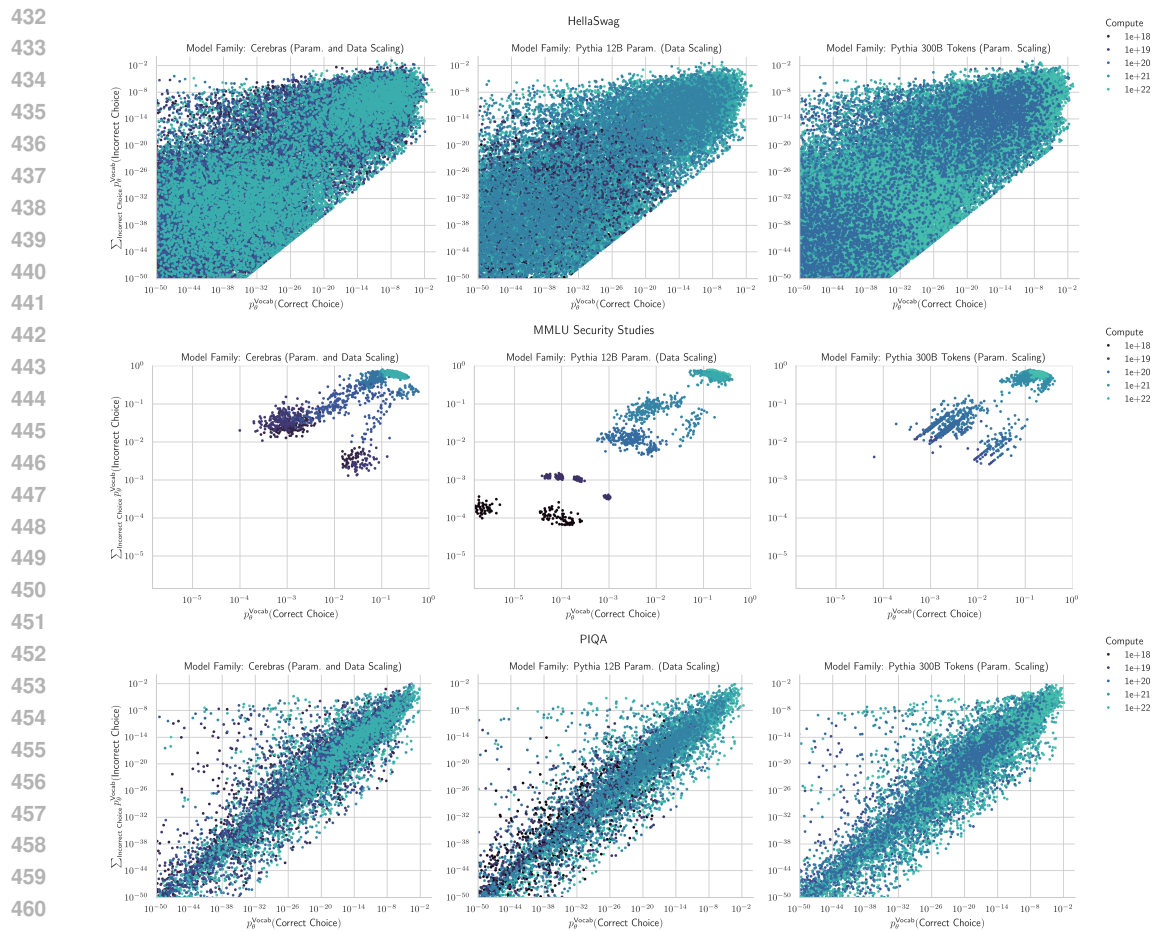
409
410
411
412
413
414
415
416
417
418
419
420
421
422
423
424
425
426
427
428
429
430
431

Figure 5: Predictability deteriorates because of probability mass fluctuating on specific incorrect choices with scale. **Left:** Transitioning from $p_\theta^{\text{Vocab}}(\text{Correct Choice})$ to $p_\theta^{\text{Choices}}(\text{Correct Choice})$ demonstrates that $p_\theta^{\text{Vocab}}(\text{Correct Choice})$ contains little information about $p_\theta^{\text{Choices}}(\text{Correct Choice})$ and vice versa; loosely speaking, any value of one can map to any value of the other. **Center:** While $p_\theta^{\text{Choices}}(\text{Correct Choice}) > 0.5$ must yield Accuracy = 1, for any $p_\theta^{\text{Choices}}(\text{Correct Choice}) < 0.5$, knowing $p_\theta^{\text{Choices}}(\text{Correct Choice})$ contains little information about Accuracy and vice versa. **Right:** Brier Score is more predictable from $p_\theta^{\text{Choices}}(\text{Correct Choice})$ than Accuracy, but still quite variable. Three benchmarks shown: MathQA Amini et al. (2019), MMLU Conceptual Physics Hendrycks et al. (2020), SciQ Welbl et al. (2017).

- $p_\theta^{\text{Choices}}(\text{Correct Choice})$, Accuracy or Brier Score - nearly any value of a score under one metric can map to any value of $p_\theta^{\text{Vocab}}(\text{Correct Choice})$ or $p_\theta^{\text{Choices}}(\text{Correct Choice})$ respectively (Fig. 5), thereby breaking the chain along which one can cleanly infer compute from an observed metric. We can see that Brier Score, a metric meant to produce more continuous scores (Schaeffer et al., 2023), is less variable than Accuracy, provided a known $p_\theta^{\text{Choices}}(\text{Correct Choice})$, but it cannot recover information about $p_\theta^{\text{Vocab}}(\text{Correct Choice})$ that is lost when shifting to $p_\theta^{\text{Choices}}(\text{Correct Choice})$. We next show that this is because of the additional information regarding the underdetermined values of $p_\theta^{\text{Choices}}(\text{Incorrect Choice})$ for each incorrect choice.

6 SCALING BEHAVIOR OF PROBABILITY MASS ON INCORRECT CHOICES

In general, aggregate performance over a distribution is often of interest. Such a focus on aggregate performance leads to an important insight: in MCQA, probability mass fluctuations on incorrect



486
 487 **Takeaway #1: Think through your metrics!**
 488 If one cares about scaling-predictable evaluations, then one needs to think through how their
 489 evaluations transform raw model outputs into useful signals to know what to expect.
 490
 491 **Takeaway #2: Continuous metrics are insufficient to guarantee predictable changes.**
 492 As shown by $p_\theta^{\text{Choices}}$ (Correct Choice) & Brier Score, even “continuous” metrics can be
 493 unpredictable, e.g., if the metric weighs correct behavior against specific incorrect behaviors.
 494
 495 **Takeaway #3: Recommended scaling-predictable metrics for pretraining practitioners.**
 496 Pretraining practitioners seeking scaling-predictable signals for capabilities are advised to
 497 focus on p_θ^{Vocab} (Correct Choice) on relevant benchmarks. Scores under this metric provide
 498 smoother scaling trends and are arguably more interpretable than the pretraining loss.
 499
 500 **Takeaway #4: Evaluations should be reshaped based on intended desiderata.**
 501 Too often, we take evaluations as frozen static objects, but evaluations should be adapted
 502 to pertinent goals. For instance, if the goal is to predict capabilities with scale, evaluations
 503 should be designed or adapted to be scaling-predictable.

7 DISCUSSION, RELATED WORK AND FUTURE DIRECTIONS

504
 505 This work identifies a factor that induces unpredictability in multiple-choice assessments of frontier AI
 506 models, as well as the underlying mechanism: probability mass on incorrect choices. Our results have
 507 implications for the design of future evaluations of frontier AI models that are reliably predictable
 508 with scaling. We hope that our work will be extended to further the science of scaling-predictable
 509 evaluation of AI systems, especially for complex and important model capabilities. We note several
 510 future directions for extension of our work, and we hope that the community also adopts our framing
 511 to further improve scaling-predictable evaluations.
 512

513 **Related Work** We intentionally wove key related work into our main text, with a particular
 514 emphasis in the Introduction. For a longer and more comprehensive exposition, see Appendix A.
 515

516 **Direction 1: Beyond Multiple Choice Benchmarks** Our study is restricted to benchmarks evaluated
 517 via log likelihood-based multiple-choice formats. While we believe this is inherently valuable
 518 due to the usefulness and prevalence of such tasks, this limits the application of our findings. We hope
 519 that our discoveries and proposed mechanisms may be used to inform the study of predictable and
 520 reliable evaluation writ large, and that future work should explore the extent to which our findings
 521 can be generalized to more complex capabilities. Our findings corroborate those of Lyu et al. (2024),
 522 who find that multiple-choice answer scores often diverge from generative evaluations. Consequently,
 523 a particularly important direction for further study is to investigate generative evaluations, which may
 524 contain similar transformations distancing performance from the observed loss.
 525

526 **Direction 2: Predicting Benchmark Performance A Priori** Our work provides an explanation
 527 why multiple-choice benchmark performance is not easily predictable for metrics such as Accuracy
 528 and Brier Score, as observed in the literature (Du et al., 2024). However, our analyses assume
 529 access to entire model families’ scores across several orders of magnitude of pretraining FLOPs, and
 530 do not employ backtesting, as sensibly recommended by (Alabdulmohsin et al., 2022; Owen, 2024).
 531 A predictive model should be able to identify change points well in advance on standard metrics like
 532 Accuracy or Brier Score.
 533
 534
 535
 536
 537
 538
 539

540 REFERENCES
541

- 542 Josh Achiam, Steven Adler, Sandhini Agarwal, Lama Ahmad, Ilge Akkaya, Florencia Leoni Aleman,
543 Diogo Almeida, Janko Altenschmidt, Sam Altman, Shyamal Anadkat, et al. Gpt-4 technical report.
544 *arXiv preprint arXiv:2303.08774*, 2023.
- 545 Together AI. Releasing 3b and 7b redpajama-incite family of models including base, instruction-
546 tuned & chat models. <https://www.together.ai/blog/redpajama-models-v1>,
547 2023. Accessed: 2024-05-19.
- 548 Ibrahim Alabdulmohsin, Behnam Neyshabur, and Xiaohua Zhai. Revisiting neural scaling laws in
549 language and vision, 2022. URL <https://arxiv.org/abs/2209.06640>.
- 550 Aida Amini, Saadia Gabriel, Shanchuan Lin, Rik Koncel-Kedziorski, Yejin Choi, and Hannaneh
551 Hajishirzi. MathQA: Towards interpretable math word problem solving with operation-based
552 formalisms. In Jill Burstein, Christy Doran, and Thamar Solorio (eds.), *Proceedings of the 2019*
553 *Conference of the North American Chapter of the Association for Computational Linguistics: Human*
554 *Language Technologies, Volume 1 (Long and Short Papers)*, pp. 2357–2367, Minneapolis,
555 Minnesota, June 2019. Association for Computational Linguistics. doi: 10.18653/v1/N19-1245.
556 URL <https://aclanthology.org/N19-1245>.
- 557 Anthropic. Anthropic’s responsible scaling policy. <https://www.anthropic.com/news/anthropics-responsible-scaling-policy>, 2023. Accessed: 2024-05-19.
- 558 Anthropic. Introducing the next generation of claudie. <https://www.anthropic.com/news/claudie-3-family>, 2024. Accessed: 2024-05-19.
- 559 Edward Beeching, Clémentine Fourrier, Nathan Habib, Sheon Han, Nathan Lambert, Nazneen
560 Rajani, Omar Sanseviero, Lewis Tunstall, and Thomas Wolf. Open l1m leaderboard. https://huggingface.co/spaces/HuggingFaceH4/open_llm_leaderboard, 2023.
- 561 Tamay Besiroglu, Ege Erdil, Matthew Barnett, and Josh You. Chinchilla scaling: A replication
562 attempt, 2024.
- 563 Stella Biderman, USVSN Sai Prashanth, Lintang Sutawika, Hailey Schoelkopf, Quentin Anthony,
564 Shivanshu Purohit, and Edward Raff. Emergent and predictable memorization in large language
565 models, 2023a.
- 566 Stella Biderman, Hailey Schoelkopf, Quentin Anthony, Herbie Bradley, Kyle O’Brien, Eric Hallahan,
567 Mohammad Aflah Khan, Shivanshu Purohit, USVSN Sai Prashanth, Edward Raff, Aviya Skowron,
568 Lintang Sutawika, and Oskar van der Wal. Pythia: A suite for analyzing large language models
569 across training and scaling, 2023b.
- 570 Stella Biderman, Hailey Schoelkopf, Lintang Sutawika, Leo Gao, Jonathan Tow, Baber Abbasi,
571 Alham Fikri Aji, Pawan Sasanka Ammanamanchi, Sidney Black, Jordan Clive, Anthony DiPofi,
572 Julen Etxaniz, Benjamin Fattori, Jessica Zosa Forde, Charles Foster, Mimansa Jaiswal, Wilson Y.
573 Lee, Haonan Li, Charles Lovering, Niklas Muennighoff, Ellie Pavlick, Jason Phang, Aviya
574 Skowron, Samson Tan, Xiangru Tang, Kevin A. Wang, Genta Indra Winata, François Yvon, and
575 Andy Zou. Lessons from the trenches on reproducible evaluation of language models. *arXiv*
576 preprint, 2024.
- 577 Yonatan Bisk, Rowan Zellers, Ronan Le Bras, Jianfeng Gao, and Yejin Choi. Piqa: Reasoning about
578 physical commonsense in natural language. 2020.
- 579 Samuel R. Bowman. Eight things to know about large language models, 2023.
- 580 Glenn W Brier. Verification of forecasts expressed in terms of probability. *Monthly weather review*,
581 78(1):1–3, 1950.
- 582 Tom Brown, Benjamin Mann, Nick Ryder, Melanie Subbiah, Jared D Kaplan, Prafulla Dhariwal,
583 Arvind Neelakantan, Pranav Shyam, Girish Sastry, Amanda Askell, et al. Language models are
584 few-shot learners. *Advances in neural information processing systems*, 33:1877–1901, 2020.
- 585 Ethan Caballero, Kshitij Gupta, Irina Rish, and David Krueger. Broken neural scaling laws, 2023.

- 594 Aidan Clark, Diego De Las Casas, Aurelia Guy, Arthur Mensch, Michela Paganini, Jordan Hoffmann,
 595 Bogdan Damoc, Blake Hechtman, Trevor Cai, Sebastian Borgeaud, et al. Unified scaling laws
 596 for routed language models. In *International Conference on Machine Learning*, pp. 4057–4086.
 597 PMLR, 2022.
- 598 Peter Clark, Isaac Cowhey, Oren Etzioni, Tushar Khot, Ashish Sabharwal, Carissa Schoenick, and
 599 Oyvind Tafjord. Think you have solved question answering? try arc, the ai2 reasoning challenge.
 600 *arXiv preprint arXiv:1803.05457*, 2018.
- 601
- 602 Together Computer. Redpajama: An open source recipe to reproduce llama training dataset, 2023.
 603 URL <https://github.com/togethercomputer/RedPajama-Data>.
- 604 Wikipedia contributors. Survival function, 2023. URL https://en.wikipedia.org/wiki/Survival_function. [Online; accessed 22-May-2024].
- 605
- 606 Council of Economic Advisers. The 2024 economic report of the president, 03 2024.
 607 URL <https://www.whitehouse.gov/cea/written-materials/2024/03/21/the-2024-economic-report-of-the-president/>. Accessed on 09/29/2024.
- 608
- 609 DeepSeek-AI, :, Xiao Bi, Deli Chen, Guanting Chen, Shanhuang Chen, Damai Dai, Chengqi Deng,
 610 Hongui Ding, Kai Dong, Qiushi Du, Zhe Fu, Huazuo Gao, Kaige Gao, Wenjun Gao, Ruiqi Ge,
 611 Kang Guan, Daya Guo, Jianzhong Guo, Guangbo Hao, Zhewen Hao, Ying He, Wenjie Hu, Panpan
 612 Huang, Erhang Li, Guowei Li, Jiashi Li, Yao Li, Y. K. Li, Wenfeng Liang, Fangyun Lin, A. X.
 613 Liu, Bo Liu, Wen Liu, Xiaodong Liu, Xin Liu, Yiyuan Liu, Haoyu Lu, Shanghao Lu, Fuli Luo,
 614 Shirong Ma, Xiaotao Nie, Tian Pei, Yishi Piao, Junjie Qiu, Hui Qu, Tongzheng Ren, Zehui Ren,
 615 Chong Ruan, Zhangli Sha, Zhihong Shao, Junxiao Song, Xuecheng Su, Jingxiang Sun, Yaofeng
 616 Sun, Minghui Tang, Bingxuan Wang, Peiyi Wang, Shiyu Wang, Yaohui Wang, Yongji Wang, Tong
 617 Wu, Y. Wu, Xin Xie, Zhenda Xie, Ziwei Xie, Yiliang Xiong, Hanwei Xu, R. X. Xu, Yanhong Xu,
 618 Dejian Yang, Yuxiang You, Shuiping Yu, Xingkai Yu, B. Zhang, Haowei Zhang, Lecong Zhang,
 619 Liyue Zhang, Mingchuan Zhang, Minghua Zhang, Wentao Zhang, Yichao Zhang, Chenggang
 620 Zhao, Yao Zhao, Shangyan Zhou, Shunfeng Zhou, Qihao Zhu, and Yuheng Zou. Deepseek llm:
 621 Scaling open-source language models with longtermism, 2024.
- 622
- 623 Nolan Dey, Gurpreet Gosal, Ziming Chen, Hemant Khachane, William Marshall, Ribhu Pathria,
 624 Marvin Tom, and Joel Hestness. Cerebras-gpt: Open compute-optimal language models trained on
 625 the cerebras wafer-scale cluster, 2023.
- 626 Anca Dragan, Helen King, and Allan Dafoe. Introducing the frontier
 627 safety framework. <https://deepmind.google/discover/blog/introducing-the-frontier-safety-framework/>, 2024. Accessed: 2024-05-19.
- 628
- 629 Zhengxiao Du, Aohan Zeng, Yuxiao Dong, and Jie Tang. Understanding emergent abilities of
 630 language models from the loss perspective, 2024.
- 631
- 632 Abhimanyu Dubey, Abhinav Jauhri, Abhinav Pandey, Abhishek Kadian, Ahmad Al-Dahle, Aiesha
 633 Letman, Akhil Mathur, Alan Schelten, Amy Yang, Angela Fan, Anirudh Goyal, Anthony Hartshorn,
 634 Aobo Yang, Archi Mitra, Archie Sravankumar, Artem Korenev, Arthur Hinsvark, Arun Rao, Aston
 635 Zhang, Aurelien Rodriguez, Austen Gregerson, Ava Spataru, Baptiste Roziere, Bethany Biron,
 636 Bin Tang, Bobbie Chern, Charlotte Caucheteux, Chaya Nayak, Chloe Bi, Chris Marra, Chris
 637 McConnell, Christian Keller, Christophe Touret, Chunyang Wu, Corinne Wong, Cristian Canton
 638 Ferrer, Cyrus Nikolaidis, Damien Allonsius, Daniel Song, Danielle Pintz, Danny Livshits, David
 639 Esiobu, Dhruv Choudhary, Dhruv Mahajan, Diego Garcia-Olano, Diego Perino, Dieuwke Hupkes,
 640 Egor Lakomkin, Ehab AlBadawy, Elina Lobanova, Emily Dinan, Eric Michael Smith, Filip
 641 Radenovic, Frank Zhang, Gabriel Synnaeve, Gabrielle Lee, Georgia Lewis Anderson, Graeme
 642 Nail, Gregoire Mialon, Guan Pang, Guillem Cucurell, Hailey Nguyen, Hannah Korevaar, Hu Xu,
 643 Hugo Touvron, Iliyan Zarov, Imanol Arrieta Ibarra, Isabel Kloumann, Ishan Misra, Ivan Evtimov,
 644 Jade Copet, Jaewon Lee, Jan Geffert, Jana Vrane, Jason Park, Jay Mahadeokar, Jeet Shah,
 645 Jelmer van der Linde, Jennifer Billock, Jenny Hong, Jenya Lee, Jeremy Fu, Jianfeng Chi, Jianyu
 646 Huang, Jiawen Liu, Jie Wang, Jiecao Yu, Joanna Bitton, Joe Spisak, Jongsoo Park, Joseph
 647 Rocca, Joshua Johnstun, Joshua Saxe, Junteng Jia, Kalyan Vasuden Alwala, Kartikeya Upasani,
 Kate Plawiak, Ke Li, Kenneth Heafield, Kevin Stone, Khalid El-Arini, Krithika Iyer, Kshitiz

648 Malik, Kuenley Chiu, Kunal Bhalla, Lauren Rantala-Yeary, Laurens van der Maaten, Lawrence
 649 Chen, Liang Tan, Liz Jenkins, Louis Martin, Lovish Madaan, Lubo Malo, Lukas Blecher, Lukas
 650 Landzaat, Luke de Oliveira, Madeline Muzzi, Mahesh Pasupuleti, Mannat Singh, Manohar Paluri,
 651 Marcin Kardas, Mathew Oldham, Mathieu Rita, Maya Pavlova, Melanie Kambadur, Mike Lewis,
 652 Min Si, Mitesh Kumar Singh, Mona Hassan, Naman Goyal, Narjes Torabi, Nikolay Bashlykov,
 653 Nikolay Bogoychev, Niladri Chatterji, Olivier Duchenne, Onur Çelebi, Patrick Alrassy, Pengchuan
 654 Zhang, Pengwei Li, Petar Vasic, Peter Weng, Prajjwal Bhargava, Pratik Dubal, Praveen Krishnan,
 655 Punit Singh Koura, Puxin Xu, Qing He, Qingxiao Dong, Ragavan Srinivasan, Raj Ganapathy,
 656 Ramon Calderer, Ricardo Silveira Cabral, Robert Stojnic, Roberta Raileanu, Rohit Girdhar, Rohit
 657 Patel, Romain Sauvestre, Ronnie Polidoro, Roshan Sumbaly, Ross Taylor, Ruan Silva, Rui Hou,
 658 Rui Wang, Saghar Hosseini, Sahana Chennabasappa, Sanjay Singh, Sean Bell, Seohyun Sonia
 659 Kim, Sergey Edunov, Shaoliang Nie, Sharan Narang, Sharath Raparthi, Sheng Shen, Shengye Wan,
 660 Shruti Bhosale, Shun Zhang, Simon Vandenhende, Soumya Batra, Spencer Whitman, Sten Sootla,
 661 Stephane Collot, Suchin Gururangan, Sydney Borodinsky, Tamar Herman, Tara Fowler, Tarek
 662 Sheasha, Thomas Georgiou, Thomas Scialom, Tobias Speckbacher, Todor Mihaylov, Tong Xiao,
 663 Ujjwal Karn, Vedanuj Goswami, Vibhor Gupta, Vignesh Ramanathan, Viktor Kerkez, Vincent
 664 Gonguet, Virginie Do, Vish Vogeti, Vladan Petrovic, Weiwei Chu, Wenhan Xiong, Wenyin Fu,
 665 Whitney Meers, Xavier Martinet, Xiaodong Wang, Xiaoqing Ellen Tan, Xinfeng Xie, Xuchao Jia,
 666 Xuewei Wang, Yaelle Goldschlag, Yashesh Gaur, Yasmine Babaei, Yi Wen, Yiwen Song, Yuchen
 667 Zhang, Yue Li, Yuning Mao, Zacharie Delpierre Coudert, Zheng Yan, Zhengxing Chen, Zoe
 668 Papakipos, Aaditya Singh, Aaron Grattafiori, Abha Jain, Adam Kelsey, Adam Shajnfeld, Adithya
 669 Gangidi, Adolfo Victoria, Ahuva Goldstand, Ajay Menon, Ajay Sharma, Alex Boesenberg, Alex
 670 Vaughan, Alexei Baevski, Allie Feinstein, Amanda Kallet, Amit Sangani, Anam Yunus, Andrei
 671 Lupu, Andres Alvarado, Andrew Caples, Andrew Gu, Andrew Ho, Andrew Poulton, Andrew
 672 Ryan, Ankit Ramchandani, Annie Franco, Aparajita Saraf, Arkabandhu Chowdhury, Ashley
 673 Gabriel, Ashwin Bharambe, Assaf Eisenman, Azadeh Yazdan, Beau James, Ben Maurer, Benjamin
 674 Leonhardi, Bernie Huang, Beth Loyd, Beto De Paola, Bhargavi Paranjape, Bing Liu, Bo Wu,
 675 Boyu Ni, Braden Hancock, Bram Wasti, Brandon Spence, Brani Stojkovic, Brian Gamido, Britt
 676 Montalvo, Carl Parker, Carly Burton, Catalina Mejia, Changhan Wang, Changkyu Kim, Chao
 677 Zhou, Chester Hu, Ching-Hsiang Chu, Chris Cai, Chris Tindal, Christoph Feichtenhofer, Damon
 678 Civin, Dana Beaty, Daniel Kreymer, Daniel Li, Danny Wyatt, David Adkins, David Xu, Davide
 679 Testuggine, Delia David, Devi Parikh, Diana Liskovich, Didem Foss, Dingkang Wang, Duc Le,
 680 Dustin Holland, Edward Dowling, Eissa Jamil, Elaine Montgomery, Eleonora Presani, Emily
 681 Hahn, Emily Wood, Erik Brinkman, Esteban Arcaute, Evan Dunbar, Evan Smothers, Fei Sun, Felix
 682 Kreuk, Feng Tian, Firat Ozgenel, Francesco Caggioni, Francisco Guzmán, Frank Kanayet, Frank
 683 Seide, Gabriela Medina Florez, Gabriella Schwarz, Gada Badeer, Georgia Swee, Gil Halpern,
 684 Govind Thattai, Grant Herman, Grigory Sizov, Guangyi, Zhang, Guna Lakshminarayanan, Hamid
 685 Shojanazeri, Han Zou, Hannah Wang, Hanwen Zha, Haroun Habeeb, Harrison Rudolph, Helen
 686 Suk, Henry Aspegren, Hunter Goldman, Ibrahim Damlaj, Igor Molybog, Igor Tufanov, Irina-
 687 Elena Veliche, Itai Gat, Jake Weissman, James Geboski, James Kohli, Japhet Asher, Jean-Baptiste
 688 Gaya, Jeff Marcus, Jeff Tang, Jennifer Chan, Jenny Zhen, Jeremy Reizenstein, Jeremy Teboul,
 689 Jessica Zhong, Jian Jin, Jingyi Yang, Joe Cummings, Jon Carvill, Jon Shepard, Jonathan McPhie,
 690 Jonathan Torres, Josh Ginsburg, Junjie Wang, Kai Wu, Kam Hou U, Karan Saxena, Karthik
 691 Prasad, Kartikay Khandelwal, Katayoun Zand, Kathy Matosich, Kaushik Veeraraghavan, Kelly
 692 Michelena, Keqian Li, Kun Huang, Kunal Chawla, Kushal Lakhota, Kyle Huang, Lailin Chen,
 693 Lakshya Garg, Lavender A, Leandro Silva, Lee Bell, Lei Zhang, Liangpeng Guo, Licheng Yu,
 694 Liron Moshkovich, Luca Wehrstedt, Madiam Khabsa, Manav Avalani, Manish Bhatt, Maria
 695 Tsimpoukelli, Martynas Mankus, Matan Hasson, Matthew Lennie, Matthias Reso, Maxim Groshev,
 696 Maxim Naumov, Maya Lathi, Meghan Keneally, Michael L. Seltzer, Michal Valko, Michelle
 697 Restrepo, Mihir Patel, Mik Vyatskov, Mikayel Samvelyan, Mike Clark, Mike Macey, Mike Wang,
 698 Miquel Jubert Hermoso, Mo Metanat, Mohammad Rastegari, Munish Bansal, Nandhini Santhanam,
 699 Natascha Parks, Natasha White, Navyata Bawa, Nayan Singhal, Nick Egebo, Nicolas Usunier,
 700 Nikolay Pavlovich Laptev, Ning Dong, Ning Zhang, Norman Cheng, Oleg Chernoguz, Olivia
 701 Hart, Omkar Salpekar, Ozlem Kalinli, Parkin Kent, Parth Parekh, Paul Saab, Pavan Balaji, Pedro
 Rittner, Philip Bontrager, Pierre Roux, Piotr Dollar, Polina Zvyagina, Prashant Ratanchandani,
 Pritish Yuvraj, Qian Liang, Rachad Alao, Rachel Rodriguez, Rafi Ayub, Raghatham Murthy,
 Raghu Nayani, Rahul Mitra, Raymond Li, Rebekkah Hogan, Robin Battey, Rocky Wang, Rohan
 Maheswari, Russ Howes, Ruty Rinott, Sai Jayesh Bondu, Samyak Datta, Sara Chugh, Sara
 Hunt, Sargun Dhillon, Sasha Sidorov, Satadru Pan, Saurabh Verma, Seiji Yamamoto, Sharadh

- 702 Ramaswamy, Shaun Lindsay, Shaun Lindsay, Sheng Feng, Shenghao Lin, Shengxin Cindy Zha,
 703 Shiva Shankar, Shuqiang Zhang, Shuqiang Zhang, Sinong Wang, Sneha Agarwal, Soji Sajuyigbe,
 704 Soumith Chintala, Stephanie Max, Stephen Chen, Steve Kehoe, Steve Satterfield, Sudarshan
 705 Govindaprasad, Sumit Gupta, Sungmin Cho, Sunny Virk, Suraj Subramanian, Sy Choudhury,
 706 Sydney Goldman, Tal Remez, Tamar Glaser, Tamara Best, Thilo Kohler, Thomas Robinson, Tianhe
 707 Li, Tianjun Zhang, Tim Matthews, Timothy Chou, Tzook Shaked, Varun Vontimitta, Victoria Ajayi,
 708 Victoria Montanez, Vijai Mohan, Vinay Satish Kumar, Vishal Mangla, Vitor Albiero, Vlad Ionescu,
 709 Vlad Poenaru, Vlad Tiberiu Mihailescu, Vladimir Ivanov, Wei Li, Wenchen Wang, Wenwen Jiang,
 710 Wes Bouaziz, Will Constable, Xiaocheng Tang, Xiaofang Wang, Xiaojian Wu, Xiaolan Wang,
 711 Xide Xia, Xilun Wu, Xinbo Gao, Yanjun Chen, Ye Hu, Ye Jia, Ye Qi, Yenda Li, Yilin Zhang,
 712 Ying Zhang, Yossi Adi, Youngjin Nam, Yu, Wang, Yuchen Hao, Yundi Qian, Yuzi He, Zach Rait,
 713 Zachary DeVito, Zef Rosnbrick, Zhaoduo Wen, Zhenyu Yang, and Zhiwei Zhao. The llama 3 herd
 714 of models, 2024. URL <https://arxiv.org/abs/2407.21783>.
- 715 Yanai Elazar, Akshita Bhagia, Ian Helgi Magnusson, Abhilasha Ravichander, Dustin Schwenk, Alane
 716 Suhr, Evan Pete Walsh, Dirk Groeneveld, Luca Soldaini, Sameer Singh, et al. What's in my big
 717 data? In *The Twelfth International Conference on Learning Representations*, 2023.
- 718 Samir Yitzhak Gadre, Georgios Smyrnis, Vaishaal Shankar, Suchin Gururangan, Mitchell Wortsman,
 719 Rulin Shao, Jean Mercat, Alex Fang, Jeffrey Li, Sedrick Keh, Rui Xin, Marianna Nezhurina, Igor
 720 Vasiljevic, Jenia Jitsev, Alexandros G. Dimakis, Gabriel Ilharco, Shuran Song, Thomas Kollar,
 721 Yair Carmon, Achal Dave, Reinhard Heckel, Niklas Muennighoff, and Ludwig Schmidt. Language
 722 models scale reliably with over-training and on downstream tasks, 2024.
- 723 Deep Ganguli, Danny Hernandez, Liane Lovitt, Amanda Askell, Yuntao Bai, Anna Chen, Tom
 724 Conerly, Nova Dassarma, Dawn Drain, Nelson Elhage, et al. Predictability and surprise in large
 725 generative models. In *2022 ACM Conference on Fairness, Accountability, and Transparency*, pp.
 726 1747–1764, 2022.
- 727 Leo Gao, Stella Biderman, Sid Black, Laurence Golding, Travis Hoppe, Charles Foster, Jason Phang,
 728 Horace He, Anish Thite, Noa Nabeshima, Shawn Presser, and Connor Leahy. The pile: An 800gb
 729 dataset of diverse text for language modeling, 2020.
- 730 Leo Gao, John Schulman, and Jacob Hilton. Scaling laws for reward model overoptimization, 2022.
- 731 Leo Gao, Jonathan Tow, Baber Abbasi, Stella Biderman, Sid Black, Anthony DiPofi, Charles Foster,
 732 Laurence Golding, Jeffrey Hsu, Alain Le Noac'h, Haonan Li, Kyle McDonell, Niklas Muennighoff,
 733 Chris Ociepa, Jason Phang, Laria Reynolds, Hailey Schoelkopf, Aviya Skowron, Lintang Sutawika,
 734 Eric Tang, Anish Thite, Ben Wang, Kevin Wang, and Andy Zou. A framework for few-shot
 735 language model evaluation, 12 2023. URL <https://zenodo.org/records/10256836>.
- 736 Mitchell A Gordon, Kevin Duh, and Jared Kaplan. Data and parameter scaling laws for neural
 737 machine translation. In *Proceedings of the 2021 Conference on Empirical Methods in Natural
 738 Language Processing*, pp. 5915–5922, 2021.
- 739 Dirk Groeneveld, Iz Beltagy, Pete Walsh, Akshita Bhagia, Rodney Kinney, Oyvind Tafjord,
 740 Ananya Harsh Jha, Hamish Ivison, Ian Magnusson, Yizhong Wang, Shane Arora, David Atkinson,
 741 Russell Author, Khyathi Raghavi Chandu, Arman Cohan, Jennifer Dumas, Yanai Elazar, Yuling Gu,
 742 Jack Hessel, Tushar Khot, William Merrill, Jacob Morrison, Niklas Muennighoff, Aakanksha Naik,
 743 Crystal Nam, Matthew E. Peters, Valentina Pyatkin, Abhilasha Ravichander, Dustin Schwenk,
 744 Saurabh Shah, Will Smith, Emma Strubell, Nishant Subramani, Mitchell Wortsman, Pradeep
 745 Dasigi, Nathan Lambert, Kyle Richardson, Luke Zettlemoyer, Jesse Dodge, Kyle Lo, Luca Sol-
 746 daini, Noah A. Smith, and Hannaneh Hajishirzi. Olmo: Accelerating the science of language
 747 models, 2024.
- 748 Dan Hendrycks, Collin Burns, Steven Basart, Andy Zou, Mantas Mazeika, Dawn Song, and
 749 Jacob Steinhardt. Measuring massive multitask language understanding. *arXiv preprint
 750 arXiv:2009.03300*, 2020.
- 751 Dan Hendrycks, Collin Burns, Saurav Kadavath, Akul Arora, Steven Basart, Eric Tang, Dawn Song,
 752 and Jacob Steinhardt. Measuring mathematical problem solving with the math dataset. 2021.

- 756 Tom Henighan, Jared Kaplan, Mor Katz, Mark Chen, Christopher Hesse, Jacob Jackson, Heewoo
 757 Jun, Tom B Brown, Prafulla Dhariwal, Scott Gray, et al. Scaling laws for autoregressive generative
 758 modeling. *arXiv preprint arXiv:2010.14701*, 2020.
- 759 Danny Hernandez, Jared Kaplan, Tom Henighan, and Sam McCandlish. Scaling laws for transfer.
 760 *arXiv preprint arXiv:2102.01293*, 2021.
- 762 Danny Hernandez, Tom Brown, Tom Conerly, Nova DasSarma, Dawn Drain, Sheer El-Showk, Nelson
 763 Elhage, Zac Hatfield-Dodds, Tom Henighan, Tristan Hume, et al. Scaling laws and interpretability
 764 of learning from repeated data. *arXiv preprint arXiv:2205.10487*, 2022.
- 765 Joel Hestness, Sharan Narang, Newsha Ardalani, Gregory Diamos, Heewoo Jun, Hassan Kianinejad,
 766 Md Patwary, Mostofa Ali, Yang Yang, and Yanqi Zhou. Deep learning scaling is predictable,
 767 empirically. *arXiv preprint arXiv:1712.00409*, 2017.
- 769 Jordan Hoffmann, Sebastian Borgeaud, Arthur Mensch, Elena Buchatskaya, Trevor Cai, Eliza
 770 Rutherford, Diego de Las Casas, Lisa Anne Hendricks, Johannes Welbl, Aidan Clark, et al.
 771 Training compute-optimal large language models. *arXiv preprint arXiv:2203.15556*, 2022.
- 772 Shengding Hu, Xin Liu, Xu Han, Xinrong Zhang, Chaoqun He, Weilin Zhao, Yankai Lin, Ning Ding,
 773 Zebin Ou, Guoyang Zeng, Zhiyuan Liu, and Maosong Sun. Predicting emergent abilities with
 774 infinite resolution evaluation, 2024.
- 776 Yuzhen Huang, Jinghan Zhang, Zifei Shan, and Junxian He. Compression represents intelligence
 777 linearly, 2024.
- 778 Andy L Jones. Scaling scaling laws with board games. *arXiv preprint arXiv:2104.03113*, 2021.
- 780 Mandar Joshi, Eunsol Choi, Daniel Weld, and Luke Zettlemoyer. triviaqa: A Large Scale Distantly
 781 Supervised Challenge Dataset for Reading Comprehension. *arXiv e-prints*, art. arXiv:1705.03551,
 782 2017.
- 783 Jared Kaplan, Sam McCandlish, Tom Henighan, Tom B Brown, Benjamin Chess, Rewon Child, Scott
 784 Gray, Alec Radford, Jeffrey Wu, and Dario Amodei. Scaling laws for neural language models.
 785 *arXiv preprint arXiv:2001.08361*, 2020.
- 786 Sakaguchi Keisuke, Le Ronan, Bhagavatula Chandra, and Choi Yejin. Winogrande: An adversarial
 787 winograd schema challenge at scale. 2019.
- 789 Maurice G Kendall. A new measure of rank correlation. *Biometrika*, 30(1/2):81–93, 1938.
- 791 David G. Kleinbaum and Mitchel Klein. *Survival Analysis: A Self-Learning Text*. Springer, 3 edition,
 792 2012. ISBN 978-1441966452. doi: 10.1007/978-1-4419-6646-9.
- 793 Tom Kwiatkowski, Jennimaria Palomaki, Olivia Redfield, Michael Collins, Ankur Parikh, Chris
 794 Alberti, Danielle Epstein, Illia Polosukhin, Matthew Kelcey, Jacob Devlin, Kenton Lee, Kristina N.
 795 Toutanova, Llion Jones, Ming-Wei Chang, Andrew Dai, Jakob Uszkoreit, Quoc Le, and Slav Petrov.
 796 Natural questions: a benchmark for question answering research. *Transactions of the Association
 797 of Computational Linguistics*, 2019.
- 798 Guokun Lai, Qizhe Xie, Hanxiao Liu, Yiming Yang, and Eduard Hovy. RACE: Large-scale ReADING
 799 comprehension dataset from examinations. In *Proceedings of the 2017 Conference on Empirical
 800 Methods in Natural Language Processing*, pp. 785–794, Copenhagen, Denmark, September
 801 2017. Association for Computational Linguistics. doi: 10.18653/v1/D17-1082. URL <https://aclanthology.org/D17-1082>.
- 803 Zhengzhong Liu, Aurick Qiao, Willie Neiswanger, Hongyi Wang, Bowen Tan, Tianhua Tao, Junbo
 804 Li, Yuqi Wang, Suqi Sun, Omkar Pangarkar, Richard Fan, Yi Gu, Victor Miller, Yonghao Zhuang,
 805 Guowei He, Haonan Li, Fajri Koto, Liping Tang, Nikhil Ranjan, Zhiqiang Shen, Xuguang Ren,
 806 Roberto Iriondo, Cun Mu, Zhiting Hu, Mark Schulze, Preslav Nakov, Tim Baldwin, and Eric P.
 807 Xing. Llm360: Towards fully transparent open-source llms, 2023.
- 809 Chenyang Lyu, Minghao Wu, and Alham Fikri Aji. Beyond probabilities: Unveiling the misalignment
 in evaluating large language models. *arXiv preprint arXiv:2402.13887*, 2024.

- 810 Alexander Maloney, Daniel A Roberts, and James Sully. A solvable model of neural scaling laws.
 811 *arXiv preprint arXiv:2210.16859*, 2022.
- 812
- 813 Sam McCandlish, Jared Kaplan, Dario Amodei, and OpenAI Dota Team. An empirical model of
 814 large-batch training, 2018.
- 815 Ian McKenzie, Alexander Lyzhov, Alicia Parrish, Ameya Prabhu, Aaron Mueller, Najoung Kim, Sam
 816 Bowman, and Ethan Perez. The inverse scaling prize, 2022. URL <https://github.com/inverse-scaling/prize>.
- 817
- 818 Todor Mihaylov, Peter Clark, Tushar Khot, and Ashish Sabharwal. Can a suit of armor conduct
 819 electricity? a new dataset for open book question answering. In *EMNLP*, 2018.
- 820
- 821 Sherin Muckatira, Vijeta Deshpande, Vladislav Lialin, and Anna Rumshisky. Emergent abilities in
 822 reduced-scale generative language models, 2024.
- 823
- 824 Niklas Muennighoff, Thomas Wang, Lintang Sutawika, Adam Roberts, Stella Biderman, Teven Le
 825 Scao, M Saiful Bari, Sheng Shen, Zheng-Xin Yong, Hailey Schoelkopf, Xiangru Tang, Dragomir
 826 Radev, Alham Fikri Aji, Khalid Almubarak, Samuel Albanie, Zaid Alyafeai, Albert Webson,
 827 Edward Raff, and Colin Raffel. Crosslingual generalization through multitask finetuning, 2023.
- 828
- 829 Niklas Muennighoff, Alexander Rush, Boaz Barak, Teven Le Scao, Nouamane Tazi, Aleksandra
 830 Piktus, Sampo Pyysalo, Thomas Wolf, and Colin A Raffel. Scaling data-constrained language
 831 models. *Advances in Neural Information Processing Systems*, 36, 2024.
- 832
- 833 Oren Neumann and Claudius Gros. Scaling laws for a multi-agent reinforcement learning model.
arXiv preprint arXiv:2210.00849, 2022.
- 834
- 835 OpenAI. Openai's approach to frontier risk. <https://openai.com/global-affairs/our-approach-to-frontier-risk/>, 2023. Accessed: 2024-05-19.
- 836
- 837 OpenAI. Hello gpt-4o. <https://openai.com/index/hello-gpt-4o/>, 2024. Accessed:
 838 2024-05-16.
- 839
- 840 OpenAI, Josh Achiam, Steven Adler, Sandhini Agarwal, Lama Ahmad, Ilge Akkaya, Florencia Leoni
 841 Aleman, Diogo Almeida, Janko Altenschmidt, Sam Altman, Shyamal Anadkat, Red Avila, Igor
 842 Babuschkin, Suchir Balaji, Valerie Balcom, Paul Baltescu, Haiming Bao, Mohammad Bavarian,
 843 Jeff Belgum, Irwan Bello, Jake Berdine, Gabriel Bernadett-Shapiro, Christopher Berner, Lenny
 844 Bogdonoff, Oleg Boiko, Madelaine Boyd, Anna-Luisa Brakman, Greg Brockman, Tim Brooks,
 845 Miles Brundage, Kevin Button, Trevor Cai, Rosie Campbell, Andrew Cann, Brittany Carey, Chelsea
 846 Carlson, Rory Carmichael, Brooke Chan, Che Chang, Fotis Chantzis, Derek Chen, Sully Chen,
 847 Ruby Chen, Jason Chen, Mark Chen, Ben Chess, Chester Cho, Casey Chu, Hyung Won Chung,
 848 Dave Cummings, Jeremiah Currier, Yunxing Dai, Cory Decareaux, Thomas Degry, Noah Deutsch,
 849 Damien Deville, Arka Dhar, David Dohan, Steve Dowling, Sheila Dunning, Adrien Ecoffet, Atty
 850 Eleti, Tyna Eloundou, David Farhi, Liam Fedus, Niko Felix, Simón Posada Fishman, Juston Forte,
 851 Isabella Fulford, Leo Gao, Elie Georges, Christian Gibson, Vik Goel, Tarun Gogineni, Gabriel
 852 Goh, Rapha Gontijo-Lopes, Jonathan Gordon, Morgan Grafstein, Scott Gray, Ryan Greene, Joshua
 853 Gross, Shixiang Shane Gu, Yufei Guo, Chris Hallacy, Jesse Han, Jeff Harris, Yuchen He, Mike
 854 Heaton, Johannes Heidecke, Chris Hesse, Alan Hickey, Wade Hickey, Peter Hoeschele, Brandon
 855 Houghton, Kenny Hsu, Shengli Hu, Xin Hu, Joost Huizinga, Shantanu Jain, Shawn Jain, Joanne
 856 Jang, Angela Jiang, Roger Jiang, Haozhun Jin, Denny Jin, Shino Jomoto, Billie Jonn, Heewoo
 857 Jun, Tomer Kaftan, Łukasz Kaiser, Ali Kamali, Ingmar Kanitscheider, Nitish Shirish Keskar,
 858 Tabarak Khan, Logan Kilpatrick, Jong Wook Kim, Christina Kim, Yongjik Kim, Jan Hendrik
 859 Kirchner, Jamie Kiros, Matt Knight, Daniel Kokotajlo, Łukasz Kondraciuk, Andrew Kondrich,
 860 Aris Konstantinidis, Kyle Kosic, Gretchen Krueger, Vishal Kuo, Michael Lampe, Ikai Lan, Teddy
 861 Lee, Jan Leike, Jade Leung, Daniel Levy, Chak Ming Li, Rachel Lim, Molly Lin, Stephanie
 862 Lin, Mateusz Litwin, Theresa Lopez, Ryan Lowe, Patricia Lue, Anna Makaju, Kim Malfacini,
 863 Sam Manning, Todor Markov, Yaniv Markovski, Bianca Martin, Katie Mayer, Andrew Mayne,
 Bob McGrew, Scott Mayer McKinney, Christine McLeavey, Paul McMillan, Jake McNeil, David
 Medina, Aalok Mehta, Jacob Menick, Luke Metz, Andrey Mishchenko, Pamela Mishkin, Vinnie
 Monaco, Evan Morikawa, Daniel Mossing, Tong Mu, Mira Murati, Oleg Murk, David Mély,
 Ashvin Nair, Reiichiro Nakano, Rajeev Nayak, Arvind Neelakantan, Richard Ngo, Hyeonwoo

- 864 Noh, Long Ouyang, Cullen O’Keefe, Jakub Pachocki, Alex Paino, Joe Palermo, Ashley Pantuliano,
 865 Giambattista Parascandolo, Joel Parish, Emry Parparita, Alex Passos, Mikhail Pavlov, Andrew Peng,
 866 Adam Perelman, Filipe de Avila Belbute Peres, Michael Petrov, Henrique Ponde de Oliveira Pinto,
 867 Michael, Pokorny, Michelle Pokrass, Vitchyr H. Pong, Tolly Powell, Alethea Power, Boris Power,
 868 Elizabeth Proehl, Raul Puri, Alec Radford, Jack Rae, Aditya Ramesh, Cameron Raymond, Francis
 869 Real, Kendra Rimbach, Carl Ross, Bob Rotsted, Henri Roussez, Nick Ryder, Mario Saltarelli, Ted
 870 Sanders, Shibani Santurkar, Girish Sastry, Heather Schmidt, David Schnurr, John Schulman, Daniel
 871 Selsam, Kyla Sheppard, Toki Sherbakov, Jessica Shieh, Sarah Shoker, Pranav Shyam, Szymon
 872 Sidor, Eric Sigler, Maddie Simens, Jordan Sitkin, Katarina Slama, Ian Sohl, Benjamin Sokolowsky,
 873 Yang Song, Natalie Staudacher, Felipe Petroski Such, Natalie Summers, Ilya Sutskever, Jie Tang,
 874 Nikolas Tezak, Madeleine B. Thompson, Phil Tillet, Amin Tootoonchian, Elizabeth Tseng, Preston
 875 Tuggle, Nick Turley, Jerry Tworek, Juan Felipe Cerón Uribe, Andrea Vallone, Arun Vijayvergiya,
 876 Chelsea Voss, Carroll Wainwright, Justin Jay Wang, Alvin Wang, Ben Wang, Jonathan Ward, Jason
 877 Wei, CJ Weinmann, Akila Welihinda, Peter Welinder, Jiayi Weng, Lilian Weng, Matt Wiethoff,
 878 Dave Willner, Clemens Winter, Samuel Wolrich, Hannah Wong, Lauren Workman, Sherwin Wu,
 879 Jeff Wu, Michael Wu, Kai Xiao, Tao Xu, Sarah Yoo, Kevin Yu, Qiming Yuan, Wojciech Zaremba,
 880 Rowan Zellers, Chong Zhang, Marvin Zhang, Shengjia Zhao, Tianhao Zheng, Juntang Zhuang,
 William Zhuk, and Barret Zoph. Gpt-4 technical report, 2024.
- 881 David Owen. How predictable is language model benchmark performance?, 2024.
- 882 Karl Pearson. VII. note on regression and inheritance in the case of two parents. *proceedings of the royal society of London*, 58(347-352):240–242, 1895.
- 883 Machel Reid, Nikolay Savinov, Denis Teplyashin, Dmitry Lepikhin, Timothy Lillicrap, Jean-baptiste
 884 Alayrac, Radu Soricut, Angeliki Lazaridou, Orhan Firat, Julian Schrittwieser, et al. Gemini
 885 1.5: Unlocking multimodal understanding across millions of tokens of context. *arXiv preprint arXiv:2403.05530*, 2024.
- 886 Jonathan S Rosenfeld, Amir Rosenfeld, Yonatan Belinkov, and Nir Shavit. A constructive prediction
 887 of the generalization error across scales. In *International Conference on Learning Representations*,
 888 2019.
- 889 Yangjun Ruan, Chris J. Maddison, and Tatsunori Hashimoto. Observational scaling laws and the
 890 predictability of language model performance, 2024.
- 891 Maarten Sap, Hannah Rashkin, Derek Chen, Ronan Le Bras, and Yejin Choi. Social iqai: Commonsense
 892 reasoning about social interactions. In *Proceedings of the 2019 Conference on Empirical Methods in Natural Language Processing and the 9th International Joint Conference on Natural Language Processing (EMNLP-IJCNLP)*, 2019a.
- 893 Maarten Sap, Hannah Rashkin, Derek Chen, Ronan LeBras, and Yejin Choi. Socialiqai: Commonsense
 894 reasoning about social interactions, 2019b.
- 895 Nikhil Sardana and Jonathan Frankle. Beyond chinchilla-optimal: Accounting for inference in
 896 language model scaling laws, 2023.
- 897 Rylan Schaeffer, Brando Miranda, and Sanmi Koyejo. Are emergent abilities of large language
 898 models a mirage? In A. Oh, T. Naumann, A. Globerson, K. Saenko, M. Hardt, and S. Levine (eds.),
 899 *Advances in Neural Information Processing Systems*, volume 36, pp. 55565–55581. Curran Associates, Inc., 2023. URL https://proceedings.neurips.cc/paper_files/paper/2023/file/adc98a266f45005c403b8311ca7e8bd7-Paper-Conference.pdf.
- 900 Charles Spearman. The proof and measurement of association between two things. 1961.
- 901 Aarohi Srivastava, Abhinav Rastogi, Abhishek Rao, Abu Awal Md Shoeb, Abubakar Abid, Adam
 902 Fisch, Adam R Brown, Adam Santoro, Aditya Gupta, Adrià Garriga-Alonso, et al. Beyond the
 903 imitation game: Quantifying and extrapolating the capabilities of language models. *arXiv preprint arXiv:2206.04615*, 2022.
- 904 Gemini Team, Rohan Anil, Sebastian Borgeaud, Yonghui Wu, Jean-Baptiste Alayrac, Jiahui Yu, Radu
 905 Soricut, Johan Schalkwyk, Andrew M Dai, Anja Hauth, et al. Gemini: a family of highly capable
 906 multimodal models. *arXiv preprint arXiv:2312.11805*, 2023.

918 Jason Wei, Yi Tay, Rishi Bommasani, Colin Raffel, Barret Zoph, Sebastian Borgeaud, Dani Yogatama,
 919 Maarten Bosma, Denny Zhou, Donald Metzler, et al. Emergent abilities of large language models.
 920 *arXiv preprint arXiv:2206.07682*, 2022.

921 Johannes Welbl, Nelson F. Liu, and Matt Gardner. Crowdsourcing multiple choice science questions.
 922 In Leon Derczynski, Wei Xu, Alan Ritter, and Tim Baldwin (eds.), *Proceedings of the 3rd Workshop
 923 on Noisy User-generated Text*, pp. 94–106, Copenhagen, Denmark, September 2017. Association
 924 for Computational Linguistics. doi: 10.18653/v1/W17-4413. URL <https://aclanthology.org/W17-4413>.

925 Rowan Zellers, Ari Holtzman, Yonatan Bisk, Ali Farhadi, and Yejin Choi. Hellaswag: Can a machine
 926 really finish your sentence? *arXiv preprint arXiv:1905.07830*, 2019.

927 Xiaohua Zhai, Alexander Kolesnikov, Neil Houlsby, and Lucas Beyer. Scaling vision transformers.
 928 In *Proceedings of the IEEE/CVF Conference on Computer Vision and Pattern Recognition*, pp.
 929 12104–12113, 2022.

930 Biao Zhang, Zhongtao Liu, Colin Cherry, and Orhan Firat. When scaling meets llm finetuning: The
 931 effect of data, model and finetuning method, 2024. URL <https://arxiv.org/abs/2402.17193>.

932 Ben Zhou, Daniel Khashabi, Qiang Ning, and Dan Roth. “going on a vacation” takes longer than
 933 “going for a walk”: A study of temporal commonsense understanding. In Kentaro Inui, Jing Jiang,
 934 Vincent Ng, and Xiaojun Wan (eds.), *Proceedings of the 2019 Conference on Empirical Methods
 935 in Natural Language Processing and the 9th International Joint Conference on Natural Language
 936 Processing (EMNLP-IJCNLP)*, pp. 3363–3369, Hong Kong, China, November 2019. Association
 937 for Computational Linguistics. doi: 10.18653/v1/D19-1332. URL <https://aclanthology.org/D19-1332>.

938

939

940

941

942

943

944

945

946

947

948

949

950

951

952

953

954

955

956

957

958

959

960

961

962

963

964

965

966

967

968

969

970

971

972 **A RELATED WORK**
 973

974 **Language Model Evaluation** The capabilities of AI models are typically evaluated using con-
 975 structed datasets to assess performance on a specific task, acting as a proxy for some real-world usage
 976 scenario. However, performing robust and reliable evaluations is a challenge, with many potential
 977 pitfalls and unsolved problems (Biderman et al., 2024). For example, we might prefer to ask models
 978 open-ended questions and evaluate their answers in natural language, but it then often becomes
 979 difficult to robustly score the resulting model outputs, especially for partial correctness. For this
 980 reason, it is common practice for evaluation benchmarks to simplify their scoring via approximations,
 981 such as extracting a sub-string from free-form outputs heuristically (Joshi et al., 2017; Kwiatkowski
 982 et al., 2019; Hendrycks et al., 2021) and checking that it matches a specific gold target string, or
 983 casting a task to a *multiple-choice* format, in which a closed set of correct and incorrect answers
 984 is known, and the model’s answer is determined by selecting the most likely option among these
 985 strings. For more details on the precise procedures typically used for multiple choice elsewhere in the
 986 literature, see Biderman et al. (2024). We believe that the multiple-choice format is valuable, due to
 987 its flexibility, popularity and relevance (Brown et al., 2020; Beeching et al., 2023; Biderman et al.,
 988 2024), but we discuss its limitations in Section 7.
 989

990 **Scaling Laws** Many neural networks exhibit power-law scaling of the pretraining loss as a function
 991 of the amount of compute, data, or parameters used for training (Hestness et al., 2017; Brown et al.,
 992 2020; Hoffmann et al., 2022). These neural scaling laws demonstrate that the pretraining loss can
 993 be highly predictable as a function of these fundamental inputs, which has a number of practical
 994 applications: Scaling laws fit to smaller training runs can be used to predict the pretraining loss of
 995 a much larger training run, and can be used to determine effective hyperparameters (McCandlish
 996 et al., 2018; DeepSeek-AI et al., 2024), or the optimal allocation of dataset and model size for a
 997 given compute budget (Hoffmann et al., 2022; Muennighoff et al., 2024; Dey et al., 2023; Sardana &
 998 Frankle, 2023; Besiroglu et al., 2024). In some cases, such laws can be used to predict performance of
 999 a larger model in a particular domain, such as coding (Achiam et al., 2023). The existence of scaling
 1000 laws turns deep learning into a predictable science at the macro level by providing a simple recipe for
 1001 improving model quality and de-risking returns on increasing investment into scale (Ganguli et al.,
 1002 2022; Bowman, 2023).

1003 **Emergent Abilities** Language models have been observed to exhibit apparent *emergent abilities*—
 1004 behaviors on downstream task performance that cannot be predicted from smaller scales (Wei et al.,
 1005 2022; Srivastava et al., 2022). Emergence appears not to be simply a product of training compute
 1006 or model size, but is also dependent on other factors such as dataset composition (Muckatira et al.,
 1007 2024; Wei et al., 2022). Schaeffer et al. (2023) find that some emergent phenomena can be a “mirage”
 1008 arising due to choices made by researchers such as the use of discontinuous metrics and insufficient
 1009 resolution. However, Du et al. (2024) note that for many tasks, emergence remains despite the use
 1010 of continuous metrics. Additionally, discontinuous metrics have been argued to often be the most
 1011 reflective of real-world usefulness, so emergence in these hard metrics is important. Hu et al. (2024)
 1012 found that for generative evaluations, infinite resolution can be achieved but requires significant
 1013 compute and that generated answer be verifiable.

1014 **Predicting Downstream Task Performance** Although predicting macroscopic pretraining loss is
 1015 useful, a far more useful goal is to predict the scaling of model performance on particular downstream
 1016 tasks or domains. If this was possible, then model developers could tune their datasets and training
 1017 procedures in a more fine-grained way before launching computationally intensive training runs.
 1018 Model performance on a particular downstream task is typically correlated with compute, albeit
 1019 with a few exceptions (McKenzie et al., 2022; Huang et al., 2024). However, despite attempts to fit
 1020 scaling laws to values other than loss, including benchmark scores (Gadre et al., 2024; Zhang et al.,
 1021 2024), model memorization (Biderman et al., 2023a), or reward (Gao et al., 2022), these downstream
 1022 performance metrics are usually more noisy or require more compute to fit accurately. Owen (2024)
 1023 and Gadre et al. (2024) both find that while *aggregate* benchmark performance with more compute
 1024 can be predicted, the scaling behaviour of individual tasks can be noisy. Additionally, Owen (2024),
 1025 Du et al. (2024) and Gadre et al. (2024) claim that predicting scaling behavior on a task without
 1026 access to models exhibiting better-than-random performance (i.e., “before emergence occurs”) cannot
 1027 be done reliably. Concurrently to our work, Ruan et al. (2024) propose Observational Scaling Laws

1026 by mapping model capabilities from compute to a shared low-dimensional space of capabilities across
 1027 model families before predicting performance on novel tasks. Our goal in this work is to investigate
 1028 the comparative unpredictability of individual downstream performance scores, and advise how to
 1029 create more scaling-predictable evaluations that are closely coupled with real-world use-cases.
 1030

1031 B DEFINITION OF SURVIVAL FUNCTION

1032 The survival function $S_X(x)$ – also known as the reliability function, the tail distribution, or the
 1033 complementary cumulative distribution function – gives the probability that a random variable X
 1034 exceeds a certain value x Kleinbaum & Klein (2012); contributors (2023):
 1035

$$1036 S_X(x) \stackrel{\text{def}}{=} \Pr[X > x] = \int_x^\infty f_X(x') dx' = 1 - F_X(x) \quad (7)$$

1037 where $F_X(x) = \Pr[X \leq x]$ is the cumulative distribution function (CDF) and $f_X(x)$ is the
 1038 probability density function (pdf) or probability mass function (pmf) of the random variable X . The
 1039 CDF $F_X(x)$ gives the probability that the random variable X is at most x , while the survival function
 1040 $S_X(x)$ gives the probability that X exceeds x .
 1041

1042 When the true distribution of X is unknown, we can use the empirical CDF (ECDF) $\hat{F}_X(x)$ and the
 1043 empirical survival function (ESF) $\hat{S}_X(x)$:
 1044

$$1045 \hat{S}_X(x) \stackrel{\text{def}}{=} \frac{1}{n} \sum_{i=1}^n 1\{x_i > x\} = 1 - \hat{F}_X(x) \quad (8)$$

1046 where n is the number of observations, x_i is the realized value of the random variable X for
 1047 observation i , and $1\{x_i > x\}$ is the indicator function. The empirical survival function $\hat{S}_X(x)$
 1048 specifies the fraction of observations for which the sampled random variable X exceeds x .
 1049

1050 C COMPUTE RESOURCES FOR EXPERIMENTS

1051 Experiments were done across a wide family of model families and sizes. The GPUs we used for
 1052 medium-sized models (7B parameters and above) used a single A100s with 80GB of vRAM. For
 1053 smaller models (≤ 8 B) we used A100s with 80GB of vRAM, Quadro RTX 8000 with 48GB of vRAM,
 1054 or RTX A4000 with 16GB of vRAM. For 70B parameter models, we used at least 2 A100 GPUs with
 1055 80GB of vRAM.

1056 D ADDITIONAL MODEL FAMILY DETAILS

1057 Here we provide further experimental details regarding our selection of model families.
 1058

1. **Pythia** (Biderman et al., 2023b): We consider two “families” for Pythia in our experiments. **Pythia (Parameter Scaling)** refers to the use of fully-trained checkpoints from 9 different model sizes (all model sizes documented in Biderman et al. (2023), as well as a 14M parameter model trained later by the authors). **Pythia-12B (Data Scaling)** refers to the use of 8 checkpoints across training for the Pythia-12B model, namely having seen 2M, 64M, 2B, 6B, 20B, 60B, 200B, and 300B tokens in training.
2. **Cerebras-GPT** (Dey et al., 2023): **Cerebras (Parameter and Data Scaling)** refers to our use of 1 checkpoint per model in the Cerebras-GPT family, each fully trained for differing quantities of data as documented by the model creators, for 7 checkpoints in total.
3. **OLMo** (Groeneveld et al., 2024): **OLMo (7B Data Scaling)** refers to the use of 7 checkpoints for OLMo-7B across training, namely, checkpoints having seen 4B, 44B, 133B, 442B, 885B, 1.5T, and 2.4T tokens.
4. **INCITE** (AI, 2023): **INCITE-7B (Data Scaling)** considers 6 checkpoints over training for the 7B parameter model, having seen 240B, 280B, 400B, 500B, 700B, and 1T tokens.
5. **LLM360** (Liu et al., 2023): **LLM360 Amber (Data Scaling)** considers 13 checkpoints of the Amber model, having seen 0B, 3.5B, 7B, 10.5B, 17.5B, 31.5B, 49B, 87.5B, 147B, 252B, 430B, 738B, and 1.26T tokens.

E BROADER IMPACT

This paper contributes to a better understanding of the predictability of large language models (LLMs), which can have both positive and negative societal impacts. On the positive side, by making LLM benchmarks more predictable, this research can help society anticipate and plan for potential challenges associated with their development and deployment. This increased predictability can facilitate proactive measures to mitigate risks and ensure the responsible use of AI technologies.

However, the increased predictability of LLMs could theoretically be exploited by malicious actors to accelerate the development of AI systems designed for malicious purposes. We also stress the importance of proactive risk assessment and the implementation of safeguards to prevent the misuse of AI technologies.

1080
1081
1082
1083
1084
1085
1086
1087
1088
1089
1090
1091
1092
1093
1094
1095
1096
1097
1098
1099
1100
1101
1102
1103
1104
1105
1106
1107
1108
1109
1110
1111
1112
1113
1114
1115
1116
1117
1118
1119
1120
1121
1122
1123
1124
1125
1126
1127
1128
1129
1130
1131
1132
1133

1134
1135

F SCORE-COMPUTE CORRELATION DISTRIBUTIONS' STATISTICS

1136
1137

F.1 PEARSON CORRELATIONS

1138

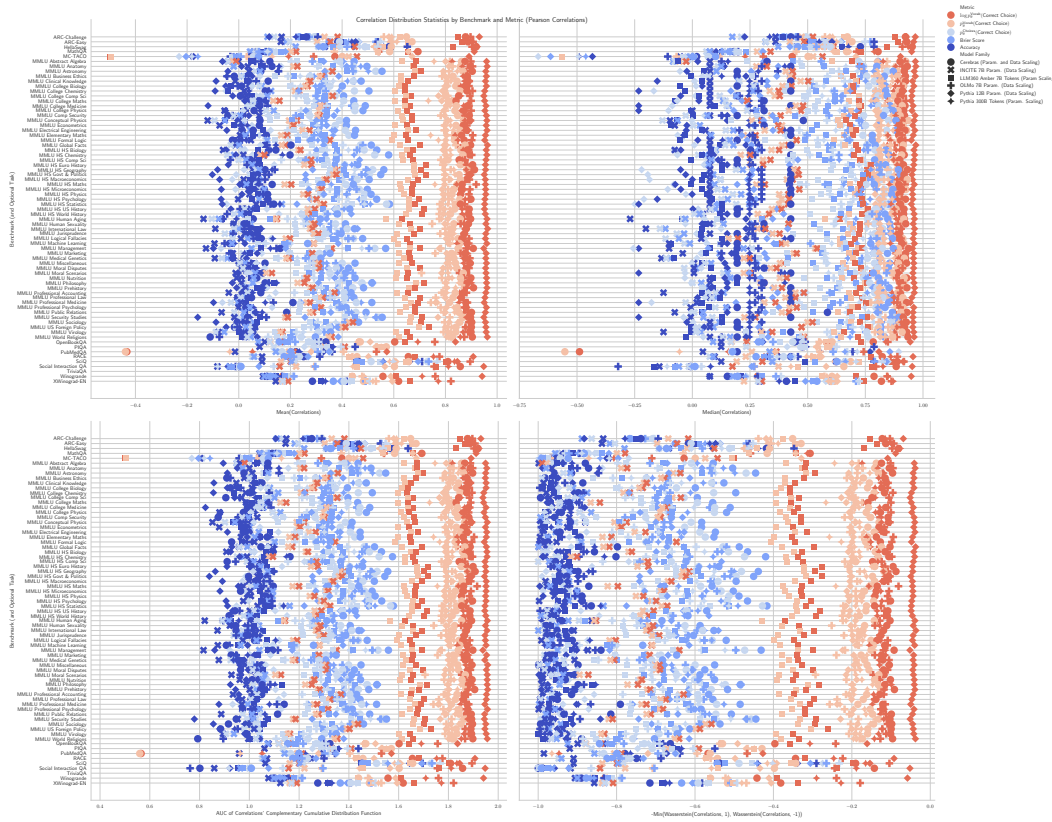


Figure 7: Statistics for empirical distributions of correlations between scores and compute for all benchmarks and model families. These correlation values were computed with Pearson correlation and are consistent with the main text’s results computed with Spearman correlation (Fig. 4): The sequence of transformations from $\log p_\theta^{\text{Vocab}}(\text{Correct Choice}) \rightarrow p_\theta^{\text{Vocab}}(\text{Correct Choice}) \rightarrow p_\theta^{\text{Choices}}(\text{Correct Choice}) \rightarrow \text{Accuracy}$ degrades predictability.

1170
1171
1172
1173
1174
1175
1176
1177
1178
1179
1180
1181
1182
1183
1184
1185
1186
1187

1188
1189

F.2 SPEARMAN CORRELATIONS

1190

1191

1192

1193

1194

1195

1196

1197

1198

1199

1200

1201

1202

1203

1204

1205

1206

1207

1208

1209

1210

1211

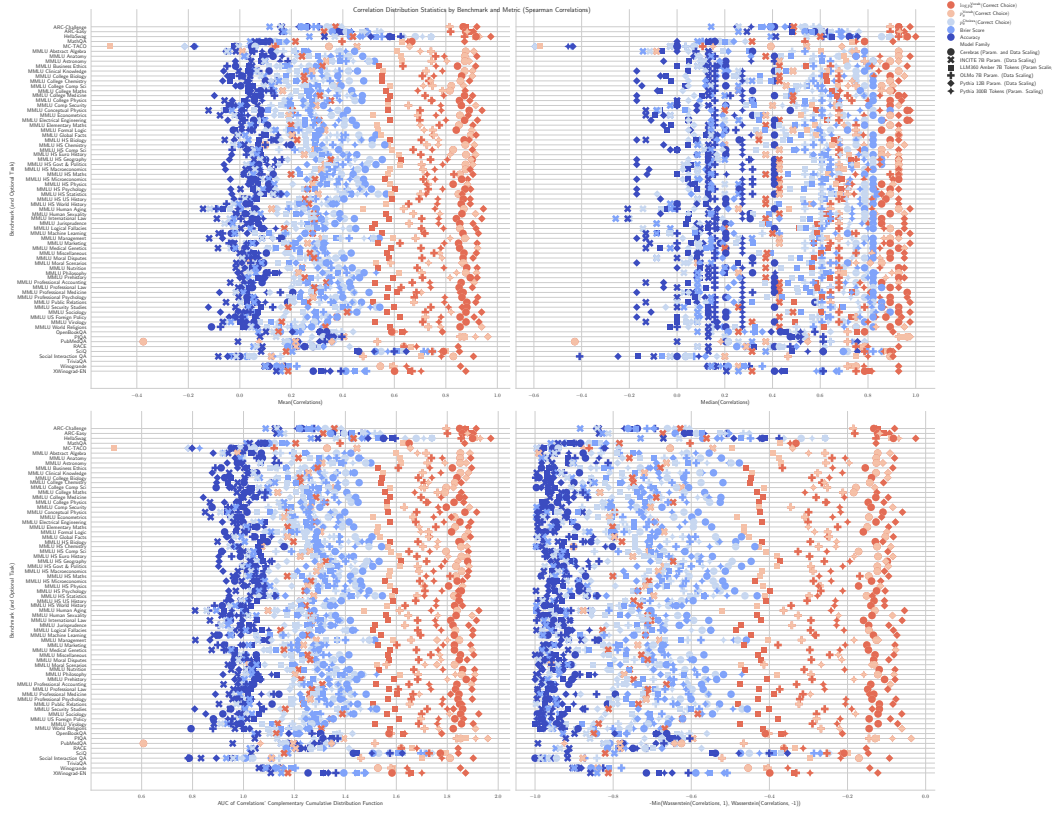
1212

1213

1214

1215

1216



1217

Figure 8: Statistics for empirical distributions of correlations between scores and compute for all benchmarks and model families. These correlation values were computed with Spearman correlation. The sequence of transformations from $\log p_\theta^{\text{vocab}}(\text{Correct Choice}) \rightarrow p_\theta^{\text{vocab}}(\text{Correct Choice}) \rightarrow p_\theta^{\text{Choices}}(\text{Correct Choice}) \rightarrow \text{Accuracy}$ degrades predictability.

1218

1219

1220

1221

1222

1223

1224

1225

1226

1227

1228

1229

1230

1231

1232

1233

1234

1235

1236

1237

1238

1239

1240

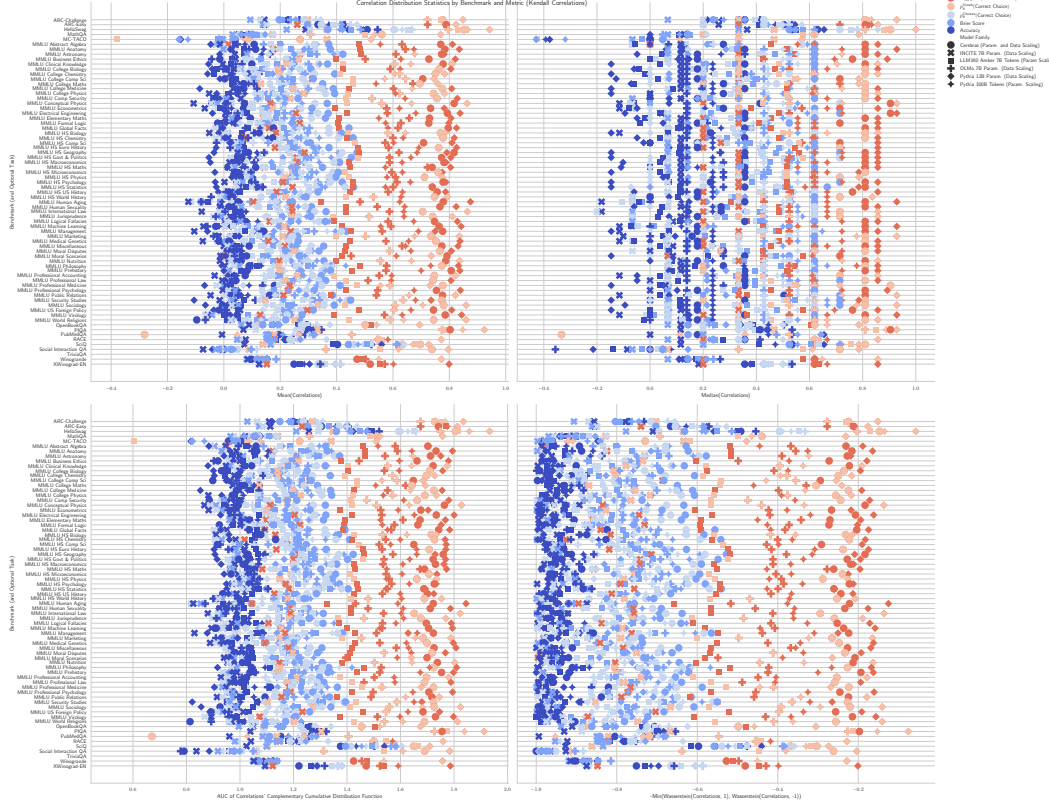
1241

1242
1243

F.3 KENDALL CORRELATIONS

1244

1245



1246

1247

1248

1249

1250

1251

1252

1253

1254

1255

1256

1257

1258

1259

1260

1261

1262

1263

1264

1265

1266

1267

1268

1269

1270

1271

Figure 9: Statistics for empirical distributions of correlations between scores and compute for all benchmarks and model families. These correlation values were computed with Kendall correlation and are consistent with the main text’s results computed with Spearman correlation (Fig. 4): The sequence of transformations from $\log p_\theta^{\text{Vocab}}(\text{Correct Choice}) \rightarrow p_\theta^{\text{Vocab}}(\text{Correct Choice}) \rightarrow p_\theta^{\text{Choices}}(\text{Correct Choice}) \rightarrow \text{Accuracy}$ degrades predictability.

1272

1273

1274

1275

1276

1277

1278

G PER-BENCHMARK SCORE-COMPUTE CORRELATION DISTRIBUTIONS

1279

1280

G.1 NLP BENCHMARK: ARC CHALLENGE CLARK ET AL. (2018)

1281

1282

1283

1284

1285

1286

1287

1288

1289

1290

1291

1292

1293

1294

1295

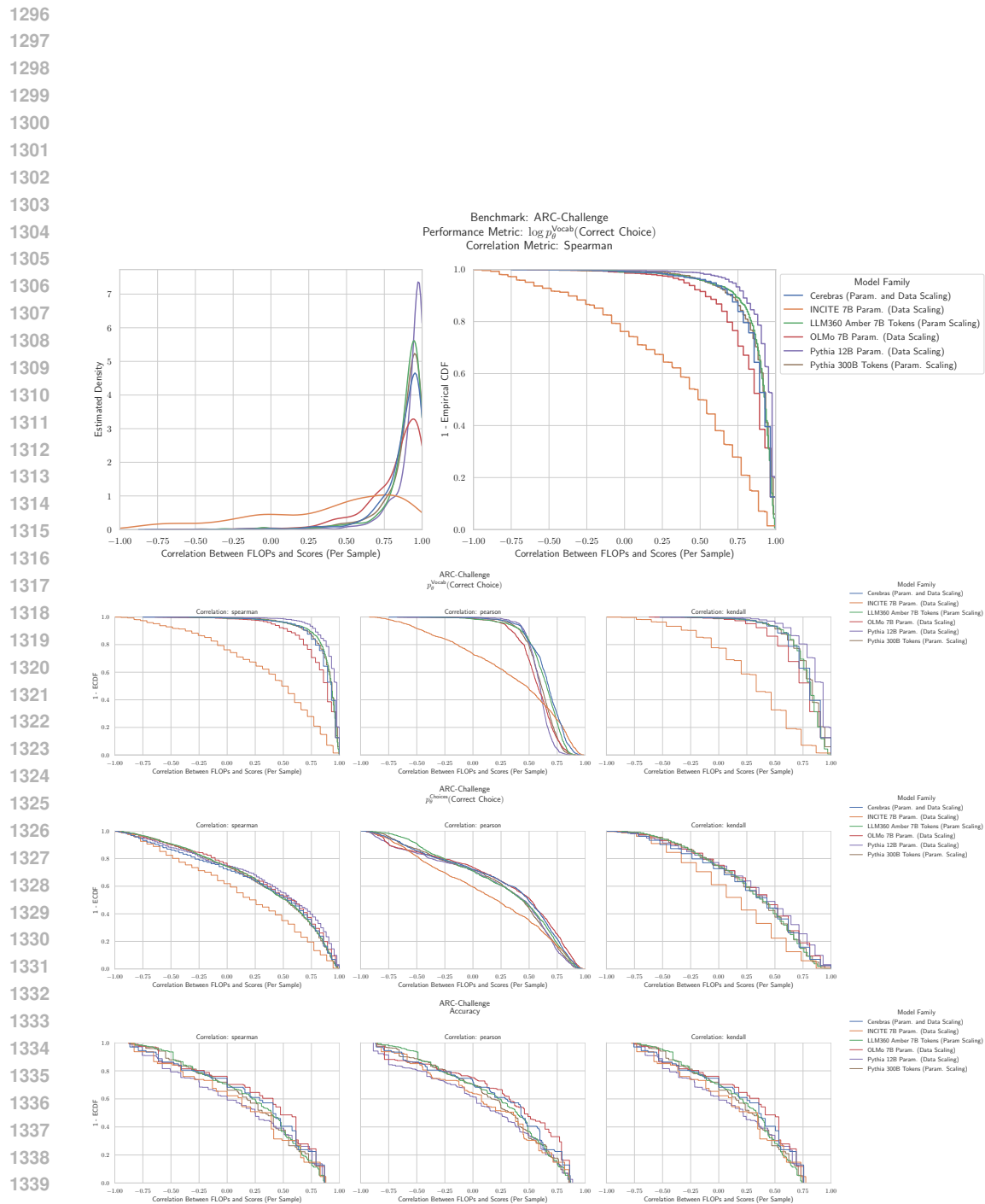


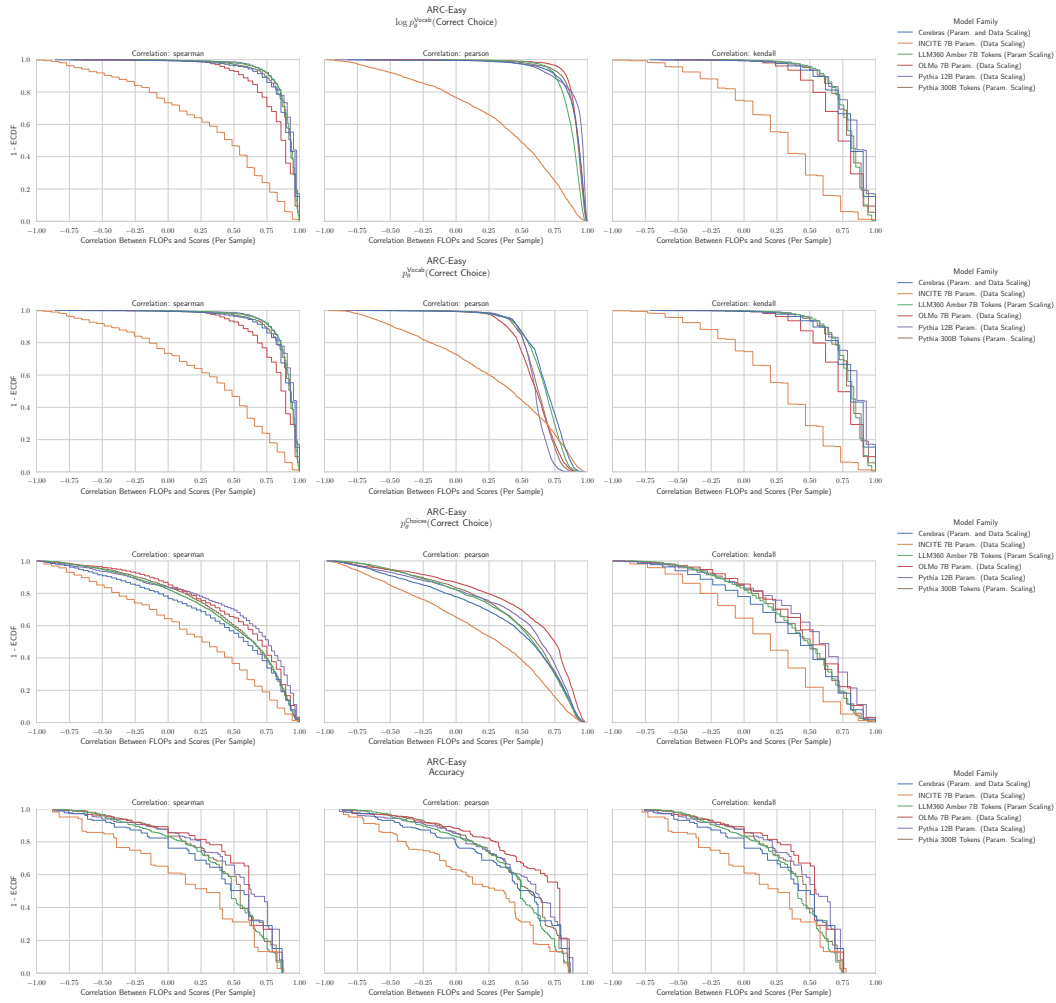
Figure 10: **ARC Challenge: Downstream performance is computed via a sequence of transformations that deteriorate correlations between scores and pretraining compute.**

1350
1351

G.2 NLP BENCHMARK: ARC EASY CLARK ET AL. (2018)

1352

1353



1354

1355

1356

1357

1358

1359

1360

1361

1362

1363

1364

1365

1366

1367

1368

1369

1370

1371

1372

1373

1374

1375

1376

1377

1378

1379

1380

1381

1382

1383

1384

Figure 11: **ARC Easy: Downstream performance is computed via a sequence of transformations that deteriorate correlations between scores and pretraining compute.**

1385

1386

1387

1388

1389

1390

1391

1392

1393

1394

1395

1396

1397

1398

1399

1400

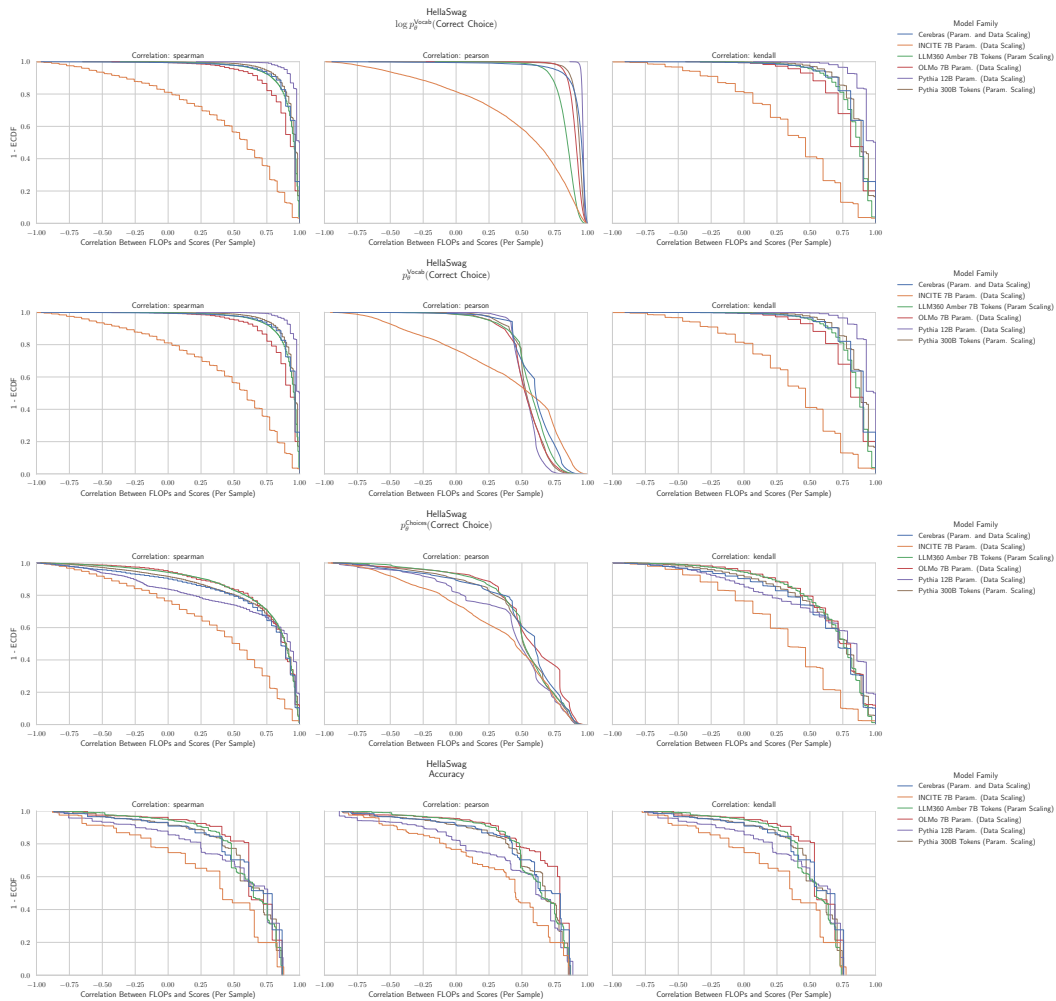
1401

1402

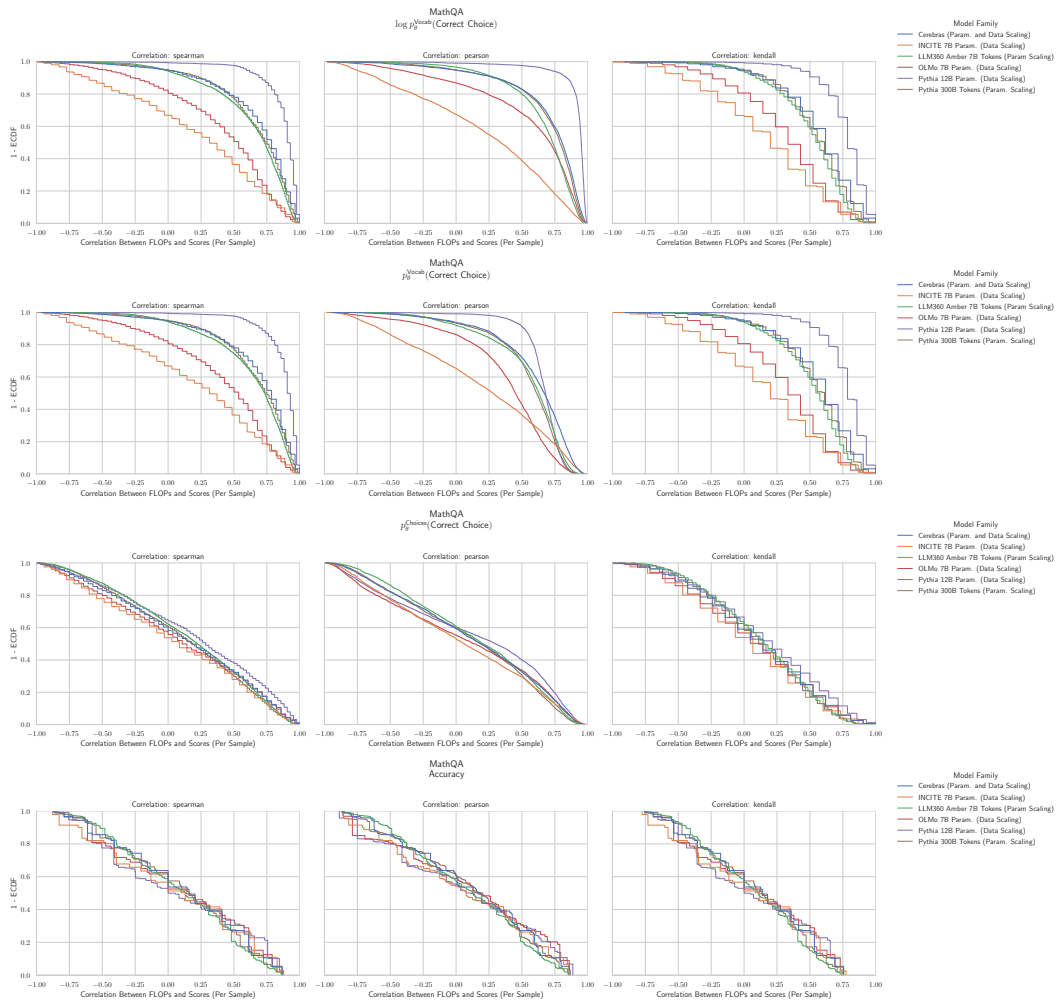
1403

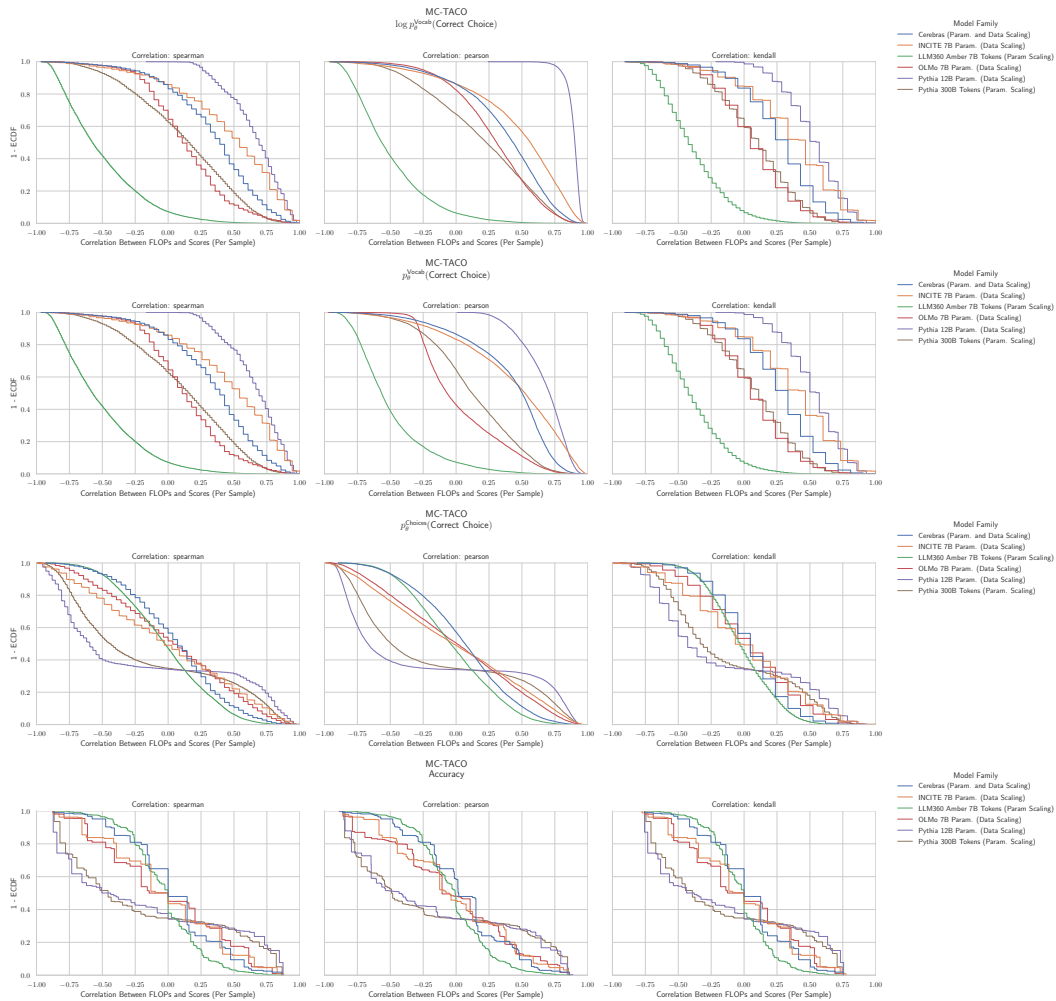
1404 **G.3 NLP BENCHMARK: HELASWAG ZELLERS ET AL. (2019)**

1405



1439 **Figure 12: Hellaswag: Downstream performance is computed via a sequence of transformations**
1440 **that deteriorate correlations between scores and pretraining compute.**

1458 G.4 NLP BENCHMARK: MATHQA AMINI ET AL. (2019)
14591493 Figure 13: HellaSwag: Downstream performance is computed via a sequence of transformations
1494 that deteriorate correlations between scores and pretraining compute.

1512 G.5 NLP BENCHMARK: MC TACO ZHOU ET AL. (2019)
15131547 **Figure 14: MC TACO: Downstream performance is computed via a sequence of transformations
1548 that deteriorate correlations between scores and pretraining compute.**
1549
1550
1551
1552
1553
1554
1555
1556
1557
1558
1559
1560
1561
1562
1563
1564
1565

1566
1567

G.6 NLP BENCHMARK: MMLU ABSTRACT ALGEBRA HENDRYCKS ET AL. (2020)

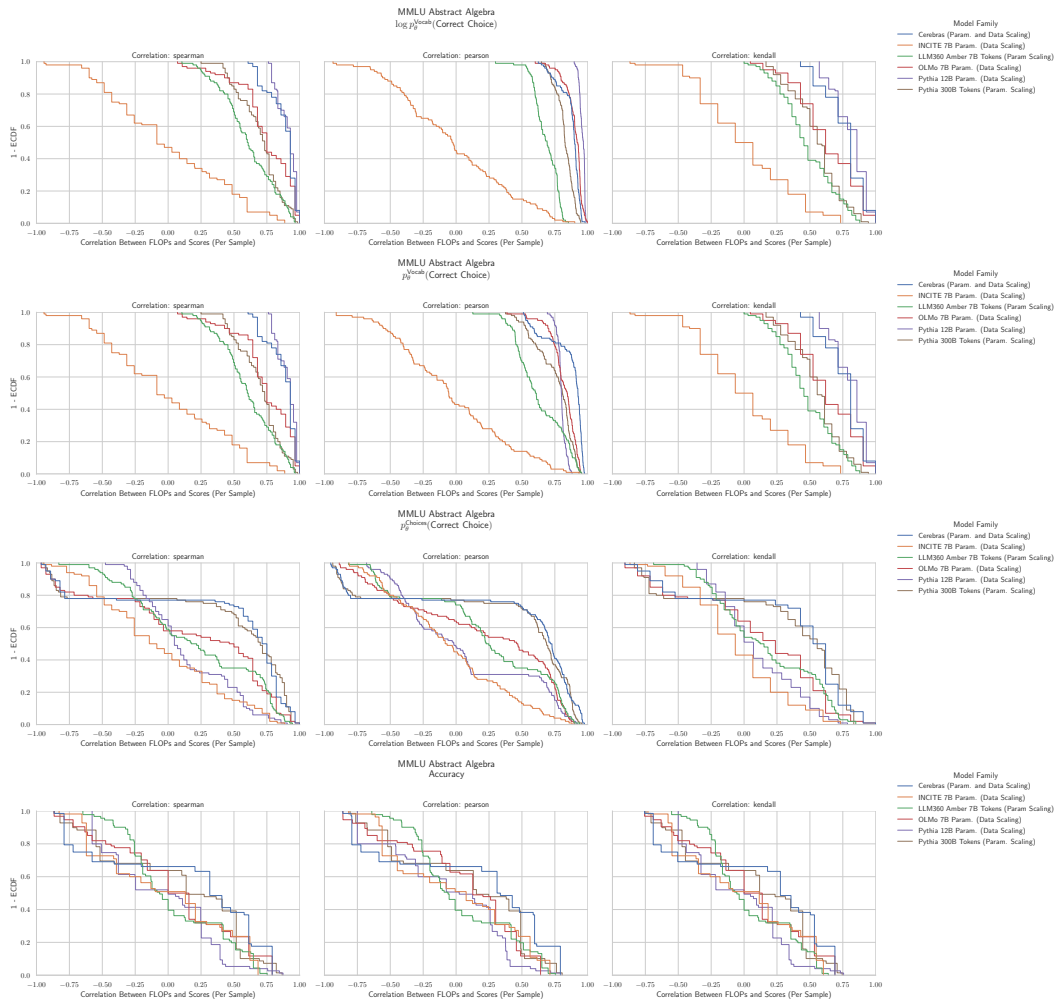
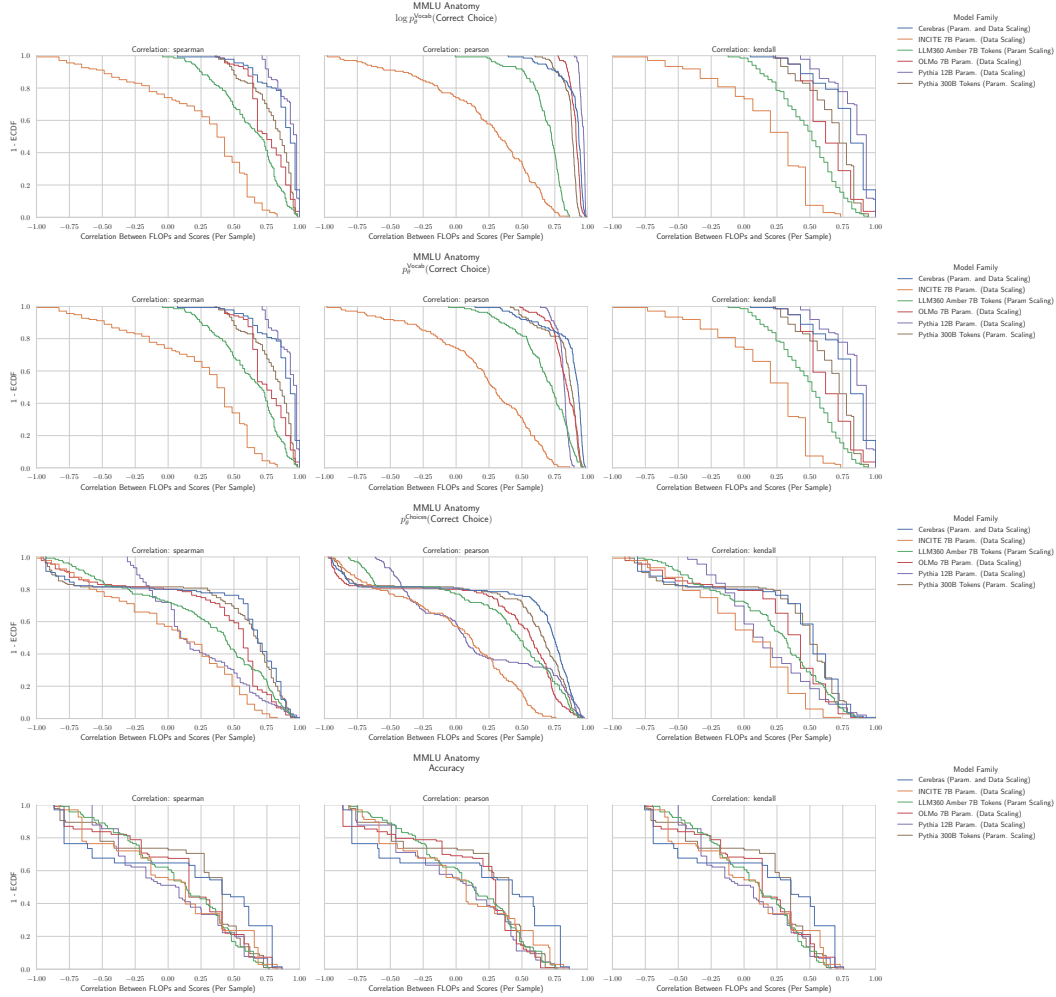
1568
1569

Figure 15: MMLU Abstract Algebra: Downstream performance is computed via a sequence of transformations that deteriorate correlations between scores and pretraining compute.

1600
1601
1602
1603
1604
1605
1606
1607
1608
1609
1610
1611
1612
1613
1614
1615
1616
1617
1618
1619

1620 **G.7 NLP BENCHMARK: MMLU ANATOMY HENDRYCKS ET AL. (2020)**



1655 **Figure 16: MMLU Anatomy: Downstream performance is computed via a sequence of transfor-**
 1656 **mations that deteriorate correlations between scores and pretraining compute.**

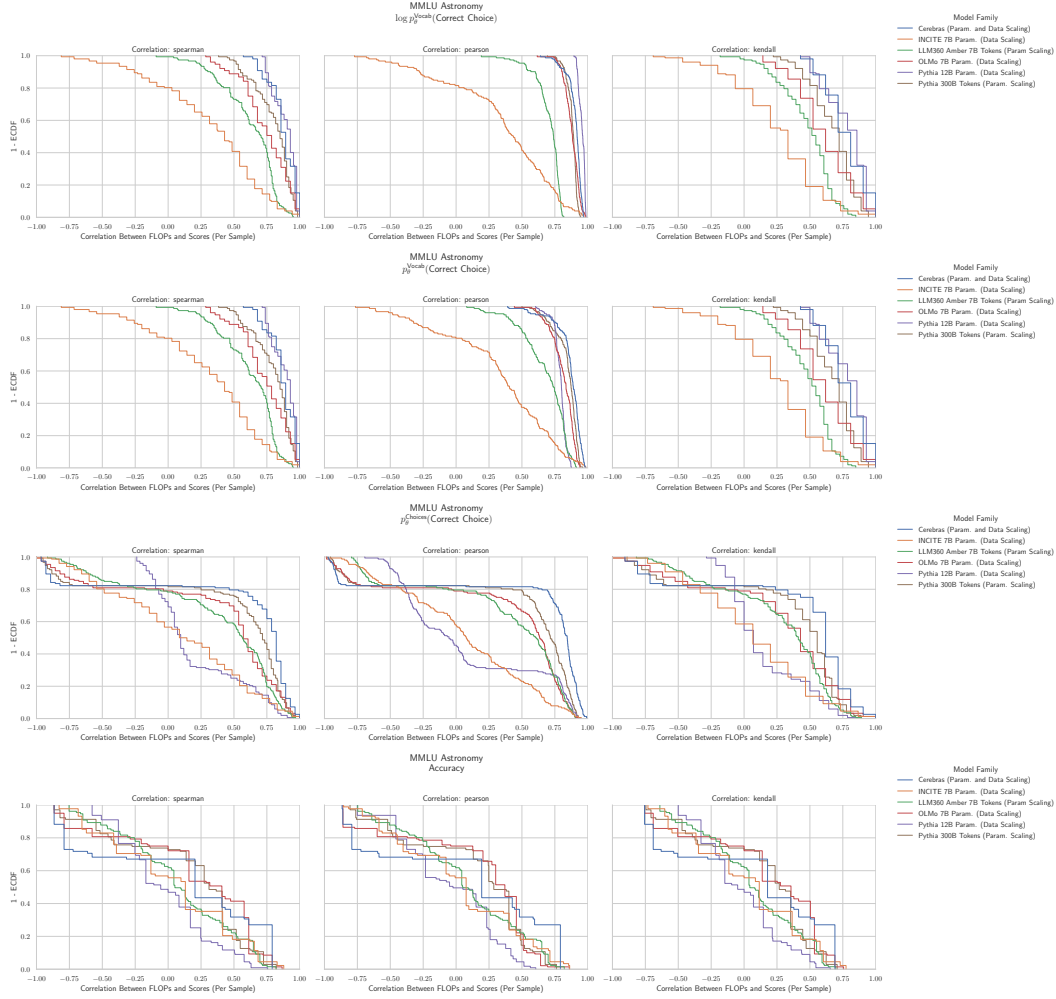
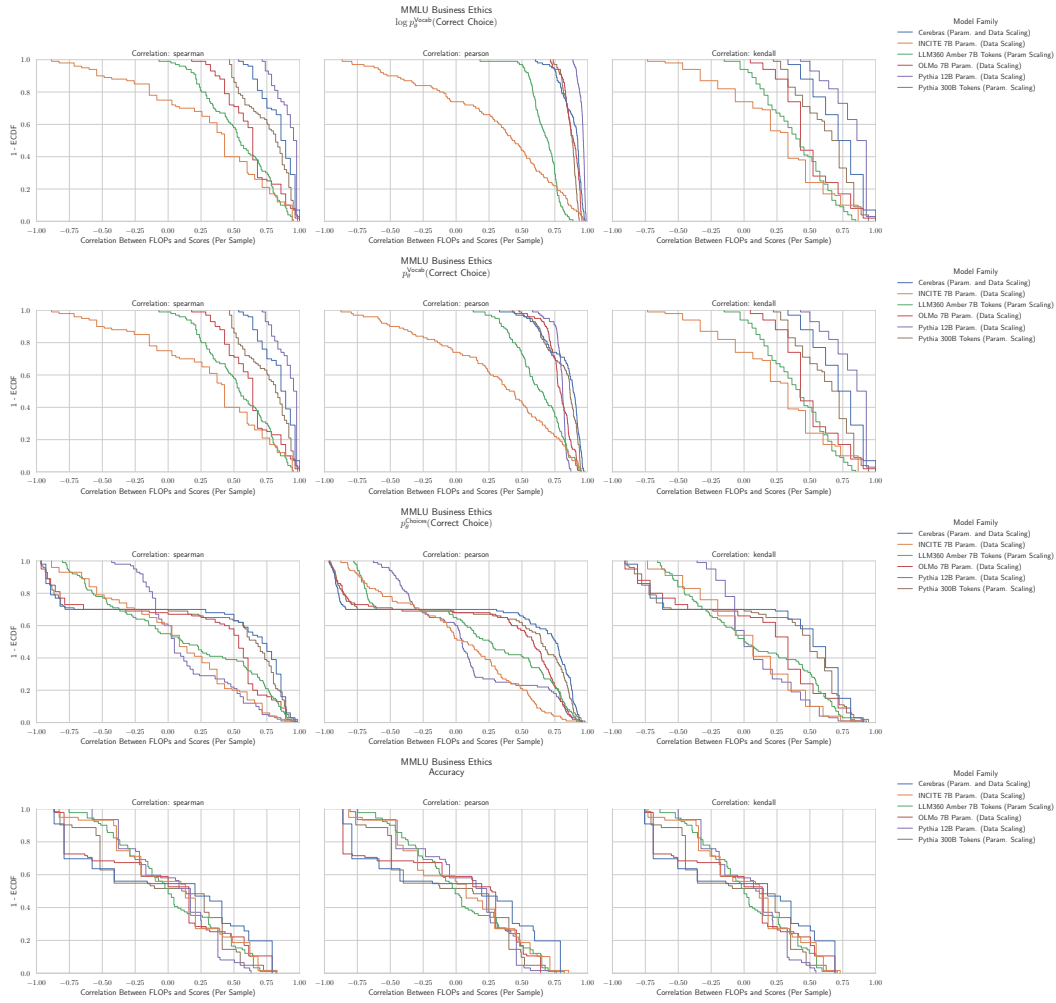
1674 G.8 NLP BENCHMARK: MMLU ASTRONOMY HENDRYCKS ET AL. (2020)
16751676
1677
1678
1679
1680
1681
1682
1683
1684
1685
1686
1687
1688
1689
1690
1691
1692
1693
1694
1695
1696
1697
1698
1699
1700
1701
1702
1703
1704
1705
1706
1707
1708
1709
1710
1711
1712
1713
1714
1715
1716
1717
1718
1719
1720
1721
1722
1723
1724
1725
1726
1727

Figure 17: MMLU Astronomy: Downstream performance is computed via a sequence of transformations that deteriorate correlations between scores and pretraining compute.

1728 G.9 NLP BENCHMARK: MMLU BUSINESS ETHICS HENDRYCKS ET AL. (2020)
17291763 Figure 18: MMLU Business Ethics: Downstream performance is computed via a sequence of
1764 transformations that deteriorate correlations between scores and pretraining compute.

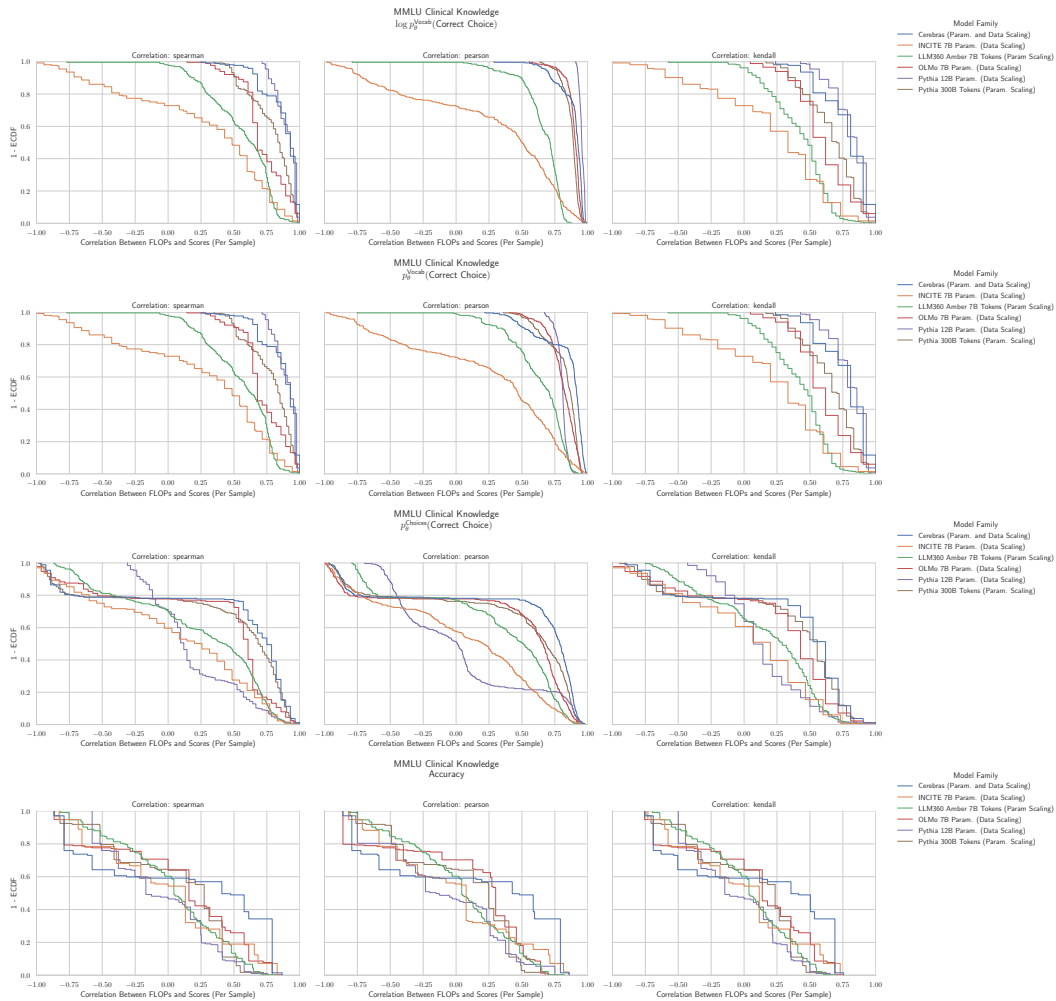
1782 G.10 NLP BENCHMARK: MMLU CLINICAL KNOWLEDGE HENDRYCKS ET AL. (2020)
17831784
1785
1786
1787
1788
1789
1790
1791
1792
1793
1794
1795
1796
1797
1798
1799
1800
1801
1802
1803
1804
1805
1806
1807
1808
1809
1810
1811
1812
1813
1814
1815
1816
1817
1818
1819
1820
1821
1822
1823
1824
1825
1826
1827
1828
1829
1830
1831
1832
1833
1834
1835

Figure 19: MMLU Clinical Knowledge: Downstream performance is computed via a sequence of transformations that deteriorate correlations between scores and pretraining compute.

1836
1837

G.11 NLP BENCHMARK: MMLU COLLEGE BIOLOGY HENDRYCKS ET AL. (2020)

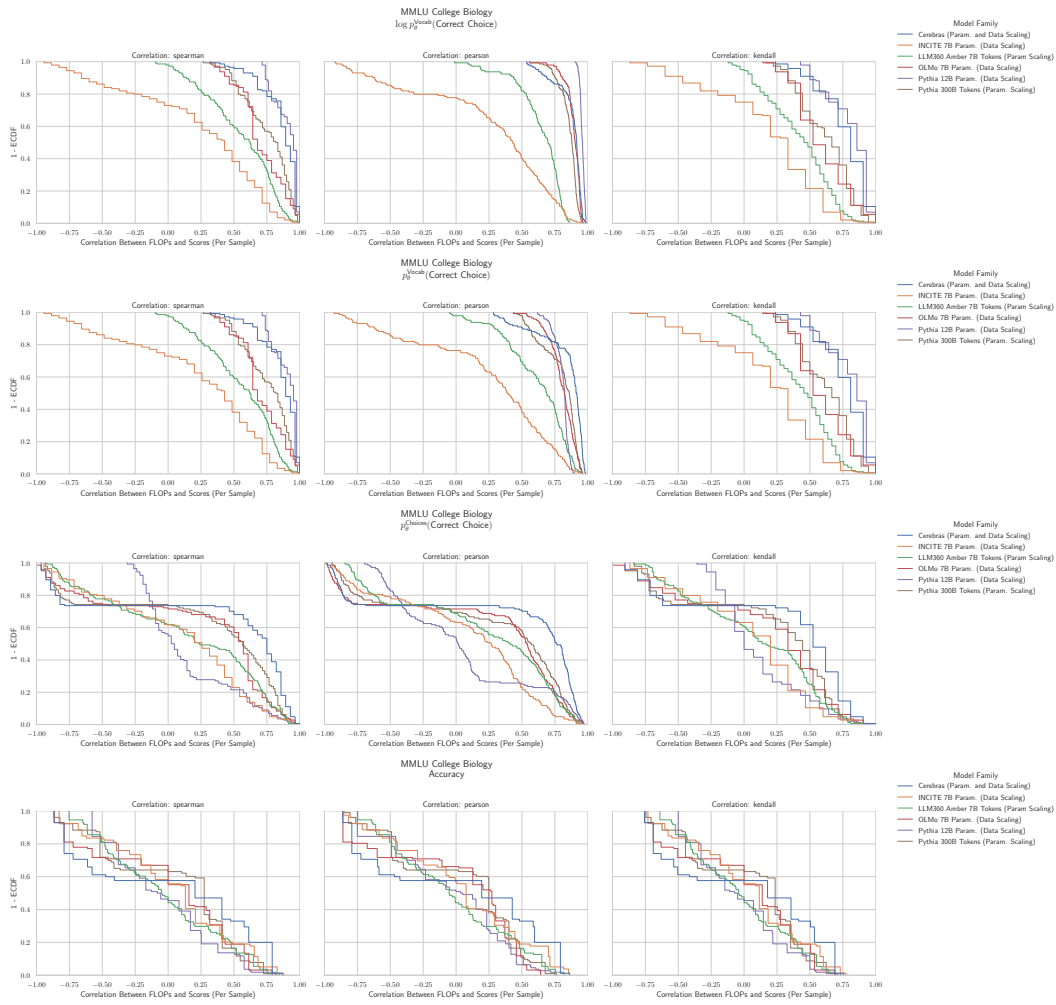
1838
1839

Figure 20: MMLU College Biology: Downstream performance is computed via a sequence of transformations that deteriorate correlations between scores and pretraining compute.

1870

1871

1872

1873

1874

1875

1876

1877

1878

1879

1880

1881

1882

1883

1884

1885

1886

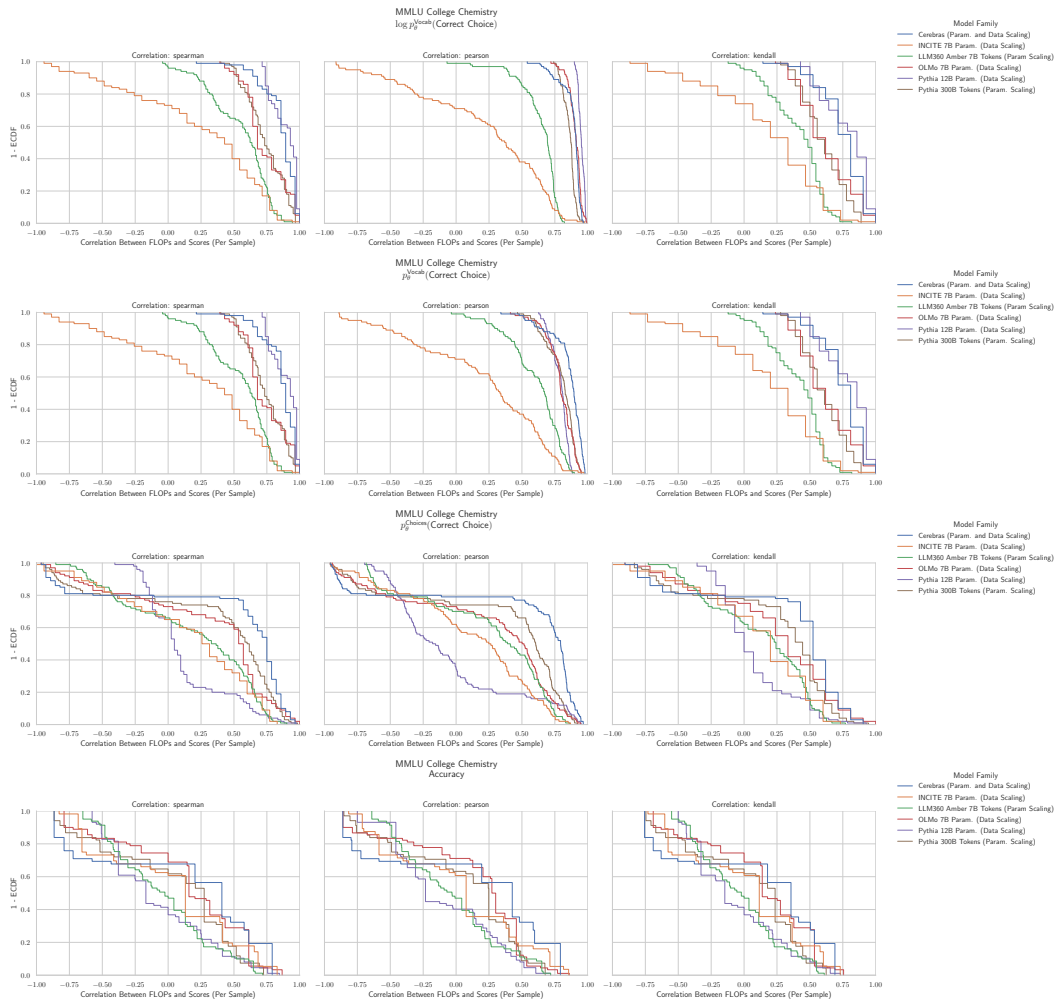
1887

1888

1889

1890
1891
1892
1893

G.12 NLP BENCHMARK: MMLU COLLEGE CHEMISTRY HENDRYCKS ET AL. (2020)

1925 **Figure 21: MMLU College Chemistry: Downstream performance is computed via a sequence of**
1926 **transformations that deteriorate correlations between scores and pretraining compute.**1927
1928
1929
1930
1931
1932
1933
1934
1935
1936
1937
1938
1939
1940
1941
1942
1943

1944
1945
1946
1947
1948
1949
1950
1951
1952
1953
1954
1955
1956
1957
1958
1959
1960
1961
1962
1963
1964
1965
1966
1967
1968
1969
1970
1971
1972
1973
1974
1975
1976
1977
1978
1979
1980
1981
1982
1983
1984
1985
1986
1987
1988
1989
1990
1991
1992
1993
1994
1995
1996
1997

G.13 NLP BENCHMARK: MMLU COLLEGE COMPUTER SCIENCE HENDRYCKS ET AL. (2020)

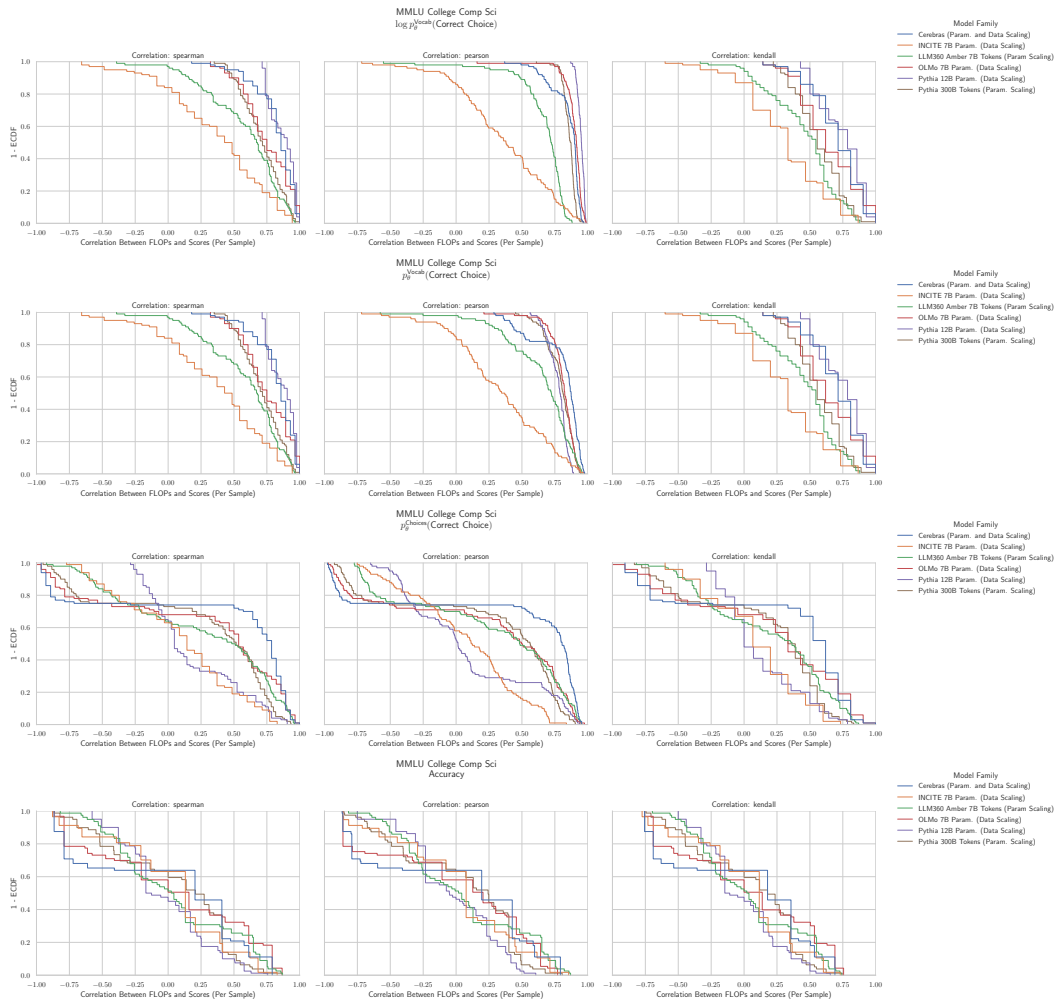


Figure 22: MMLU College Computer Science: Downstream performance is computed via a sequence of transformations that deteriorate correlations between scores and pretraining compute.

1998
1999

G.14 NLP BENCHMARK: MMLU COLLEGE MATHEMATICS HENDRYCKS ET AL. (2020)

2000

2001

2002

2003

2004

2005

2006

2007

2008

2009

2010

2011

2012

2013

2014

2015

2016

2017

2018

2019

2020

2021

2022

2023

2024

2025

2026

2027

2028

2029

2030

2031

2032

2033

2034

2035

2036

2037

2038

2039

2040

2041

2042

2043

2044

2045

2046

2047

2048

2049

2050

2051

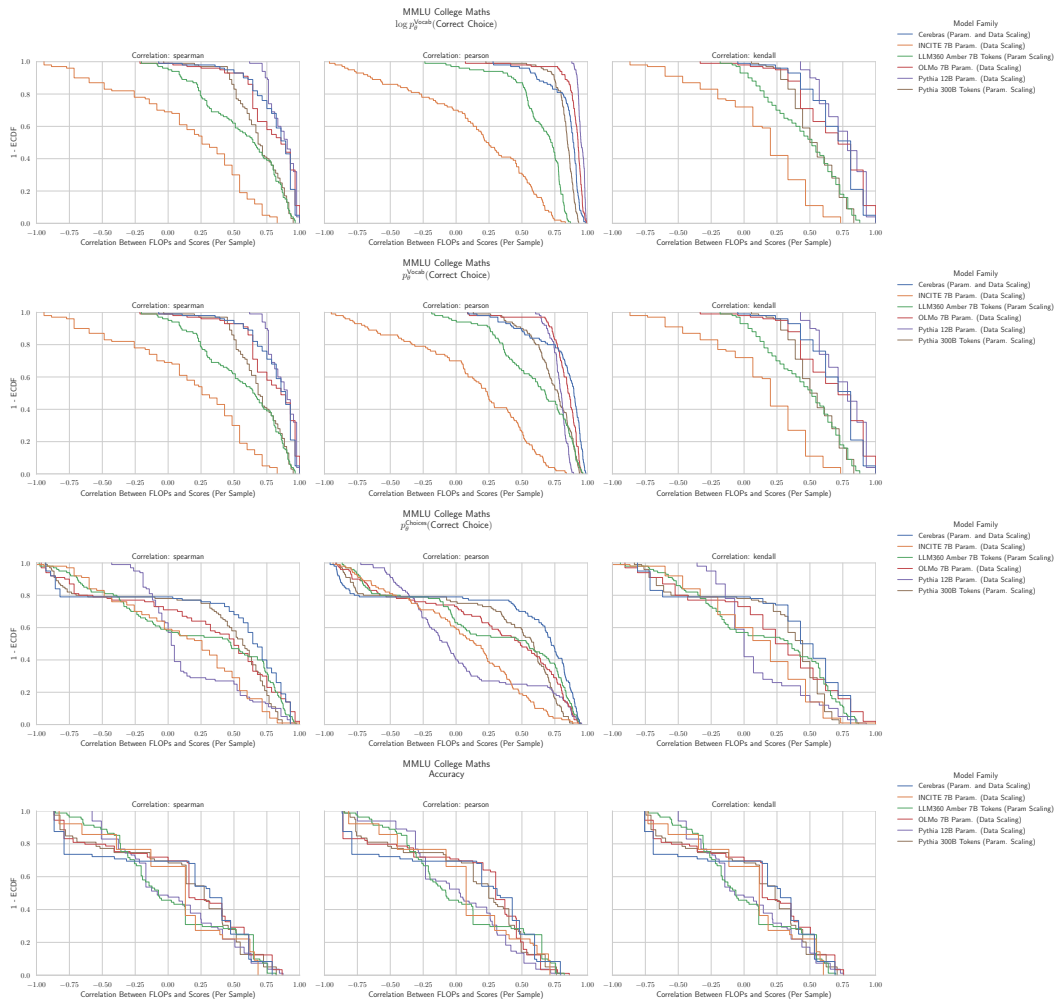


Figure 23: MMLU College Mathematics: Downstream performance is computed via a sequence of transformations that deteriorate correlations between scores and pretraining compute.

2052
2053

G.15 NLP BENCHMARK: MMLU COLLEGE MEDICINE HENDRYCKS ET AL. (2020)

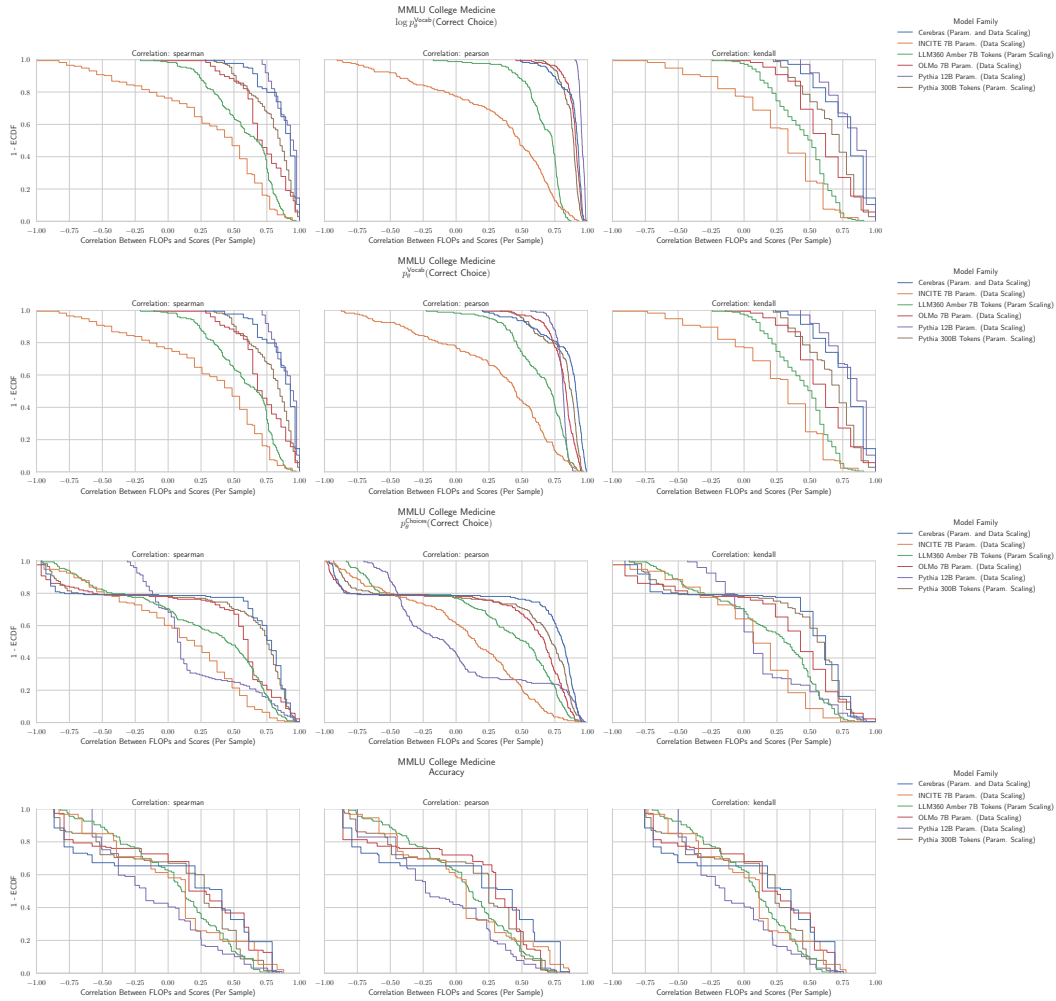
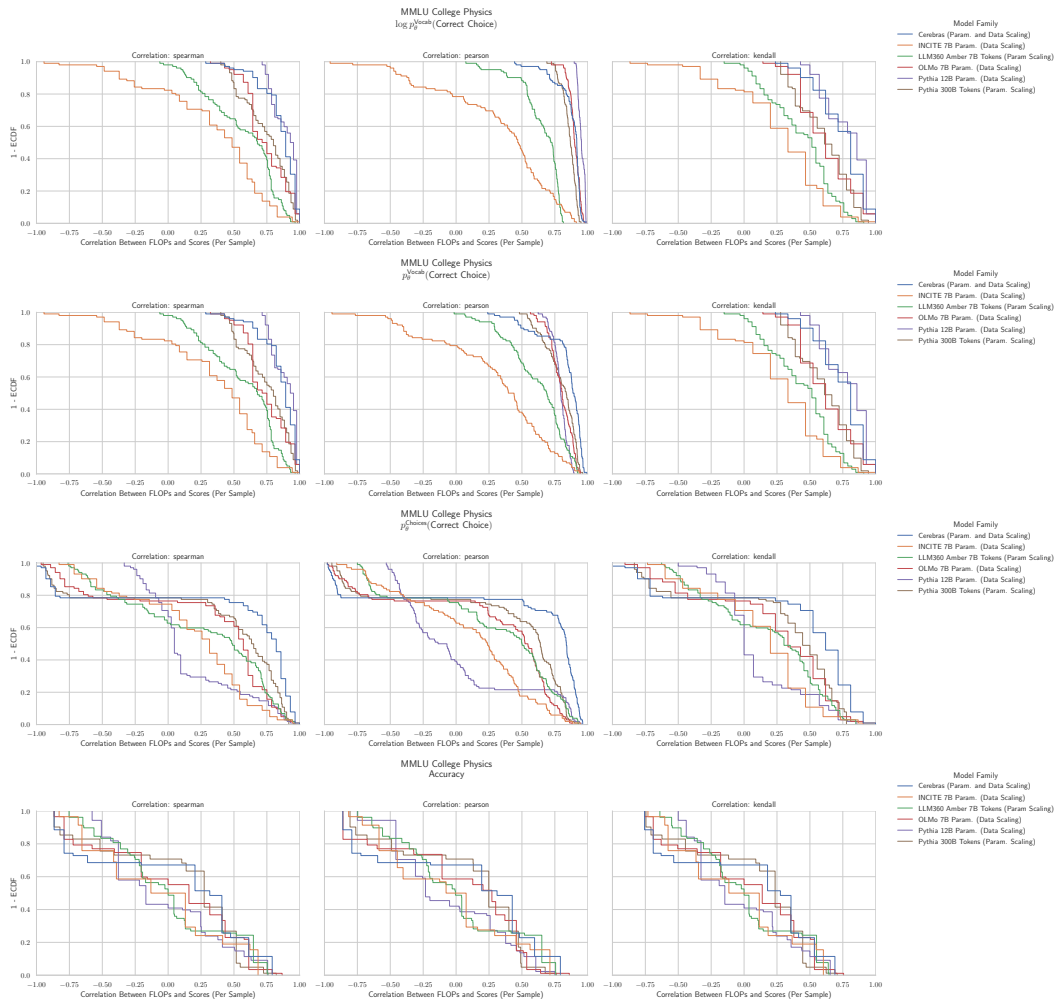
2054
2055

Figure 24: MMLU College Medicine: Downstream performance is computed via a sequence of transformations that deteriorate correlations between scores and pretraining compute.

2090
2091
2092
2093
2094
2095
2096
2097
2098
2099
2100
2101
2102
2103
2104
2105

2106
2107

G.16 NLP BENCHMARK: MMLU COLLEGE PHYSICS HENDRYCKS ET AL. (2020)

2108
21092110
2111
2112
2113
2114
2115
2116
2117
2118
2119
2120
2121
2122
2123
2124
2125
2126
2127
2128
2129
2130
2131
2132
2133
2134
2135
2136
2137
2138
2139
2140
2141
2142
2143
2144
2145
2146
2147
2148
2149
2150
2151
2152
2153
2154
2155
2156
2157
2158
2159Figure 25: **MMLU College Physics: Downstream performance is computed via a sequence of transformations that deteriorate correlations between scores and pretraining compute.**

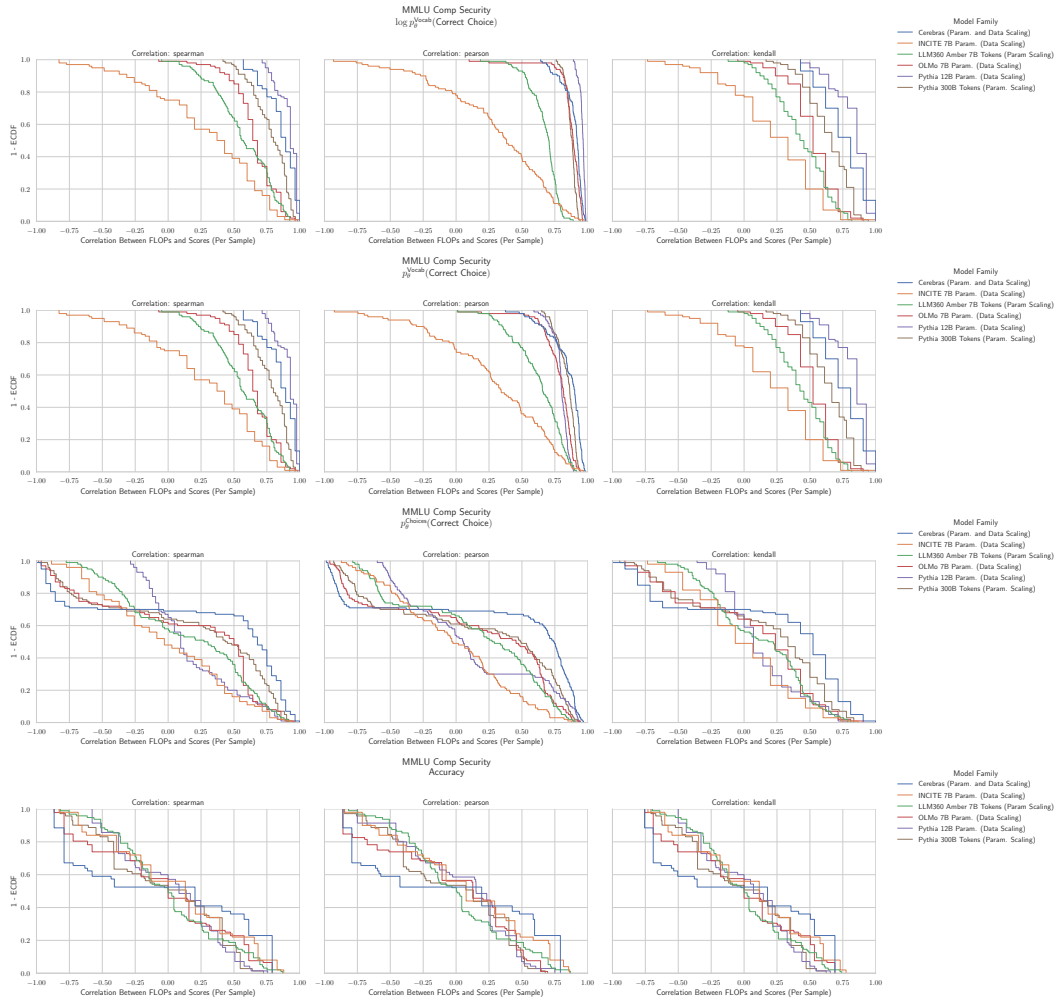
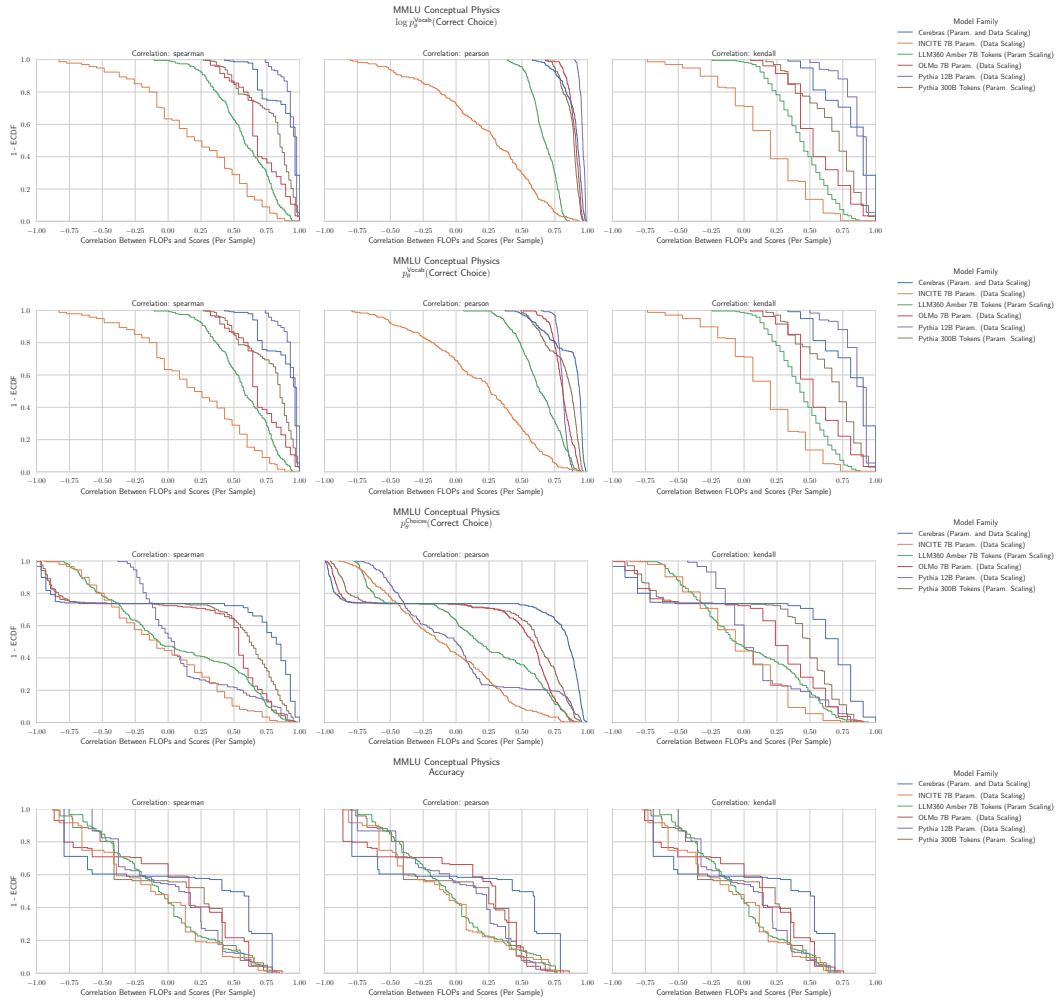
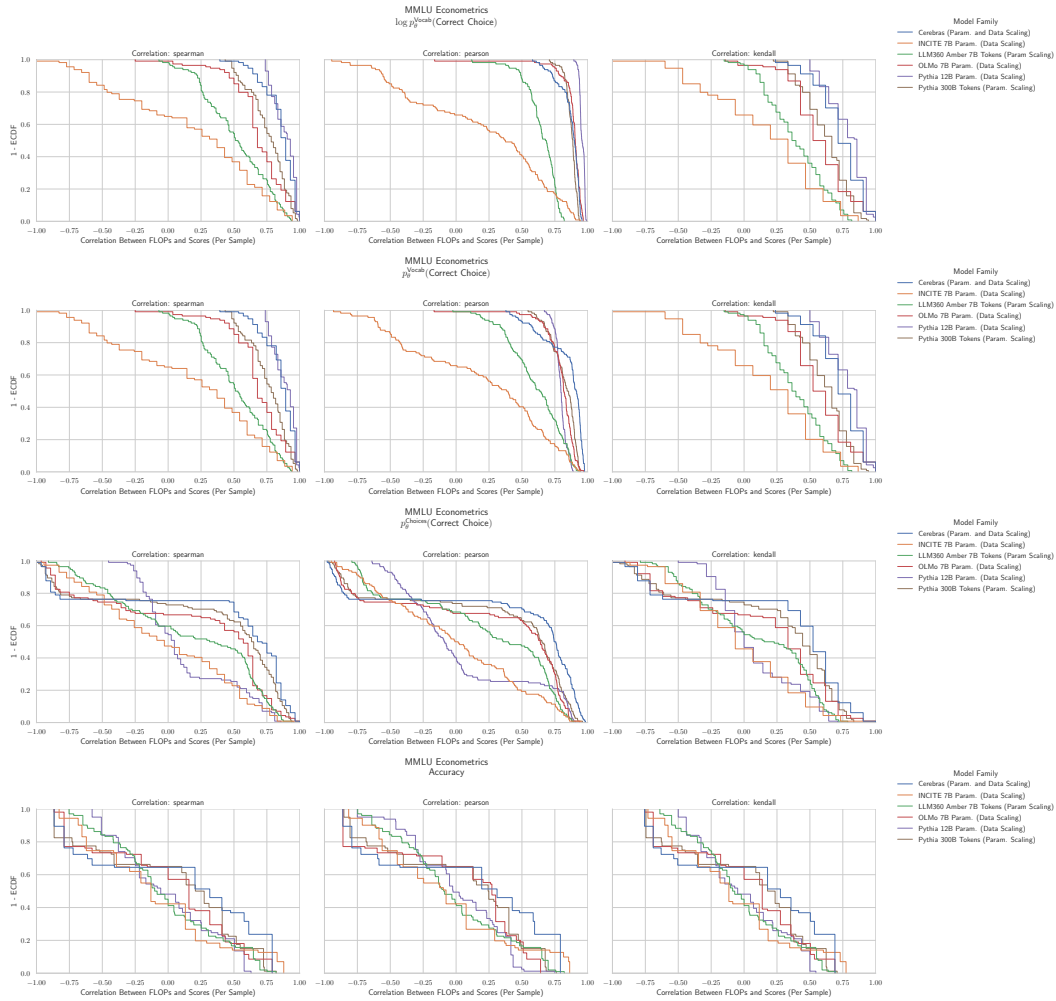
2160 G.17 NLP BENCHMARK: MMLU COMPUTER SECURITY HENDRYCKS ET AL. (2020)
21612162
2163
2164
2165
2166
2167
2168
2169
2170
2171
2172
2173
2174
2175
2176
2177
2178
2179
2180
2181
2182
2183
2184
2185
2186
2187
2188
2189
2190
2191
2192
2193
2194
2195
2196
2197
2198
2199
2200
2201
2202
2203
2204
2205
2206
2207
2208
2209
2210
2211
2212
2213

Figure 26: MMLU Computer Security: Downstream performance is computed via a sequence of transformations that deteriorate correlations between scores and pretraining compute.

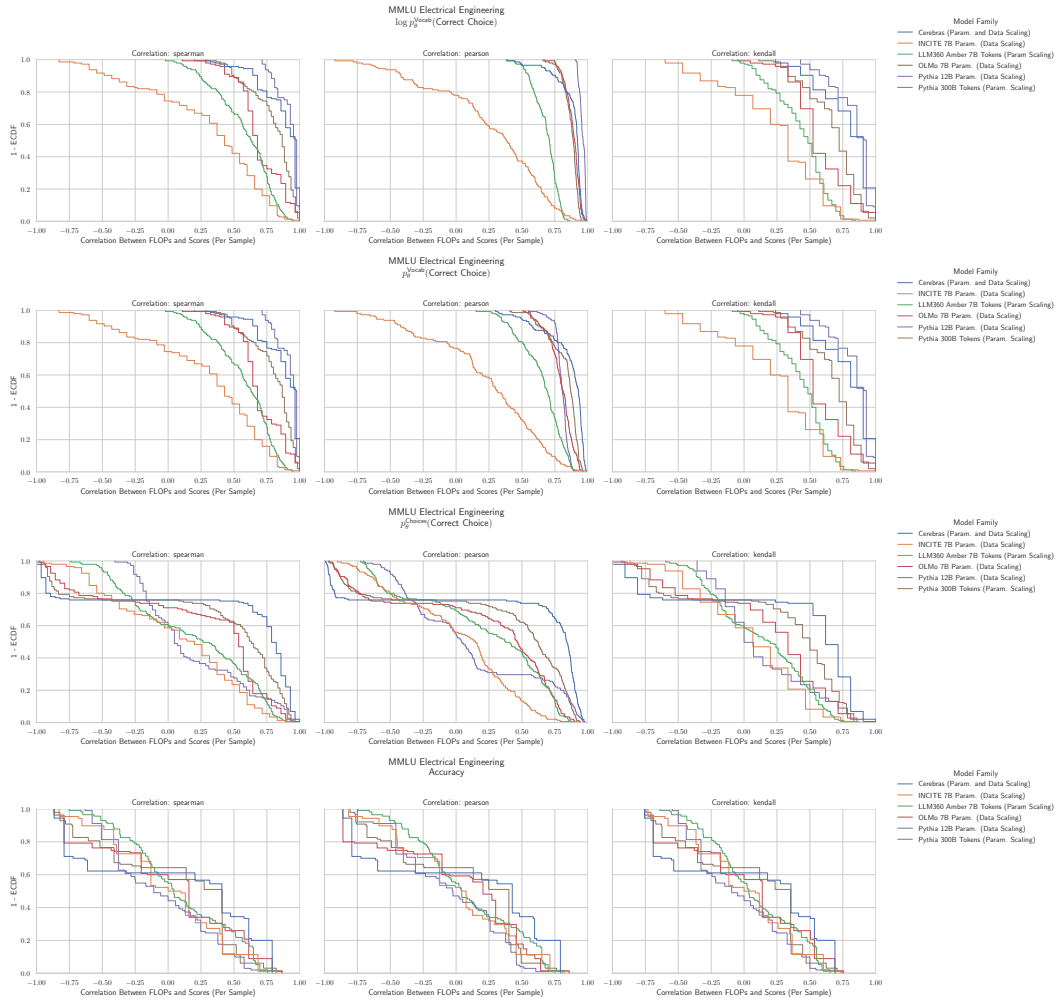
2214 G.18 NLP BENCHMARK: MMLU CONCEPTUAL PHYSICS HENDRYCKS ET AL. (2020)
22152249 **Figure 27: MMLU Conceptual Physics: Downstream performance is computed via a sequence
2250 of transformations that deteriorate correlations between scores and pretraining compute.**

2251
2252
2253
2254
2255
2256
2257
2258
2259
2260
2261
2262
2263
2264
2265
2266
2267

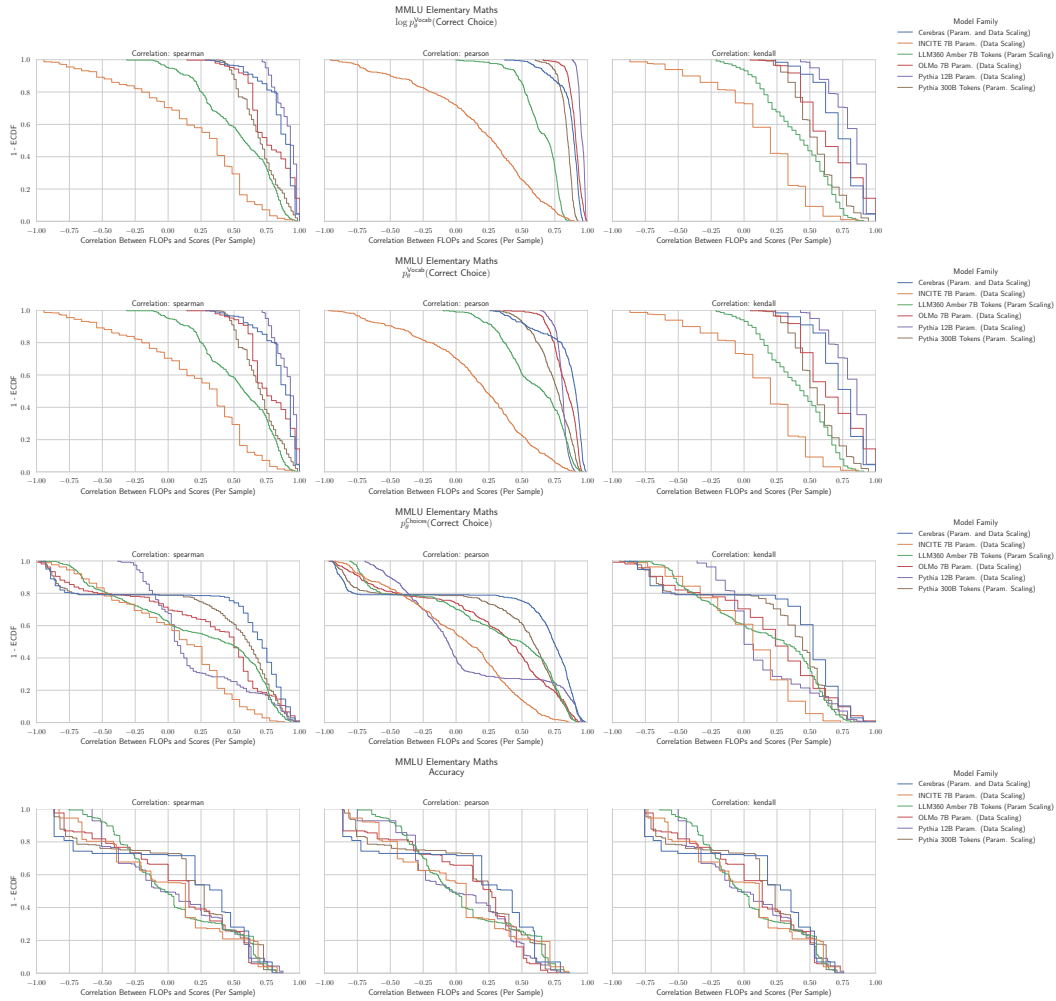
2268 G.19 NLP BENCHMARK: MMLU ECONOMETRICS HENDRYCKS ET AL. (2020)
22692303 **Figure 28: MMLU Econometrics: Downstream performance is computed via a sequence of
2304 transformations that deteriorate correlations between scores and pretraining compute.**
2305
2306
2307
2308
2309
2310
2311
2312
2313
2314
2315
2316
2317
2318
2319
2320
2321

2322
2323

G.20 NLP BENCHMARK: MMLU ELECTRICAL ENGINEERING HENDRYCKS ET AL. (2020)

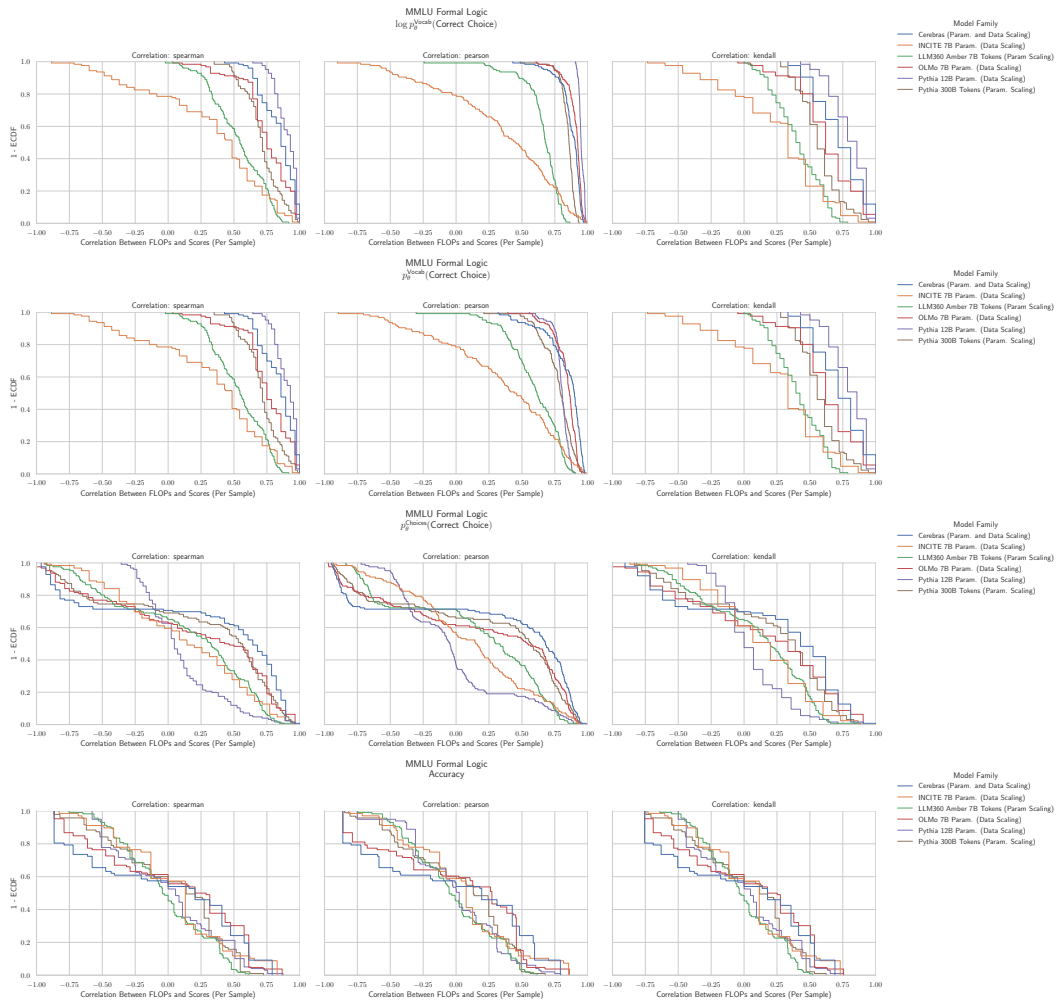
2324
2325Figure 29: **MMLU Electrical Engineering: Downstream performance is computed via a sequence of transformations that deteriorate correlations between scores and pretraining compute.**2357
2358
2359
2360
2361
2362
2363
2364
2365
2366
2367
2368
2369
2370
2371
2372
2373
2374
2375

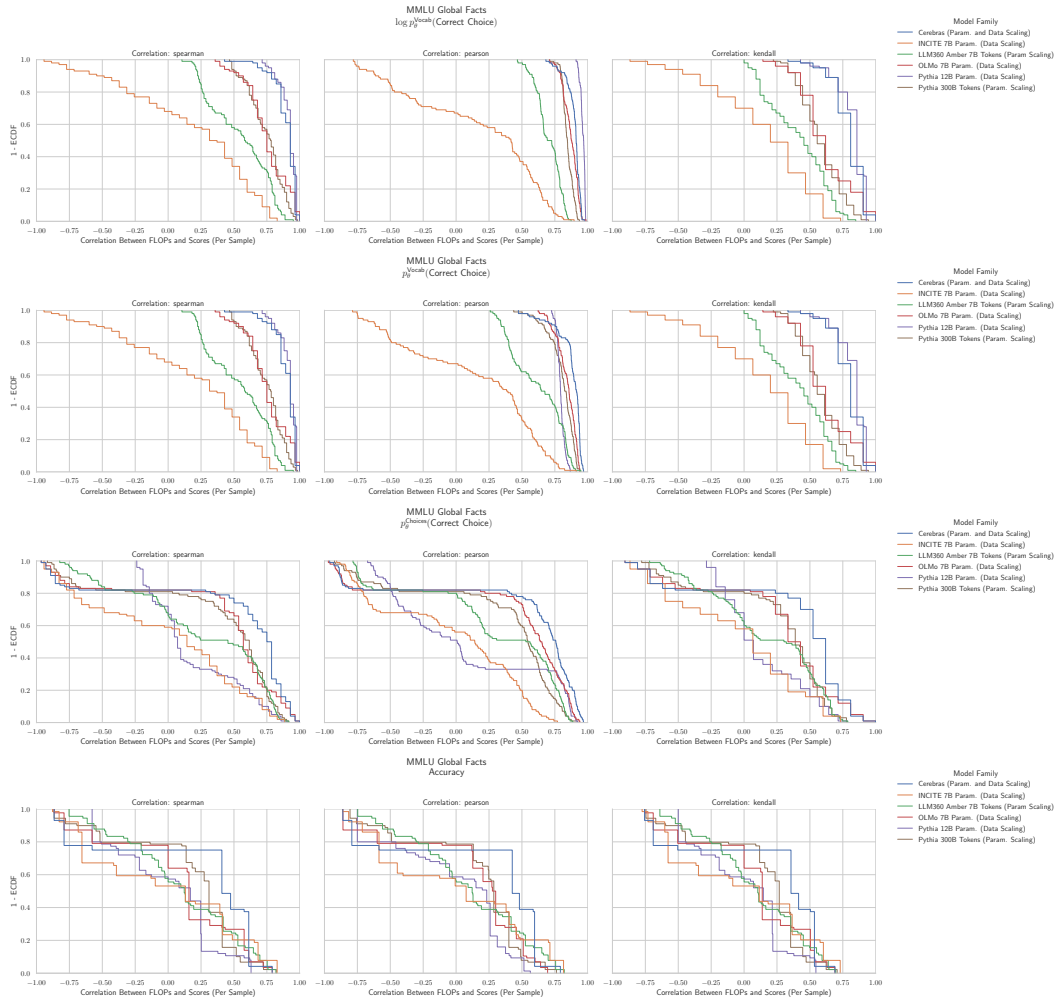
2376 **G.21 NLP BENCHMARK: MMLU ELEMENTARY MATHEMATICS HENDRYCKS ET AL. (2020)**
 2377



2411 **Figure 30: MMLU Elementary Mathematics: Downstream performance is computed via a**
 2412 **sequence of transformations that deteriorate correlations between scores and pretraining**
 2413 **compute.**

2414
 2415
 2416
 2417
 2418
 2419
 2420
 2421
 2422
 2423
 2424
 2425
 2426
 2427
 2428
 2429

2430
2431 G.22 NLP BENCHMARK: MMLU FORMAL LOGIC HENDRYCKS ET AL. (2020)
24322445
2446
2447
2448
2449
2450
2451
2452
2453
2454
2455
2456
2457
2458
2459
2460
2461
2462
2463
2464
2465 Figure 31: **MMLU Formal Logic: Downstream performance is computed via a sequence of transformations that deteriorate correlations between scores and pretraining compute.**
2466
2467
2468
2469
2470
2471
2472
2473
2474
2475
2476
2477
2478
2479
2480
2481
2482
2483

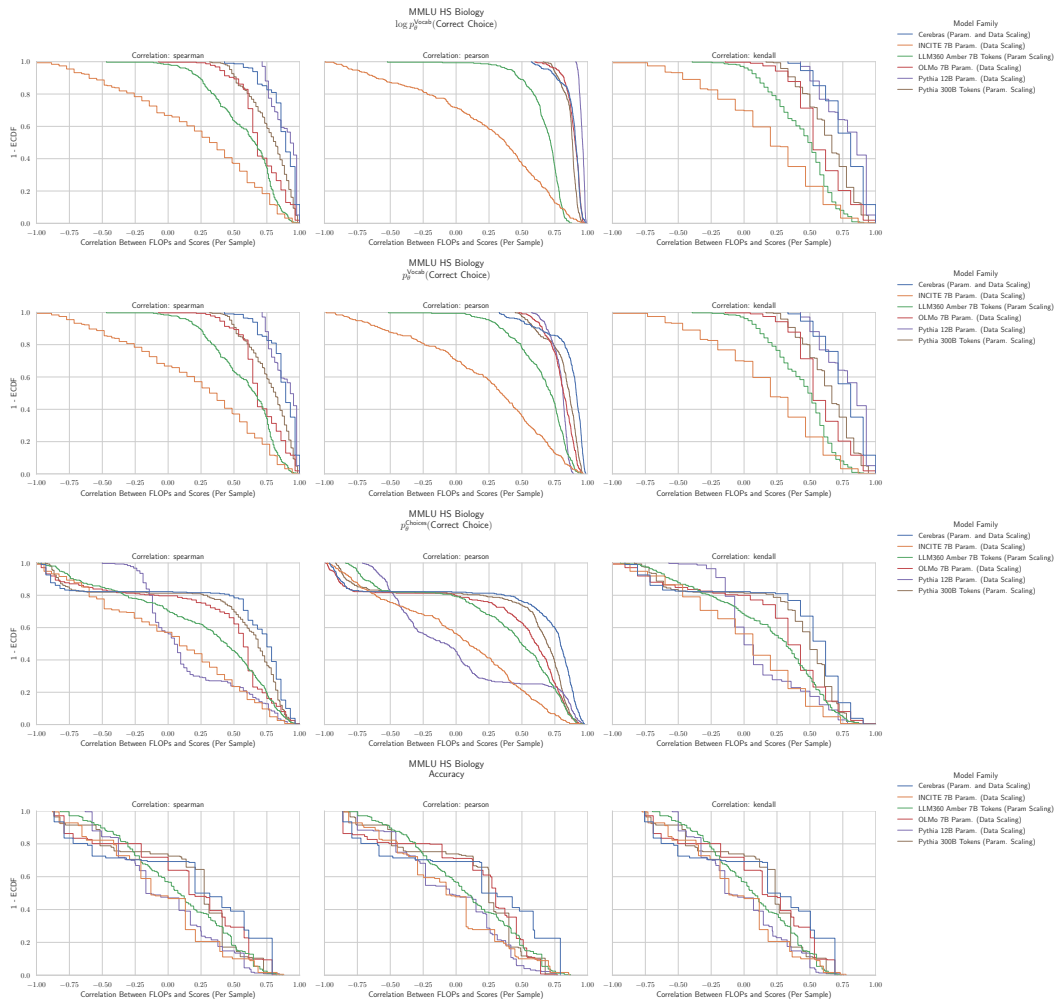
2484 G.23 NLP BENCHMARK: MMLU GLOBAL FACTS HENDRYCKS ET AL. (2020)
24852519 Figure 32: **MMLU Global Facts: Downstream performance is computed via a sequence of**
2520 **transformations that deteriorate correlations between scores and pretraining compute.**

2538
2539

G.24 NLP BENCHMARK: MMLU HIGH SCHOOL BIOLOGY HENDRYCKS ET AL. (2020)

2540

2541

Figure 33: **MMLU High School Biology:** Downstream performance is computed via a sequence of transformations that deteriorate correlations between scores and pretraining compute.

2572

2573

2574

2575

2576

2577

2578

2579

2580

2581

2582

2583

2584

2585

2586

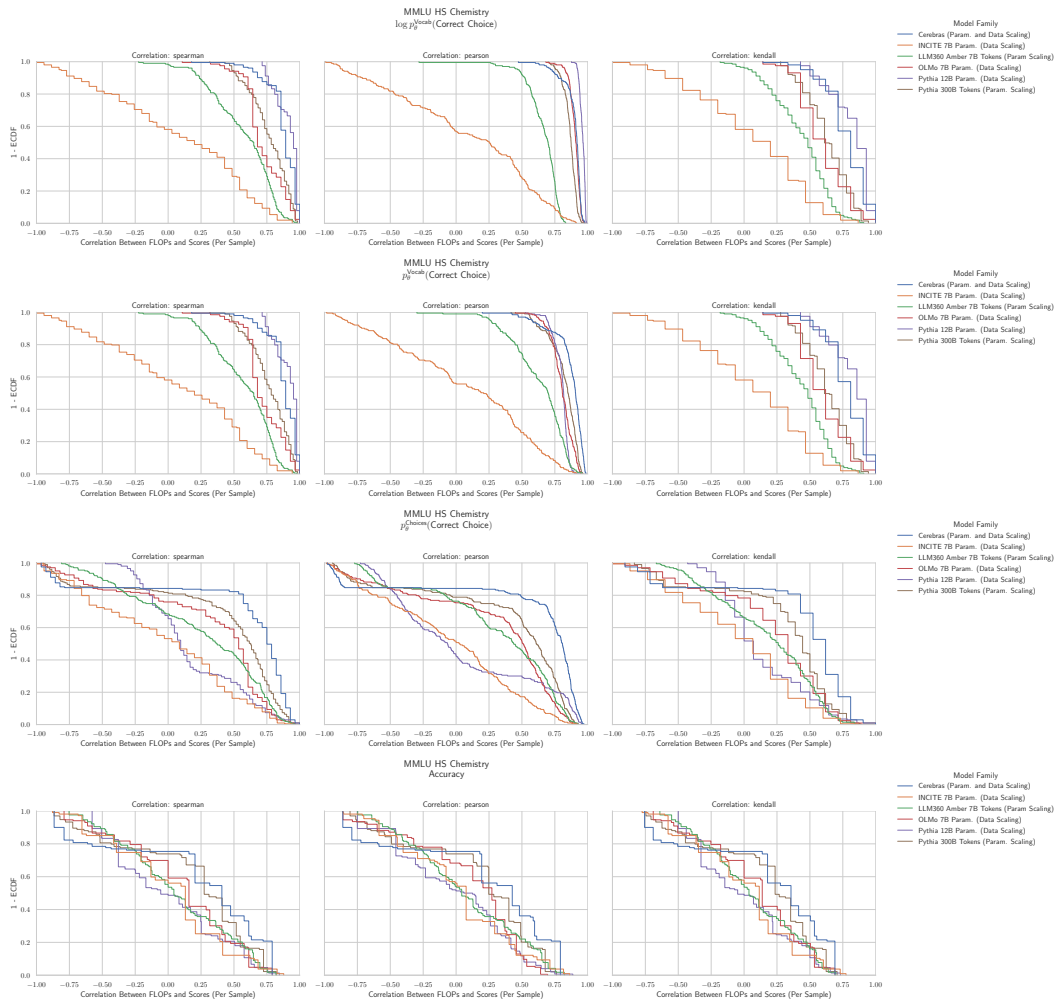
2587

2588

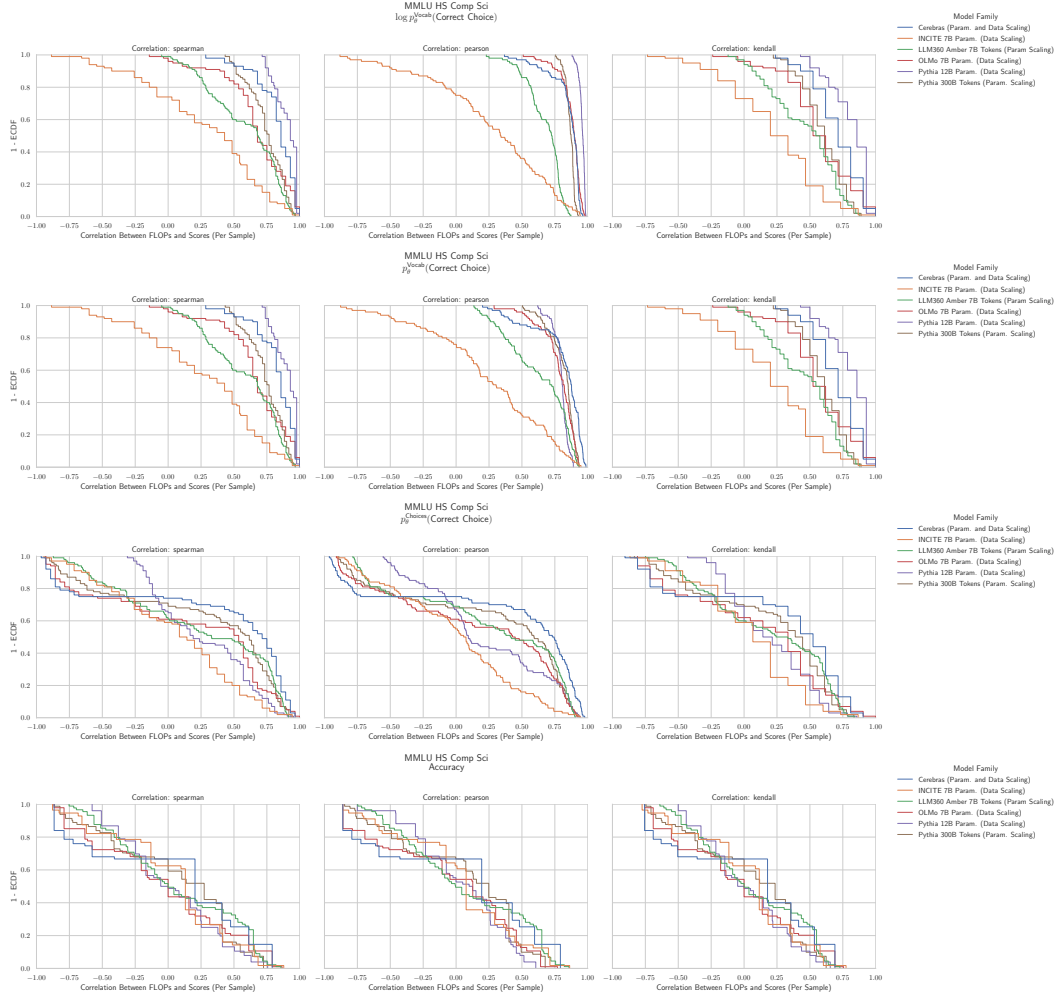
2589

2590

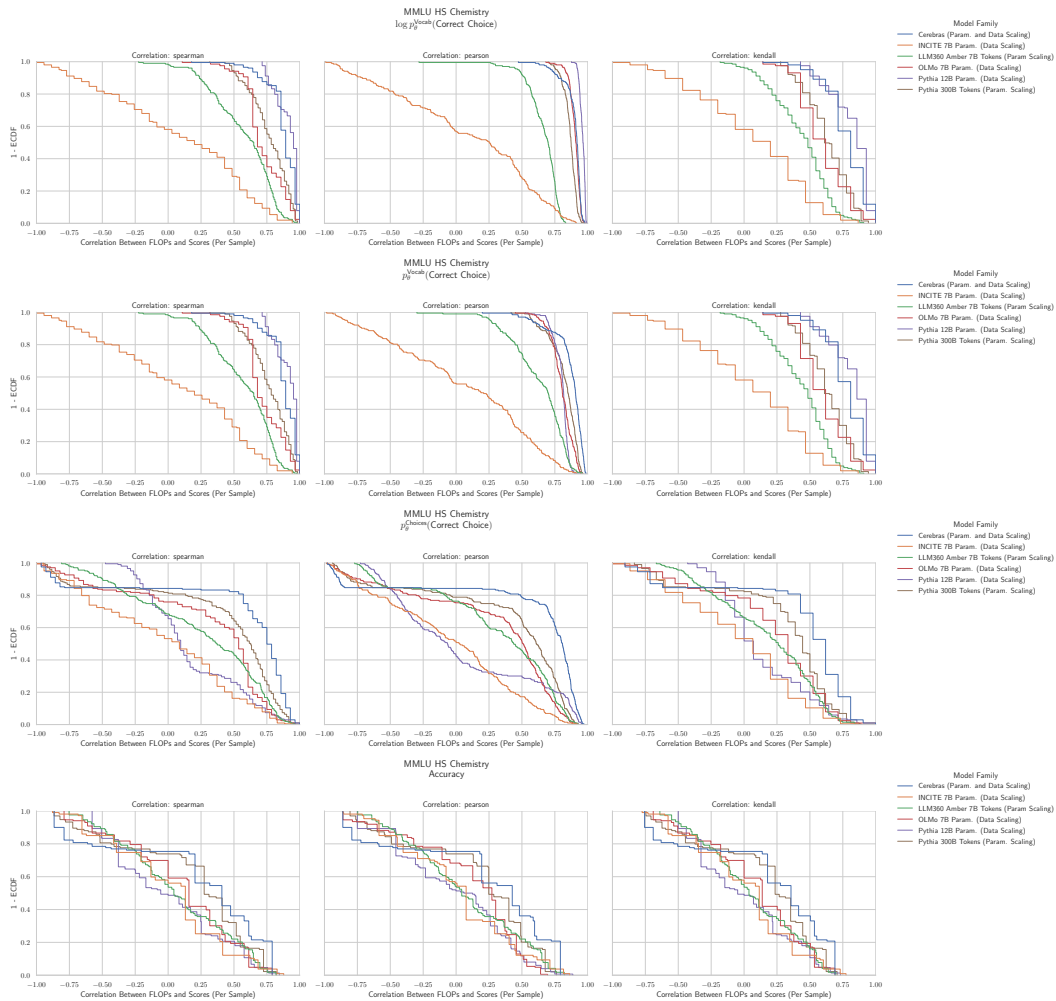
2591

2592 NLP BENCHMARK: MMLU HIGH SCHOOL CHEMISTRY HENDRYCKS ET AL. (2020)
25932627 **Figure 34: MMLU High School Chemistry: Downstream performance is computed via a
2628 sequence of transformations that deteriorate correlations between scores and pretraining
2629 compute.**

2646 **G.26 NLP BENCHMARK: MMLU HIGH SCHOOL COMPUTER SCIENCE HENDRYCKS ET AL.**
 2647 (**2020**)



2682 **Figure 35: MMLU High School Computer Science: Downstream performance is computed via
 2683 a sequence of transformations that deteriorate correlations between scores and pretraining
 2684 compute.**

2700 G.27 NLP BENCHMARK: MMLU HIGH SCHOOL CHEMISTRY HENDRYCKS ET AL. (2020)
27012735 **Figure 36: MMLU High School Chemistry: Downstream performance is computed via a
2736 sequence of transformations that deteriorate correlations between scores and pretraining
2737 compute.**
2738
2739
2740
2741
2742
2743
2744
2745
2746
2747
2748
2749
2750
2751
2752
2753

2754
2755
2756

G.28 NLP BENCHMARK: MMLU HIGH SCHOOL EUROPEAN HISTORY HENDRYCKS ET AL. (2020)

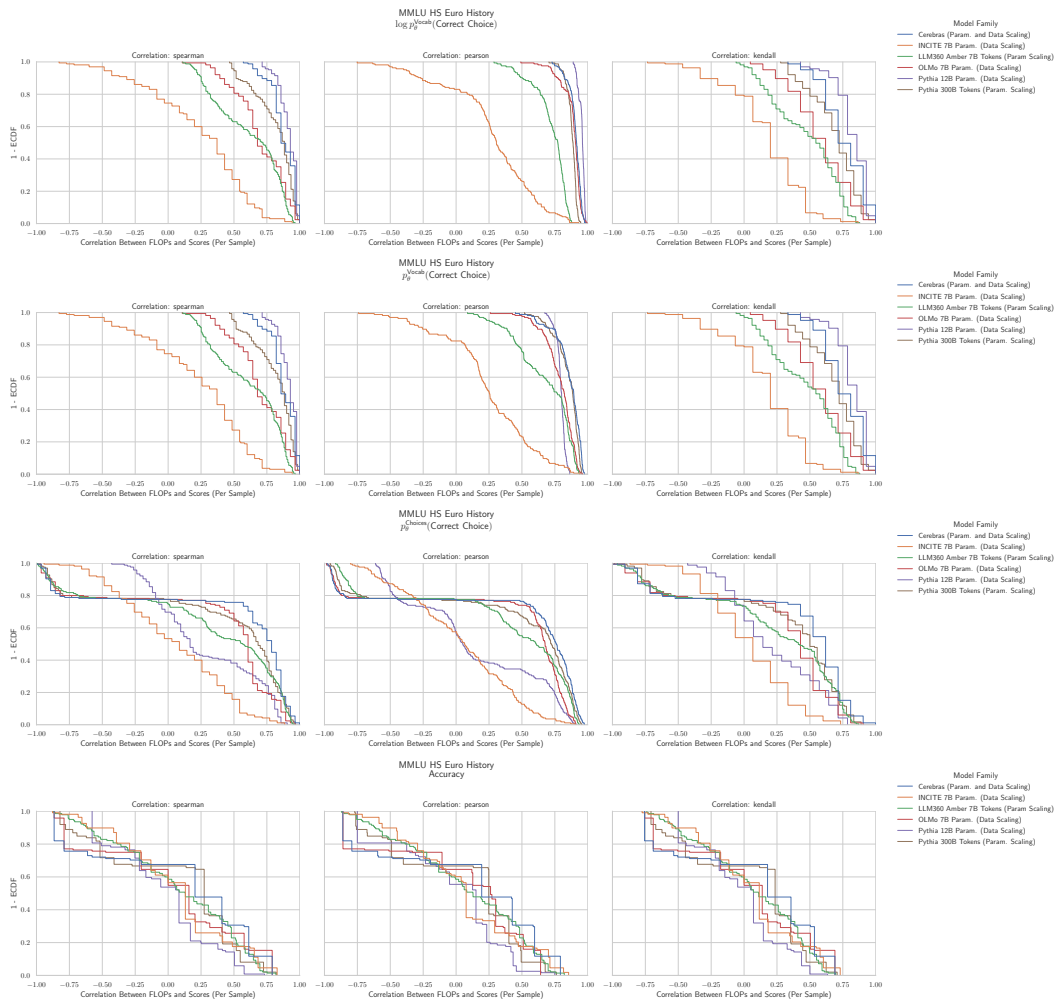
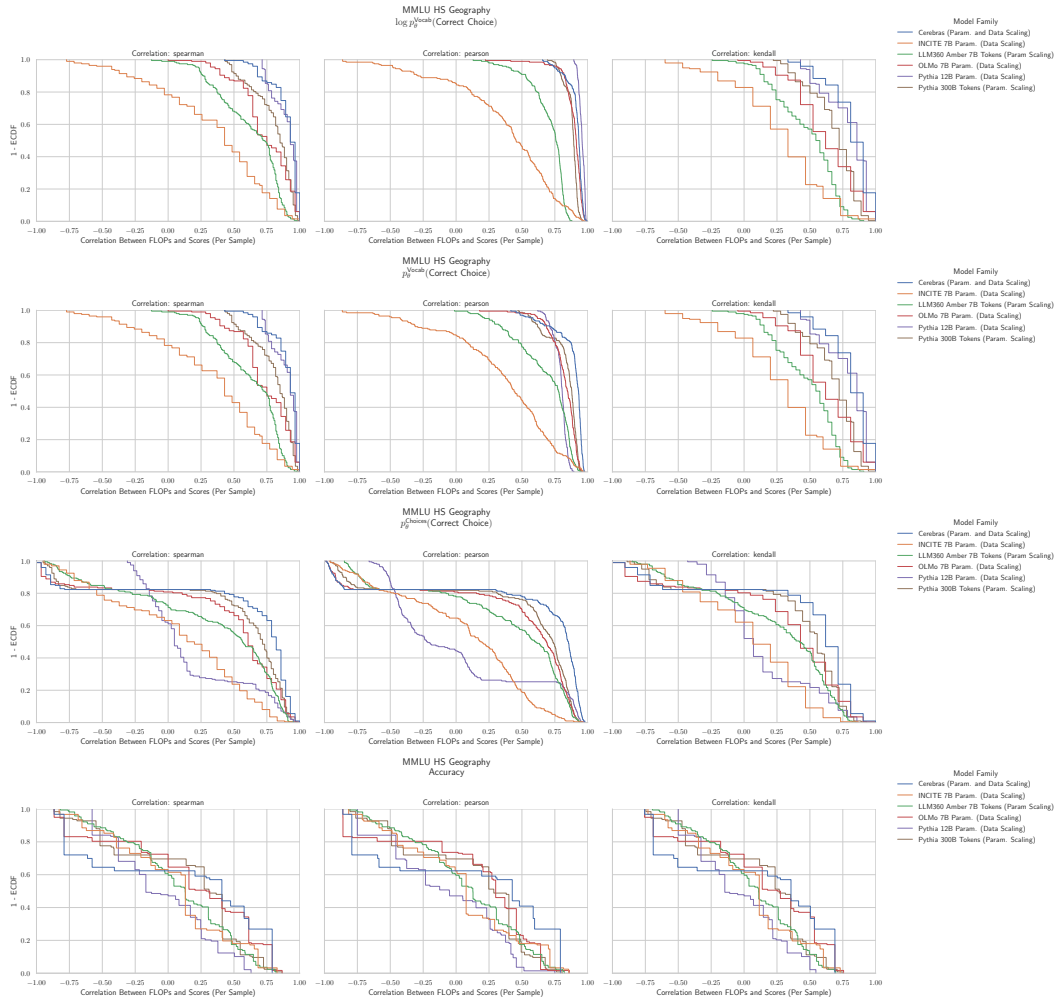
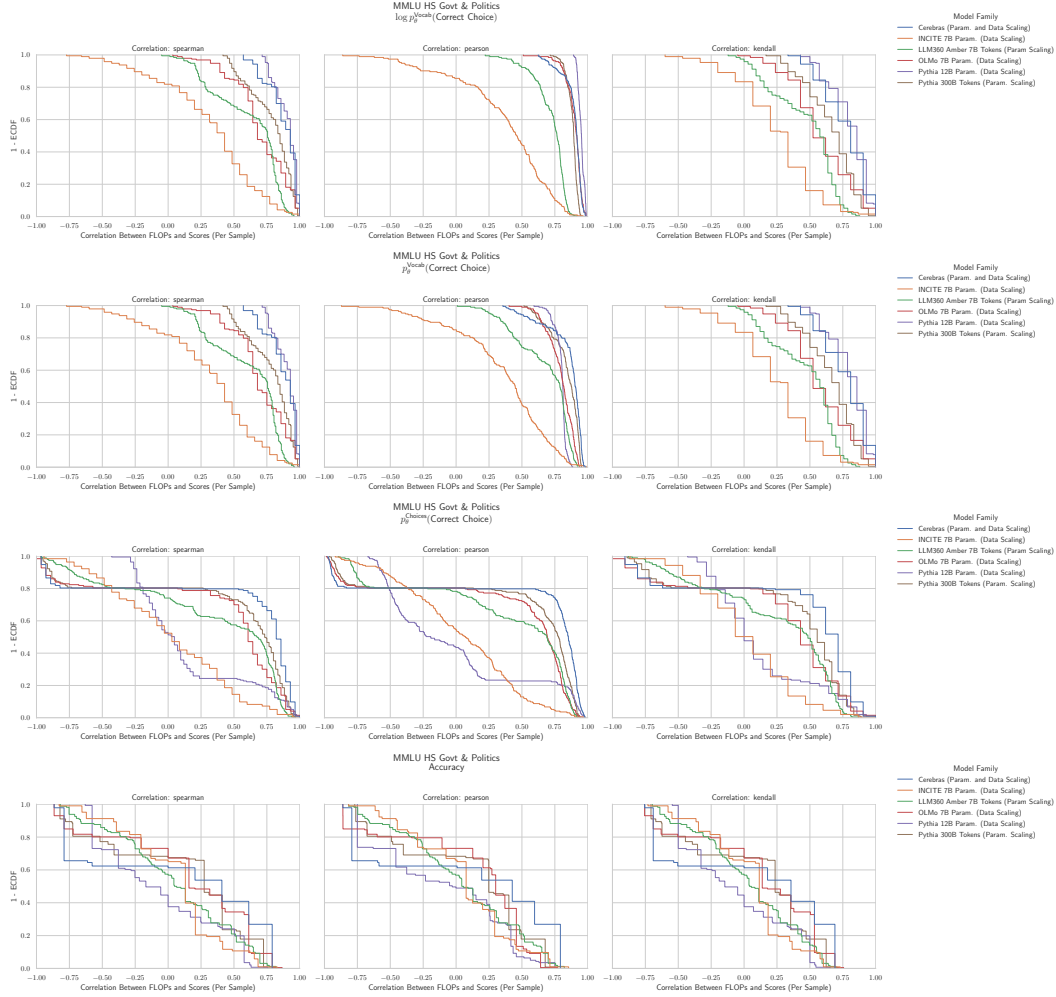


Figure 37: MMLU High School European History: Downstream performance is computed via a sequence of transformations that deteriorate correlations between scores and pretraining compute.

2793
2794
2795
2796
2797
2798
2799
2800
2801
2802
2803
2804
2805
2806
2807

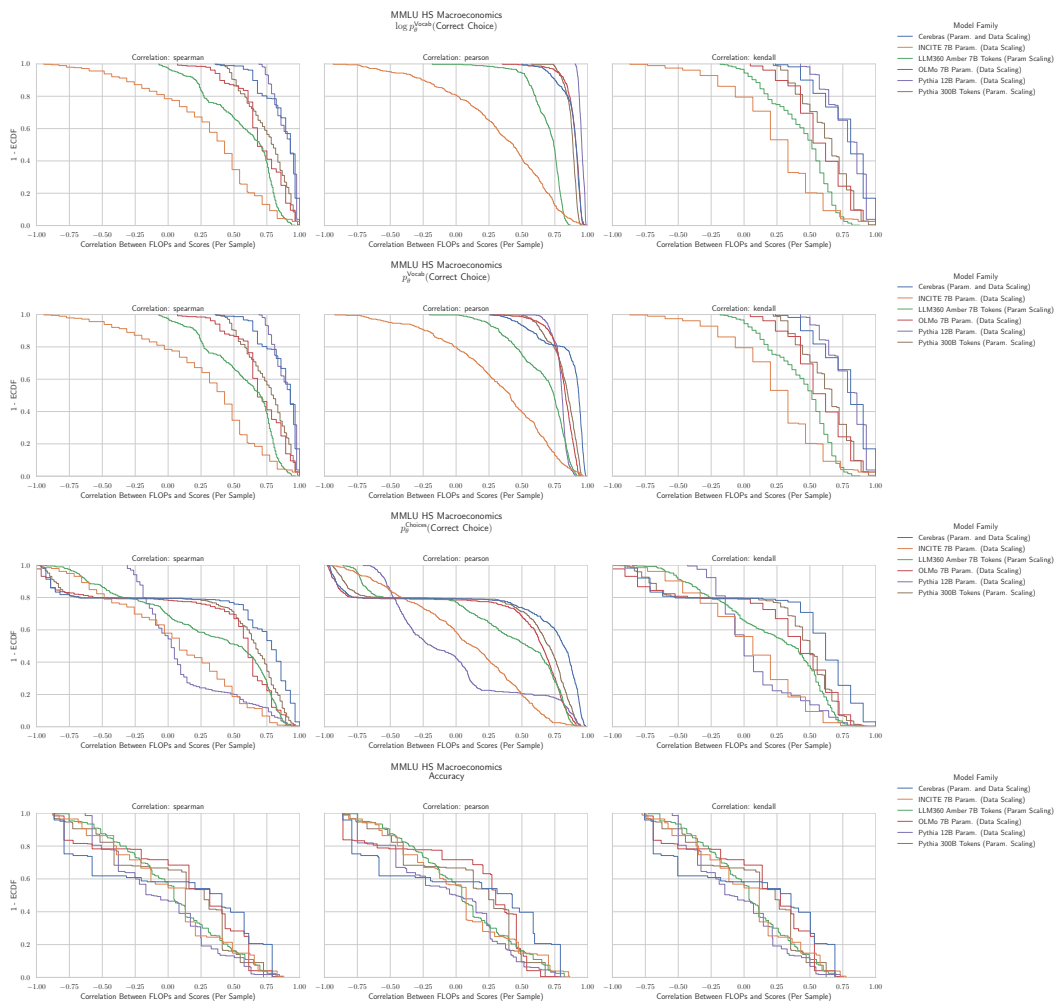
2808 G.29 NLP BENCHMARK: MMLU HIGH SCHOOL GEOGRAPHY HENDRYCKS ET AL. (2020)
28092843 **Figure 38: MMLU High School Geography: Downstream performance is computed via a
2844 sequence of transformations that deteriorate correlations between scores and pretraining
2845 compute.**

2862 G.30 NLP BENCHMARK: MMLU HIGH SCHOOL GOVERNMENT & POLITICS HENDRYCKS
 2863 ET AL. (2020)

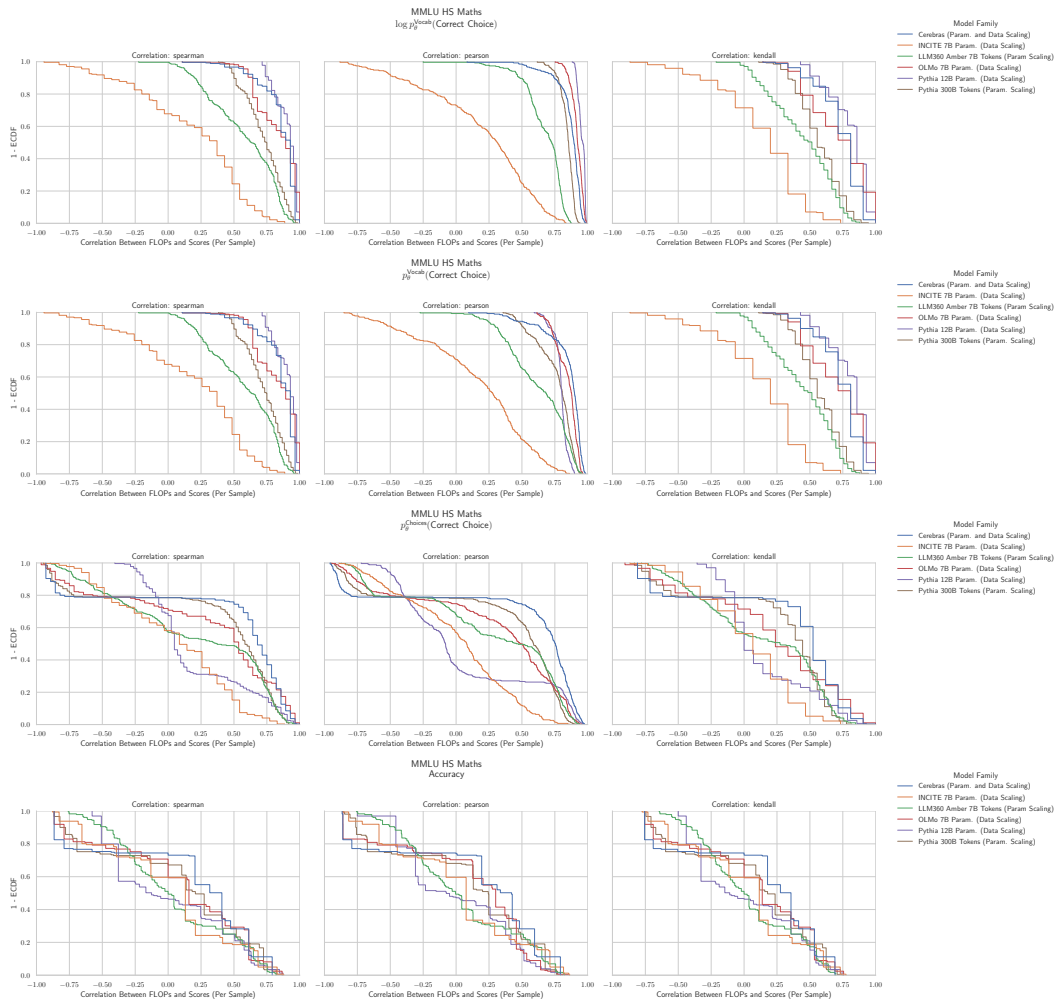


2898 **Figure 39: MMLU High School Government & Politics: Downstream performance is computed
 2899 via a sequence of transformations that deteriorate correlations between scores and pretraining
 2900 compute.**

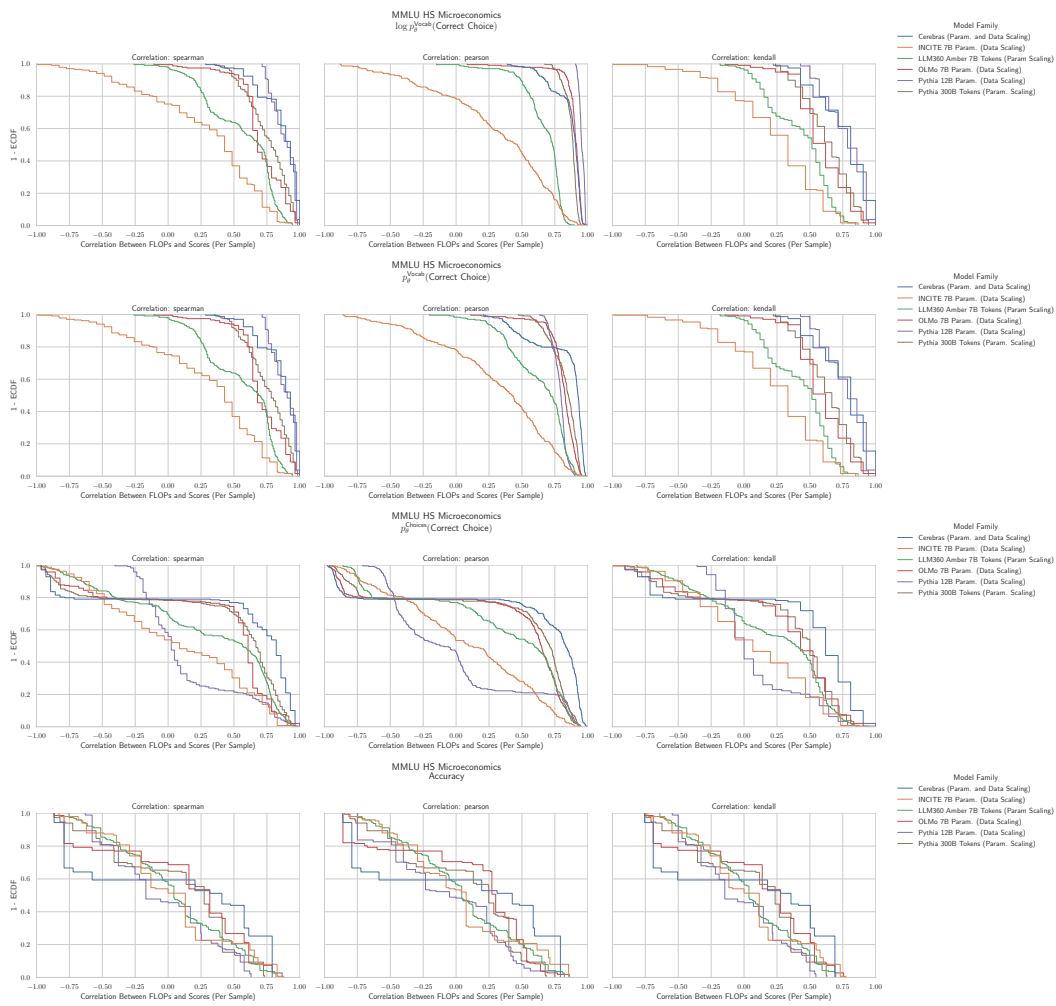
2916 G.31 NLP BENCHMARK: MMLU HIGH SCHOOL MACROECONOMICS HENDRYCKS ET AL.
 2917 (2020)



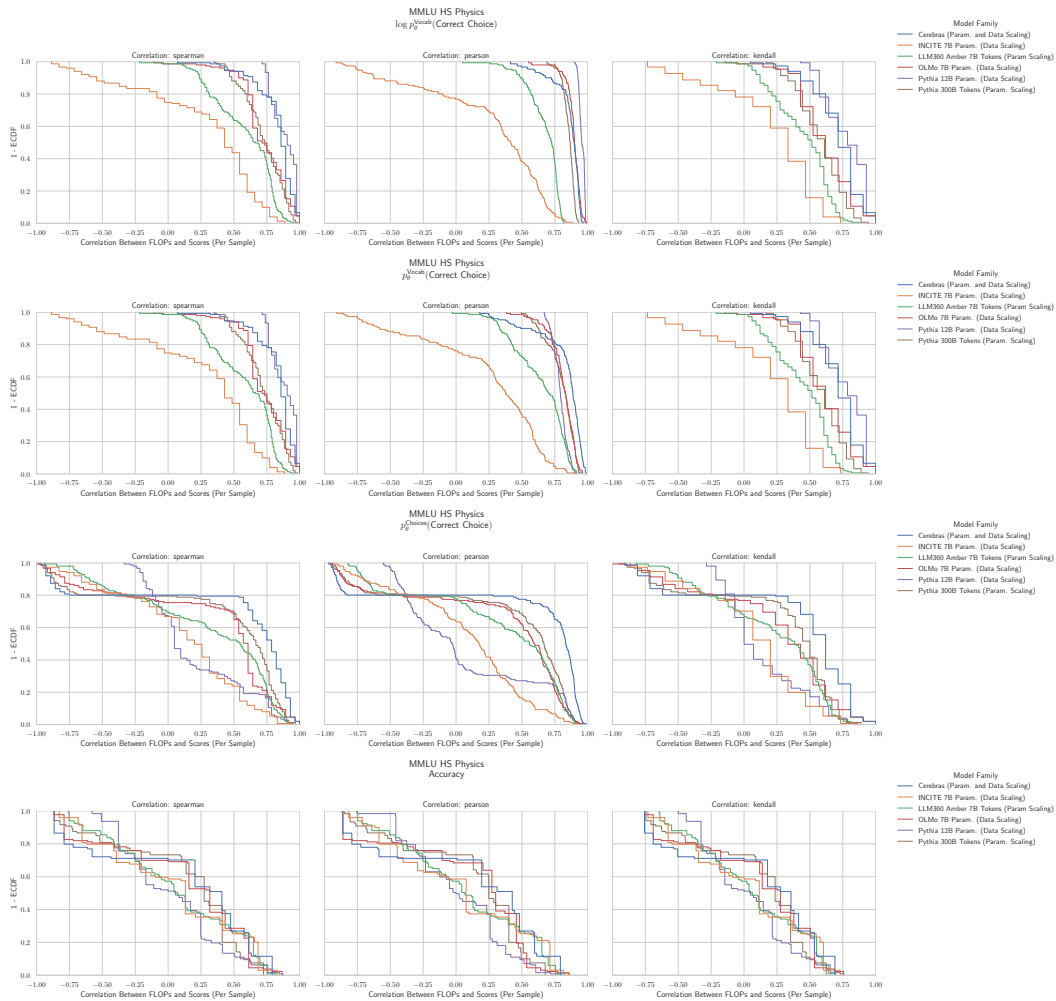
2952 **Figure 40: MMLU High School Macroeconomics: Downstream performance is computed via
 2953 a sequence of transformations that deteriorate correlations between scores and pretraining
 2954 compute.**

2970 G.32 NLP BENCHMARK: MMLU HIGH SCHOOL MATHEMATICS HENDRYCKS ET AL. (2020)
29713005 **Figure 41: MMLU High School Mathematics: Downstream performance is computed via
3006 a sequence of transformations that deteriorate correlations between scores and pretraining
3007 compute.**
3008
3009
3010
3011
3012
3013
3014
3015
3016
3017
3018
3019
3020
3021
3022
3023

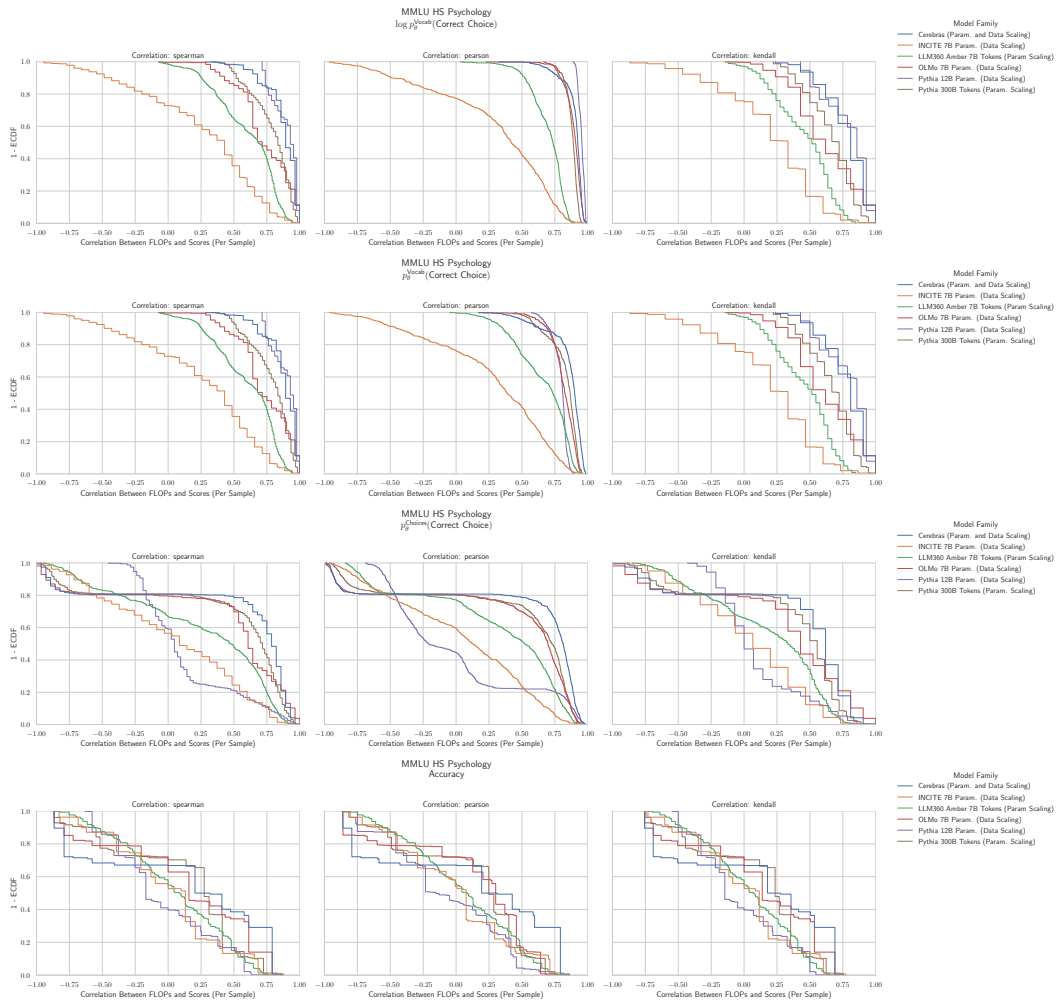
3024 **G.33 NLP BENCHMARK: MMLU HIGH SCHOOL MICROECONOMICS HENDRYCKS ET AL.**
 3025 (2020)



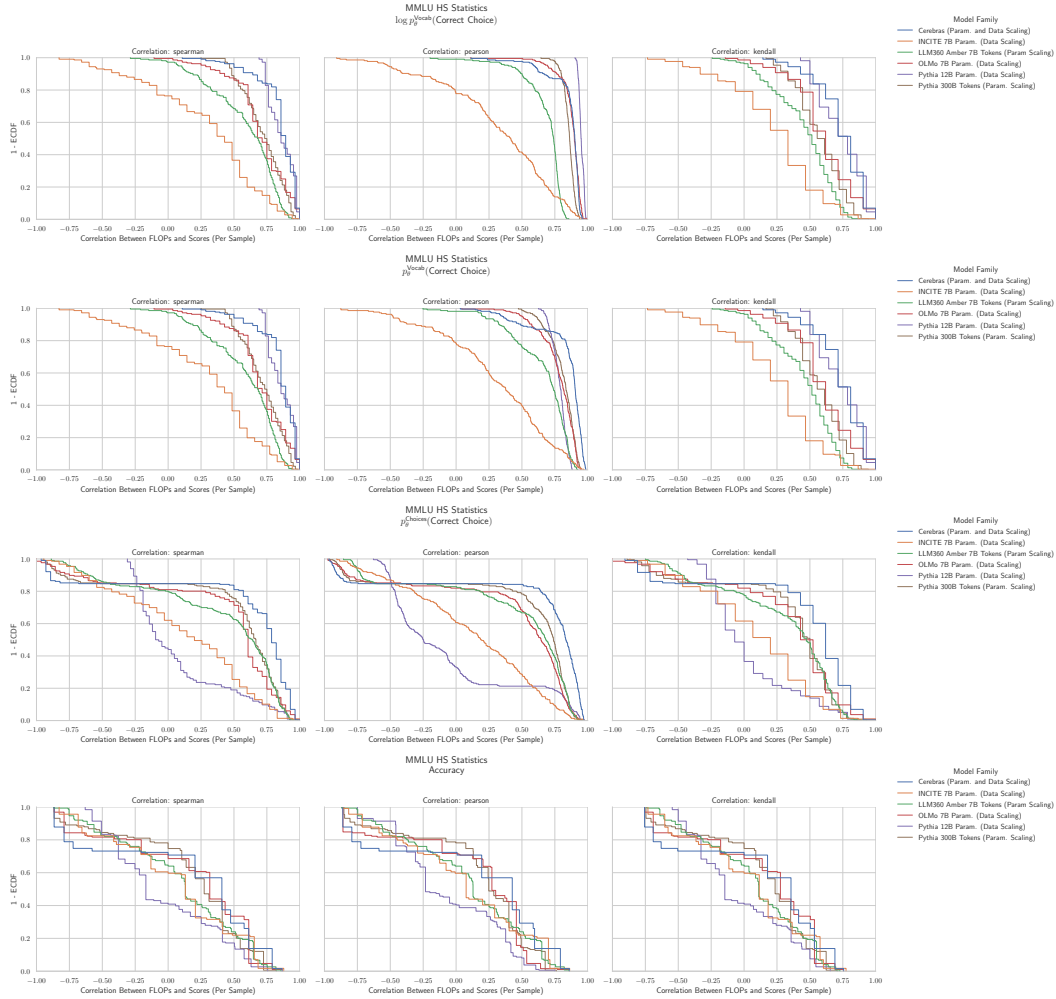
3060 **Figure 42: MMLU High School Microeconomics: Downstream performance is computed via
 3061 a sequence of transformations that deteriorate correlations between scores and pretraining
 3062 compute.**

3078 G.34 NLP BENCHMARK: MMLU HIGH SCHOOL PHYSICS HENDRYCKS ET AL. (2020)
30793113 **Figure 43: MMLU High School Physics: Downstream performance is computed via a sequence
3114 of transformations that deteriorate correlations between scores and pretraining compute.**

3115
3116
3117
3118
3119
3120
3121
3122
3123
3124
3125
3126
3127
3128
3129
3130
3131

3132 G.35 NLP BENCHMARK: MMLU HIGH SCHOOL PSYCHOLOGY HENDRYCKS ET AL. (2020)
31333167 **Figure 44: MMLU High School Psychology: Downstream performance is computed via a
3168 sequence of transformations that deteriorate correlations between scores and pretraining
3169 compute.**

3186 G.36 NLP BENCHMARK: MMLU HIGH SCHOOL STATISTICS HENDRYCKS ET AL. (2020)
 3187



3205 Figure 45: **MMLU High School Statistics: Downstream performance is computed via a sequence
 3206 of transformations that deteriorate correlations between scores and pretraining compute.**

3207
 3208
 3209
 3210
 3211
 3212
 3213
 3214
 3215
 3216
 3217
 3218
 3219
 3220
 3221
 3222
 3223
 3224
 3225
 3226
 3227
 3228
 3229
 3230
 3231
 3232
 3233
 3234
 3235
 3236
 3237
 3238
 3239

G.37 NLP BENCHMARK: MMLU HIGH SCHOOL US HISTORY HENDRYCKS ET AL. (2020)

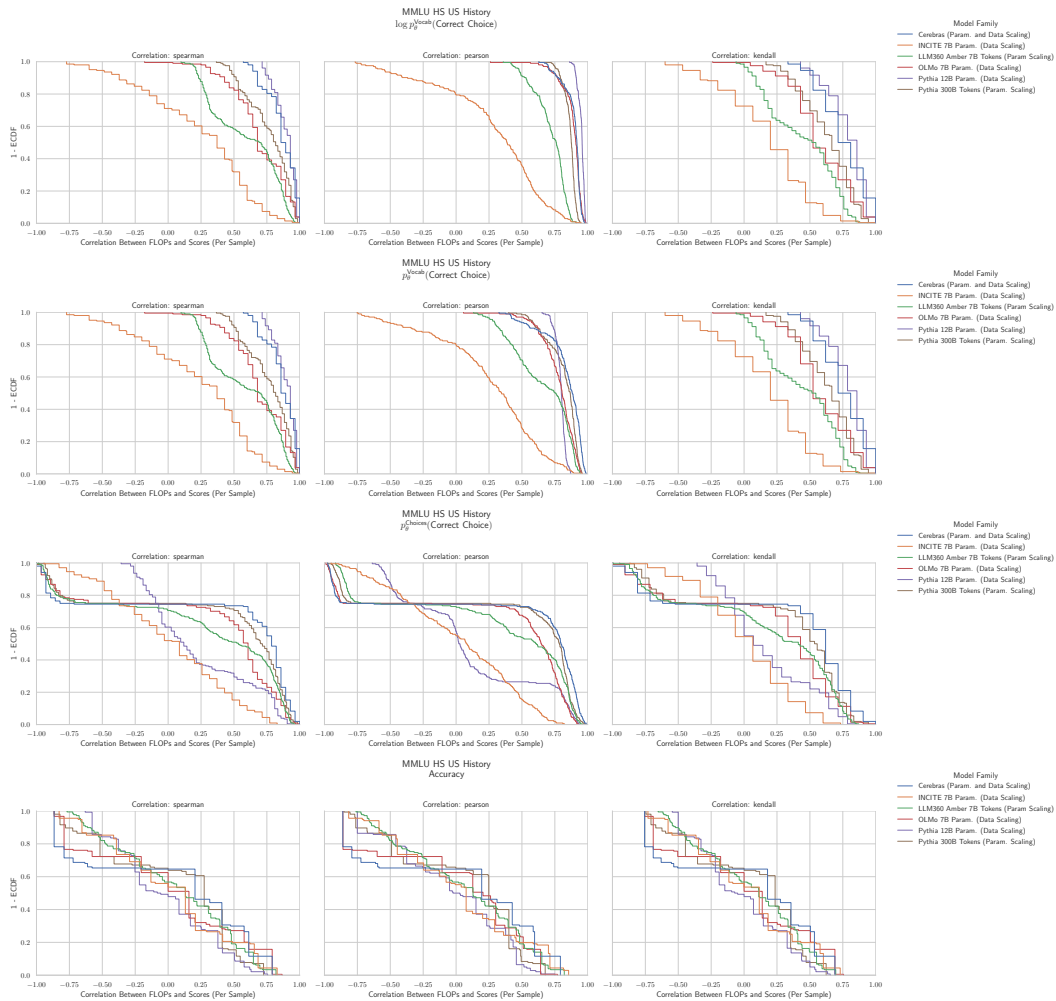
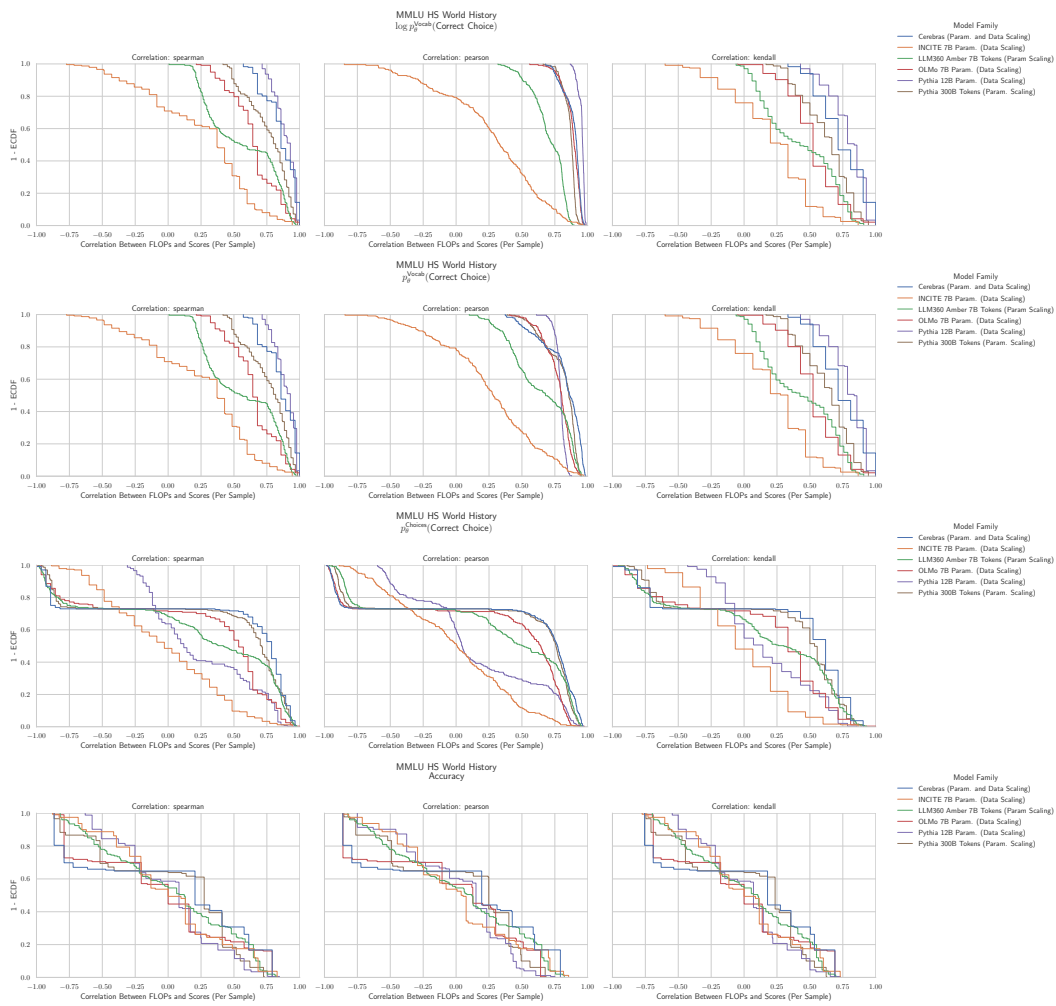


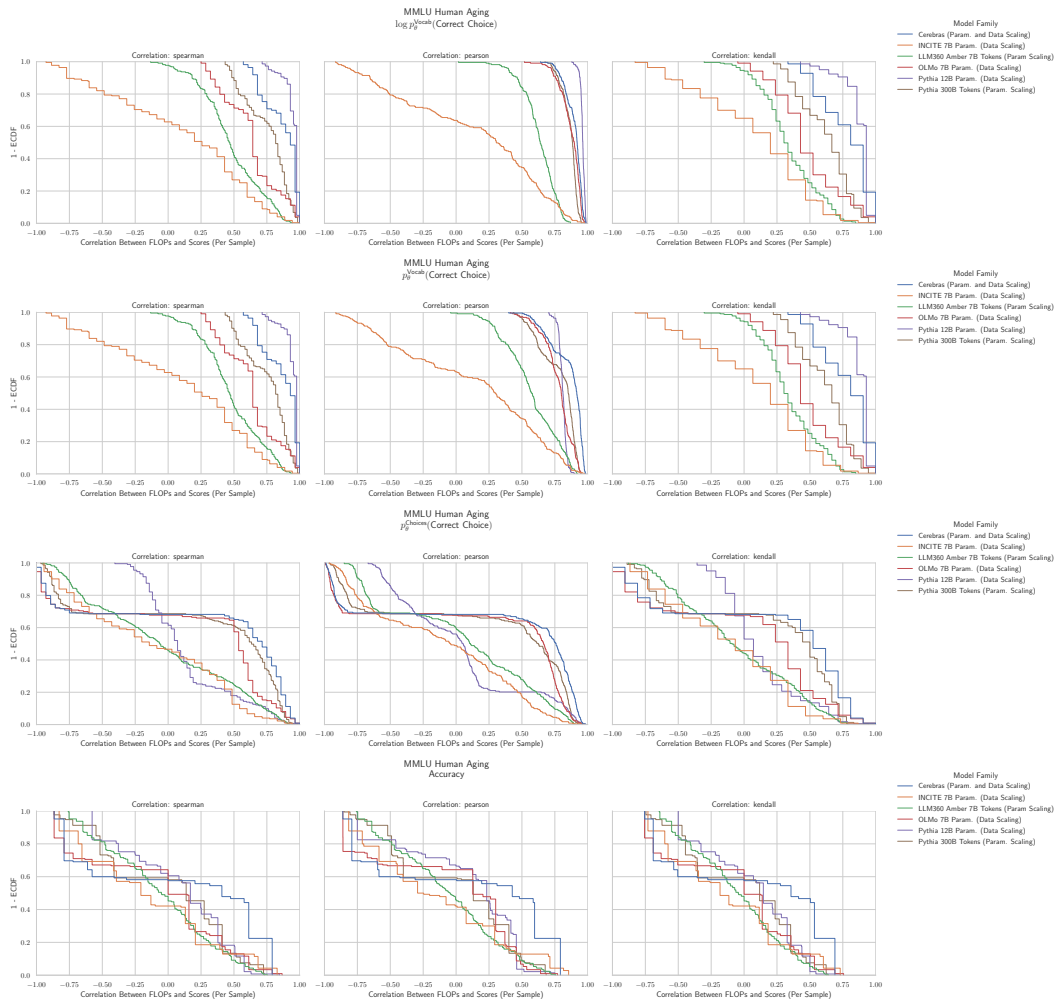
Figure 46: **MMLU High School US History:** Downstream performance is computed via a sequence of transformations that deteriorate correlations between scores and pretraining compute.

3294 G.38 NLP BENCHMARK: MMLU HIGH SCHOOL WORLD HISTORY HENDRYCKS ET AL.
 3295 (2020)

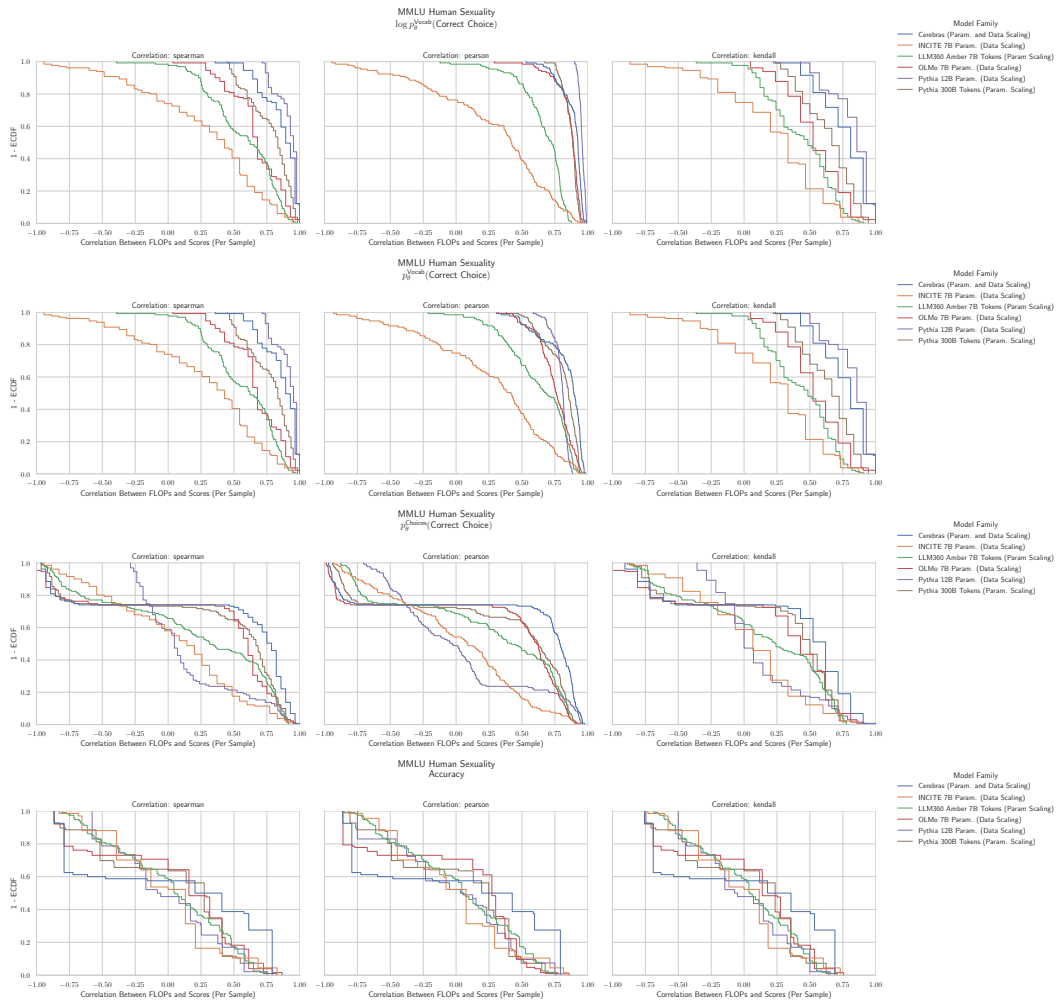


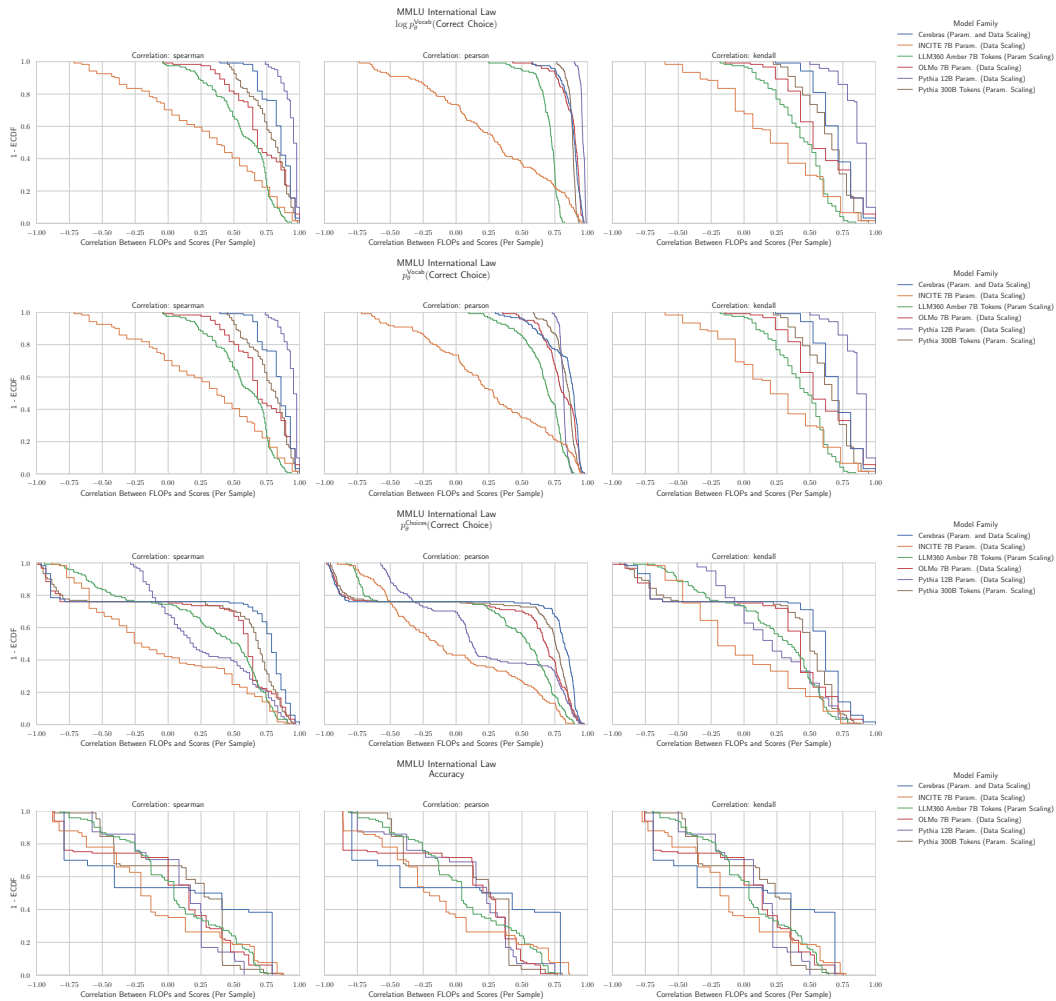
3296
 3297
 3298
 3299
 3300
 3301
 3302
 3303
 3304
 3305
 3306
 3307
 3308
 3309
 3310
 3311
 3312
 3313
 3314
 3315
 3316
 3317
 3318
 3319
 3320
 3321
 3322
 3323
 3324
 3325
 3326
 3327
 3328
 3329
 3330
 3331
 3332
 3333
 3334
 3335
 3336
 3337
 3338
 3339
 3340
 3341
 3342
 3343
 3344
 3345
 3346
 3347

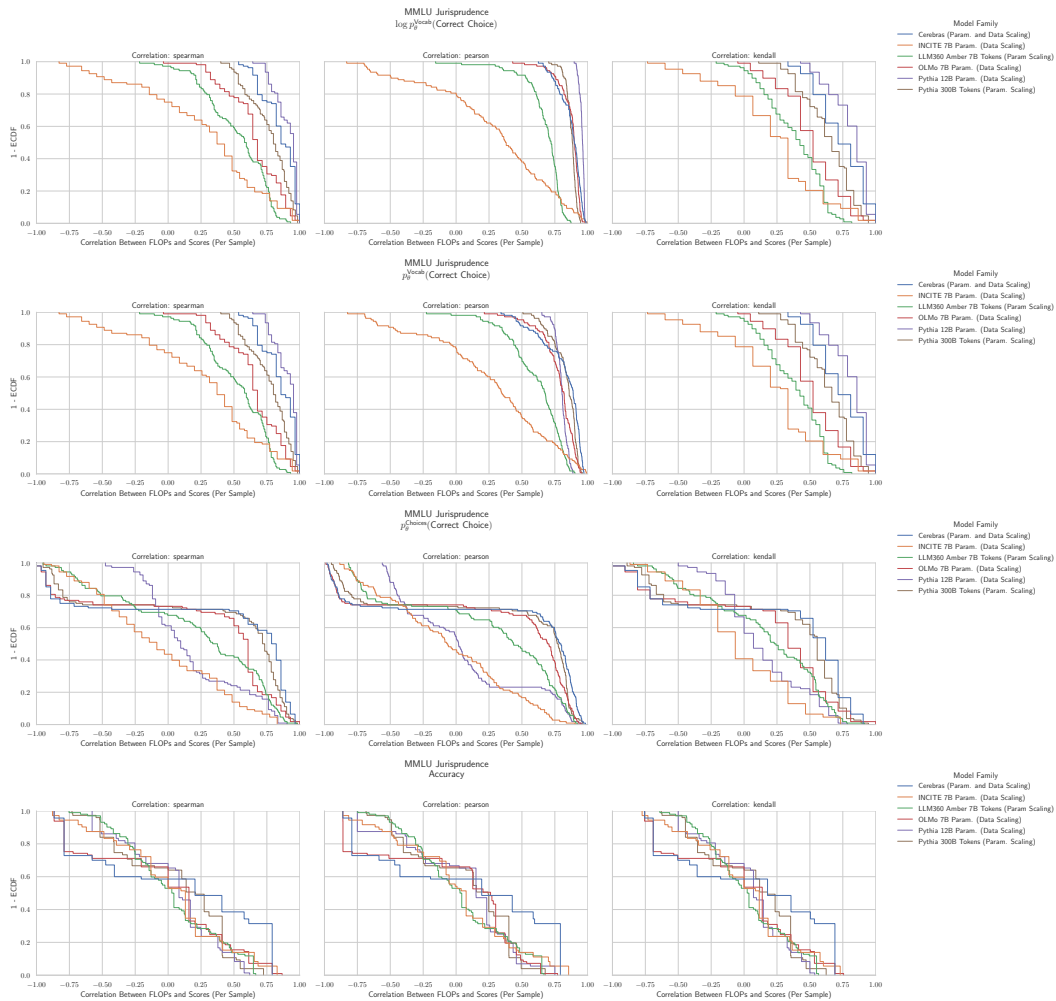
Figure 47: MMLU High School World History: Downstream performance is computed via a sequence of transformations that deteriorate correlations between scores and pretraining compute.

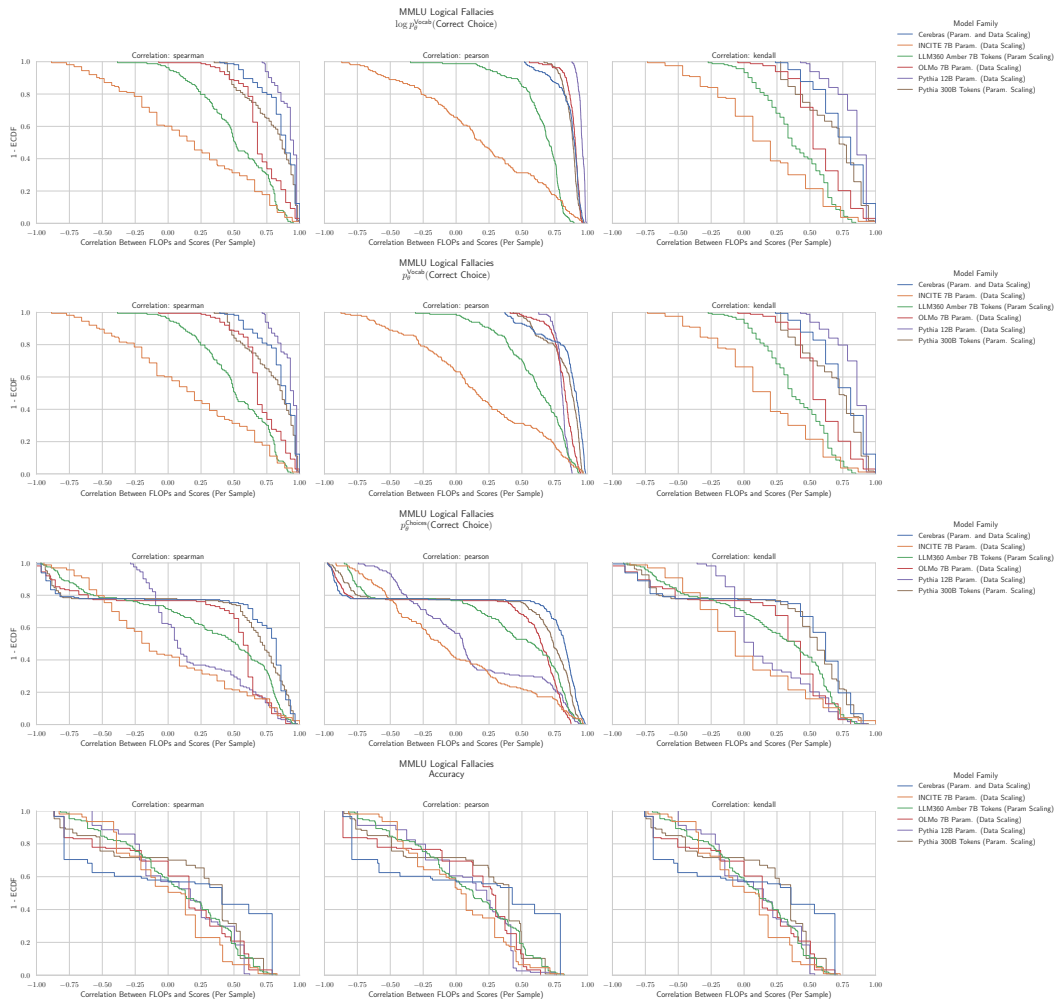
3348 G.39 NLP BENCHMARK: MMLU HUMAN AGING HENDRYCKS ET AL. (2020)
33493383 **Figure 48: MMLU Human Aging: Downstream performance is computed via a sequence of
3384 transformations that deteriorate correlations between scores and pretraining compute.**

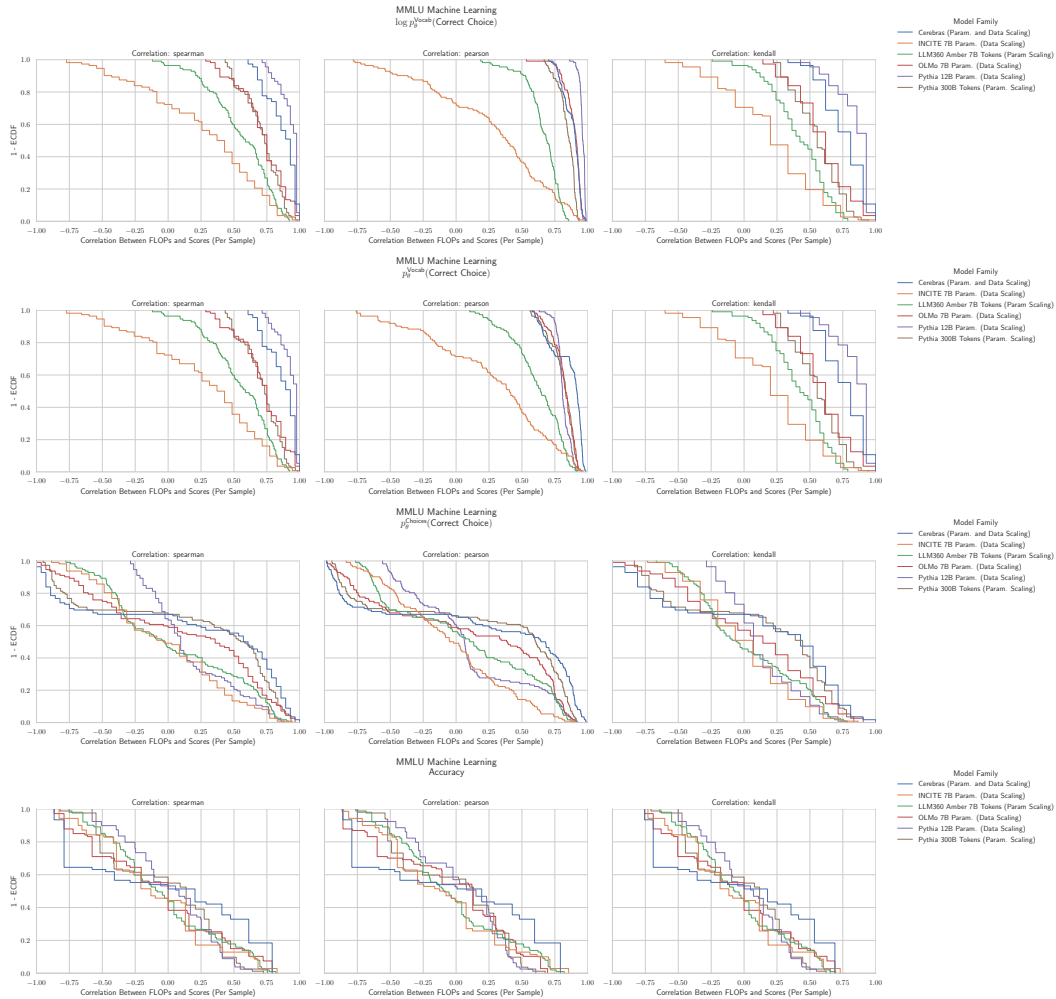
3348
3349
3350
3351
3352
3353
3354
3355
3356
3357
3358
3359
3360
3361
3362
3363
3364
3365
3366
3367
3368
3369
3370
3371
3372
3373
3374
3375
3376
3377
3378
3379
3380
3381
3382
3383
3384
3385
3386
3387
3388
3389
3390
3391
3392
3393
3394
3395
3396
3397
3398
3399
3400
3401

3402 G.40 NLP BENCHMARK: MMLU HUMAN SEXUALITY HENDRYCKS ET AL. (2020)
34033437 Figure 49: MMLU Human Sexuality: Downstream performance is computed via a sequence of
3438 transformations that deteriorate correlations between scores and pretraining compute.
3439

3456 G.41 NLP BENCHMARK: MMLU INTERNATIONAL LAW HENDRYCKS ET AL. (2020)
34573491 **Figure 50: MMLU International Law: Downstream performance is computed via a sequence of
3492 transformations that deteriorate correlations between scores and pretraining compute.**
3493
3494
3495
3496
3497
3498
3499
3500
3501
3502
3503
3504
3505
3506
3507
3508
3509

3510 G.42 NLP BENCHMARK: MMLU JURISPRUDENCE HENDRYCKS ET AL. (2020)
35113545 **Figure 51: MMLU Jurisprudence: Downstream performance is computed via a sequence of
3546 transformations that deteriorate correlations between scores and pretraining compute.**
3547
3548
3549
3550
3551
3552
3553
3554
3555
3556
3557
3558
3559
3560
3561
3562
3563

3564 G.43 NLP BENCHMARK: MMLU LOGICAL FALLACIES HENDRYCKS ET AL. (2020)
35653599 **Figure 52: MMLU Logical Fallacies: Downstream performance is computed via a sequence of
3600 transformations that deteriorate correlations between scores and pretraining compute.**
3601
3602
3603
3604
3605
3606
3607
3608
3609
3610
3611
3612
3613
3614
3615
3616
3617

3618 G.44 NLP BENCHMARK: MMLU MACHINE LEARNING HENDRYCKS ET AL. (2020)
36193653 **Figure 53: MMLU Machine Learning: Downstream performance is computed via a sequence of
3654 transformations that deteriorate correlations between scores and pretraining compute.**

3655
3656
3657
3658
3659
3660
3661
3662
3663
3664
3665
3666
3667
3668
3669
3670
3671

3672
3673

G.45 NLP BENCHMARK: MMLU MANAGEMENT HENDRYCKS ET AL. (2020)

3674

3675

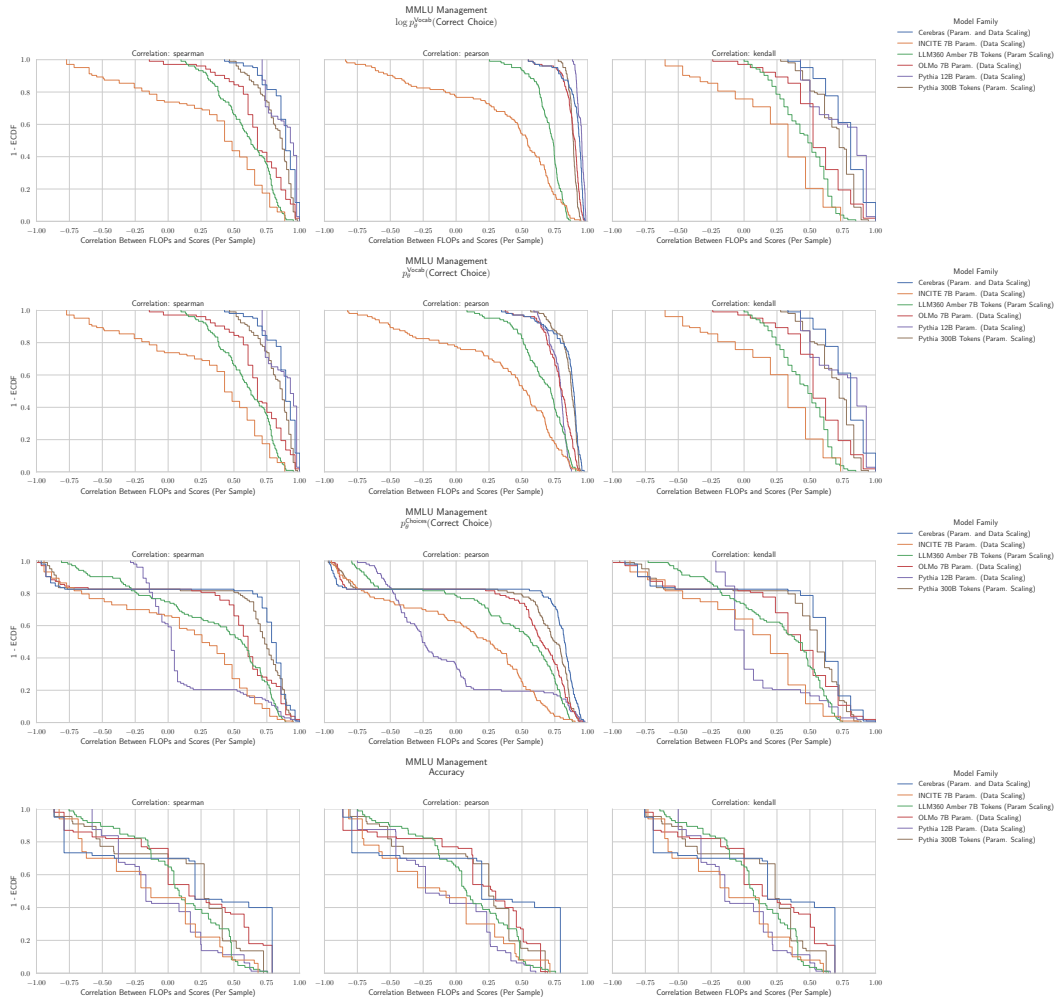


Figure 54: **MMLU Management:** Downstream performance is computed via a sequence of transformations that deteriorate correlations between scores and pretraining compute.

3706

3707

3708

3709

3710

3711

3712

3713

3714

3715

3716

3717

3718

3719

3720

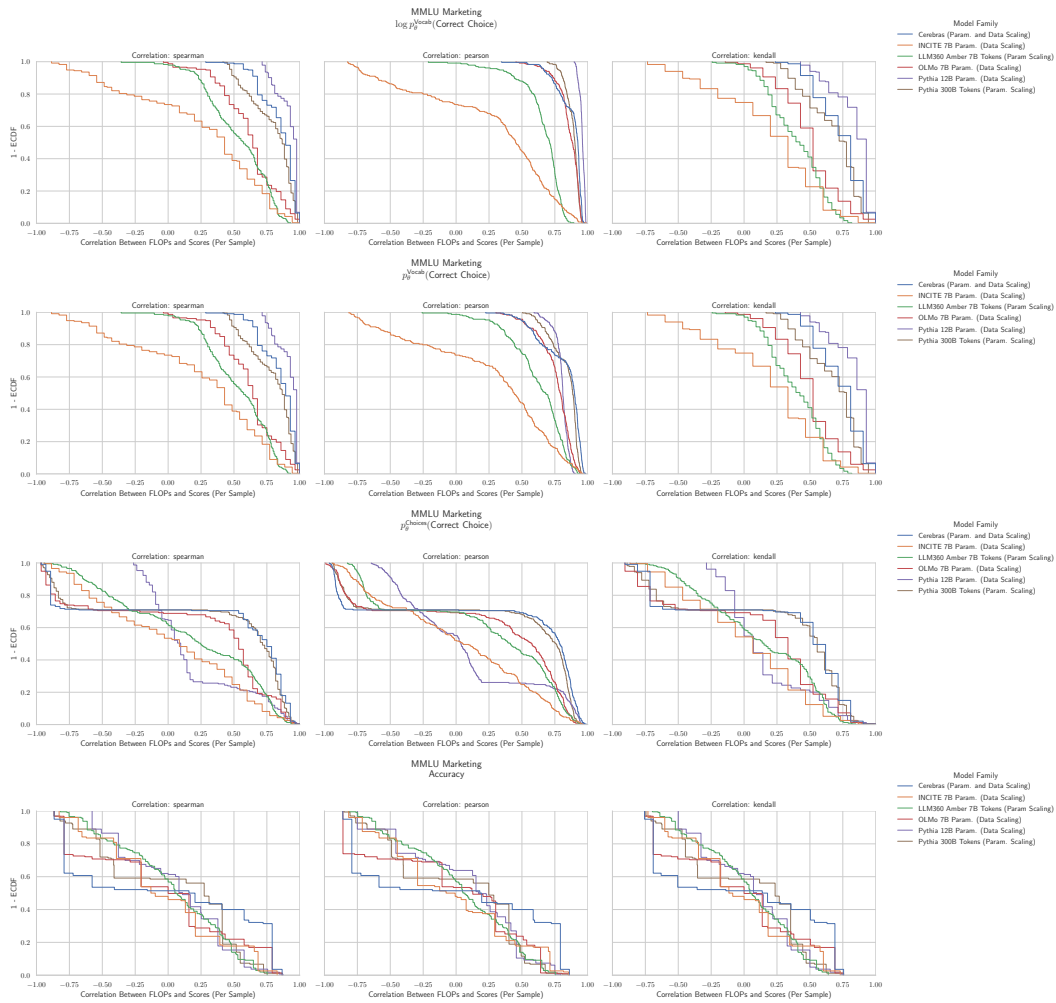
3721

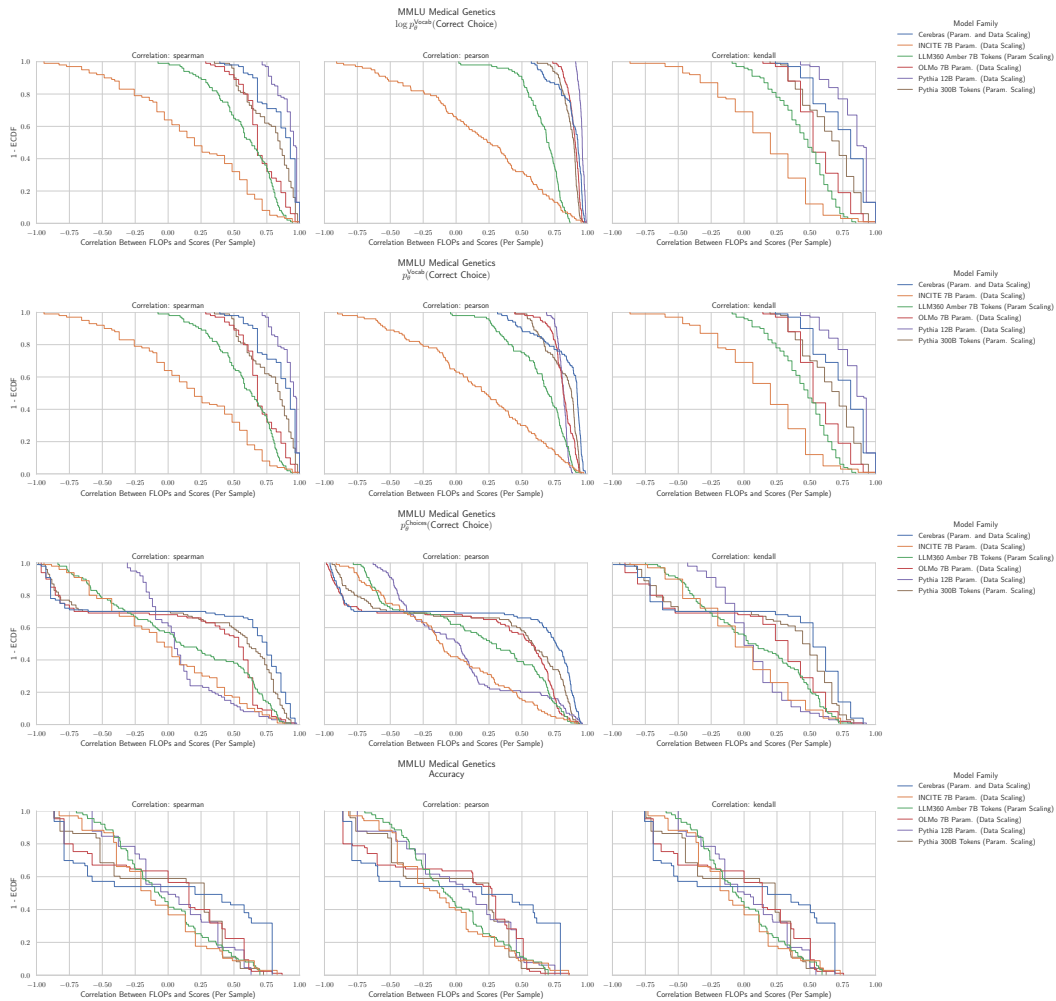
3722

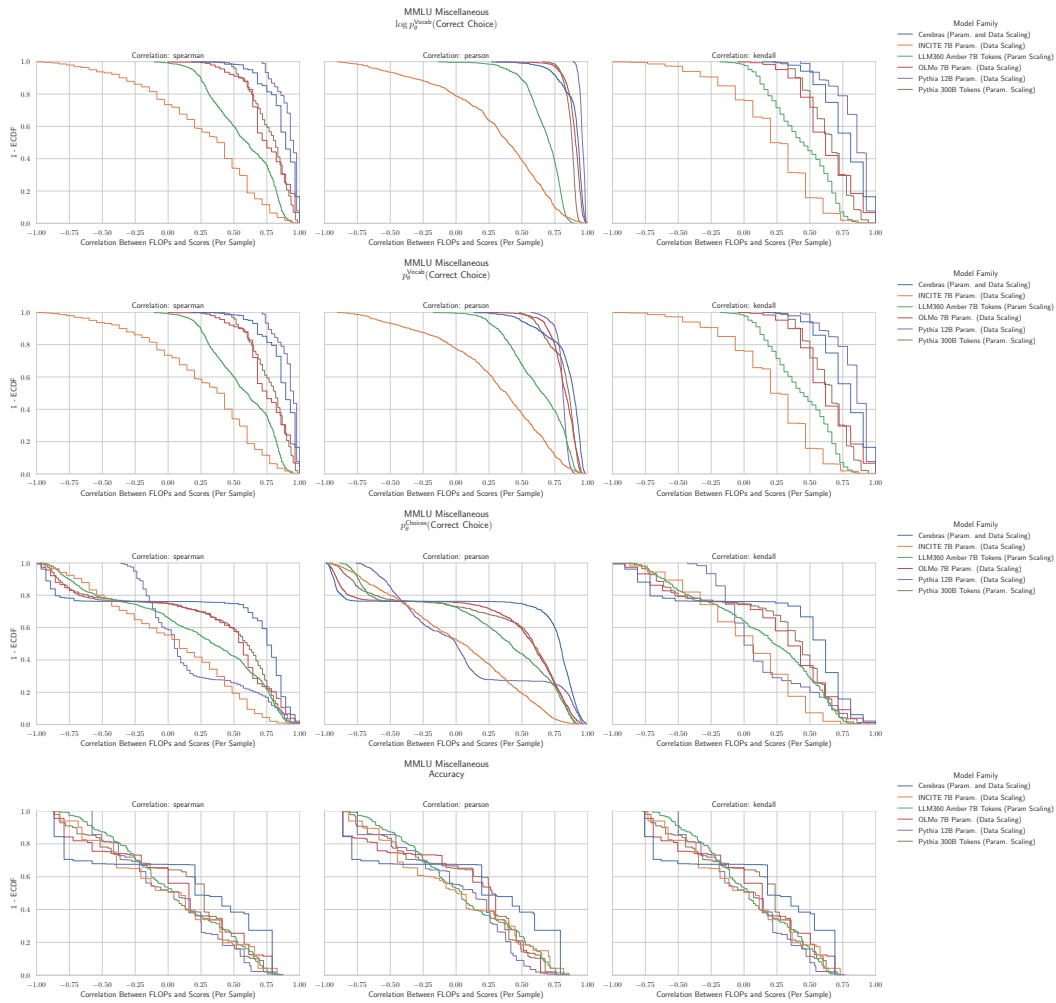
3723

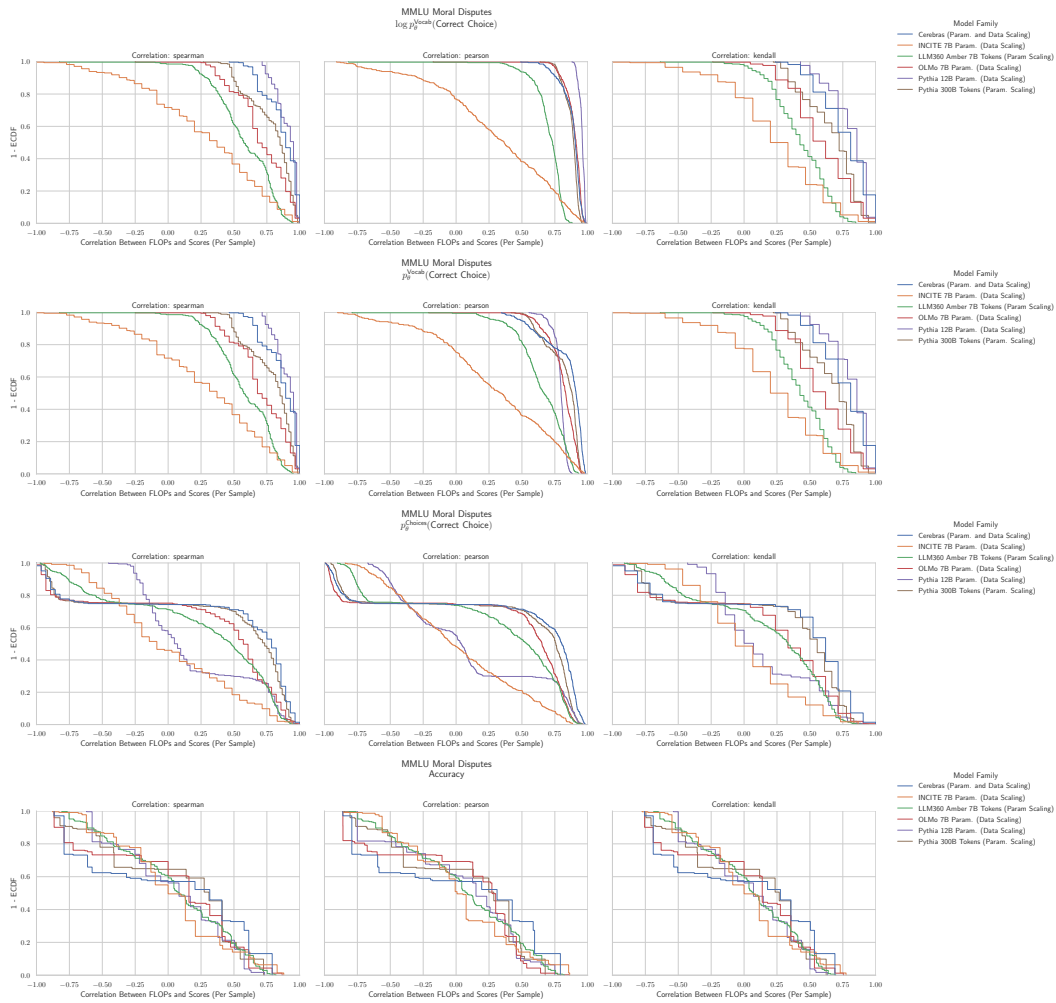
3724

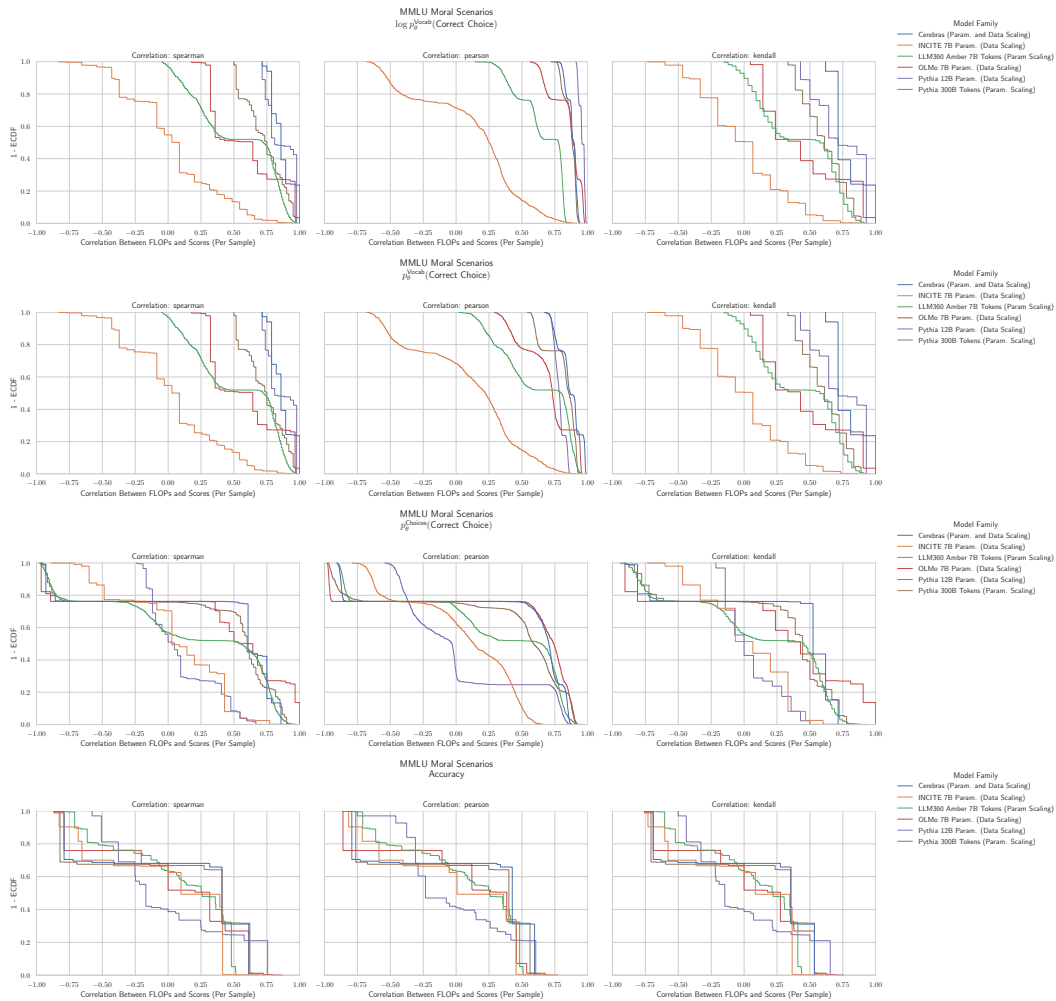
3725

3726 G.46 NLP BENCHMARK: MMLU MARKETING HENDRYCKS ET AL. (2020)
37273761 Figure 55: MMLU Marketing: Downstream performance is computed via a sequence of
3762 transformations that deteriorate correlations between scores and pretraining compute.
3763

3780 G.47 NLP BENCHMARK: MMLU MEDICAL GENETICS HENDRYCKS ET AL. (2020)
37813815 Figure 56: MMLU Medical Genetics: Downstream performance is computed via a sequence of transformations that deteriorate correlations between scores and pretraining compute.
3816

3834 G.48 NLP BENCHMARK: MMLU MISCELLANEOUS HENDRYCKS ET AL. (2020)
38353869 Figure 57: MMLU Miscellaneous: Downstream performance is computed via a sequence of
3870 transformations that deteriorate correlations between scores and pretraining compute.
3871
3872
3873
3874
3875
3876
3877
3878
3879
3880
3881
3882
3883
3884
3885
3886
3887

3888 G.49 NLP BENCHMARK: MMLU MORAL DISPUTES HENDRYCKS ET AL. (2020)
38893923 Figure 58: MMLU Moral Disputes: Downstream performance is computed via a sequence of
3924 transformations that deteriorate correlations between scores and pretraining compute.

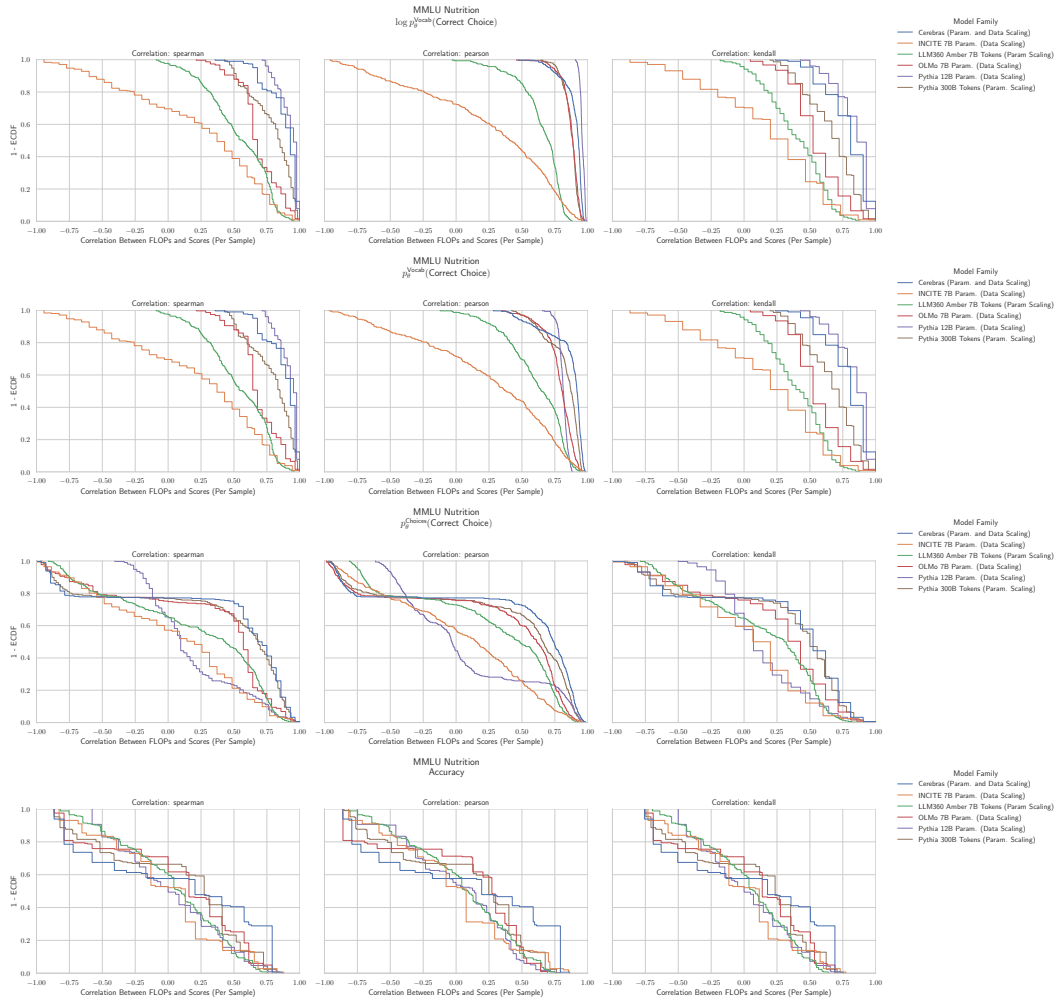
3942 G.50 NLP BENCHMARK: MMLU MORAL SCENARIOS HENDRYCKS ET AL. (2020)
39433977 Figure 59: MMLU Moral Scenarios: Downstream performance is computed via a sequence of
3978 transformations that deteriorate correlations between scores and pretraining compute.
3979
3980
3981
3982
3983
3984
3985
3986
3987
3988
3989
3990
3991
3992
3993
3994
3995

3996
3997

G.51 NLP BENCHMARK: MMLU NUTRITION HENDRYCKS ET AL. (2020)

3998

3999



4014

4015

4016

4017

4018

4019

4020

4021

4022

4023

4024

4025

4026

4027

4028

4029

4030

4031

4032

Figure 60: **MMLU Nutrition: Downstream performance is computed via a sequence of transformations that deteriorate correlations between scores and pretraining compute.**

4033

4034

4035

4036

4037

4038

4039

4040

4041

4042

4043

4044

4045

4046

4047

4048

4049

4050
4051

G.52 NLP BENCHMARK: MMLU PHILOSOPHY HENDRYCKS ET AL. (2020)

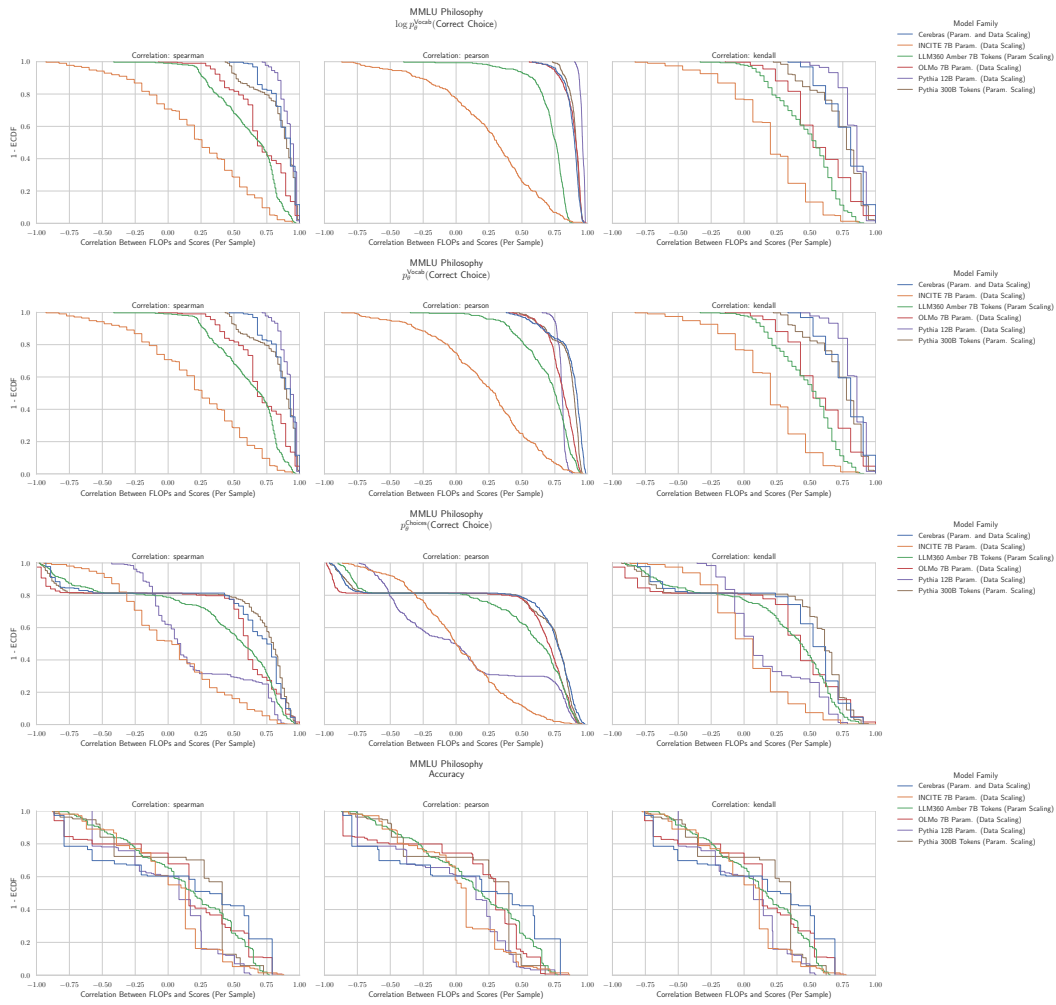
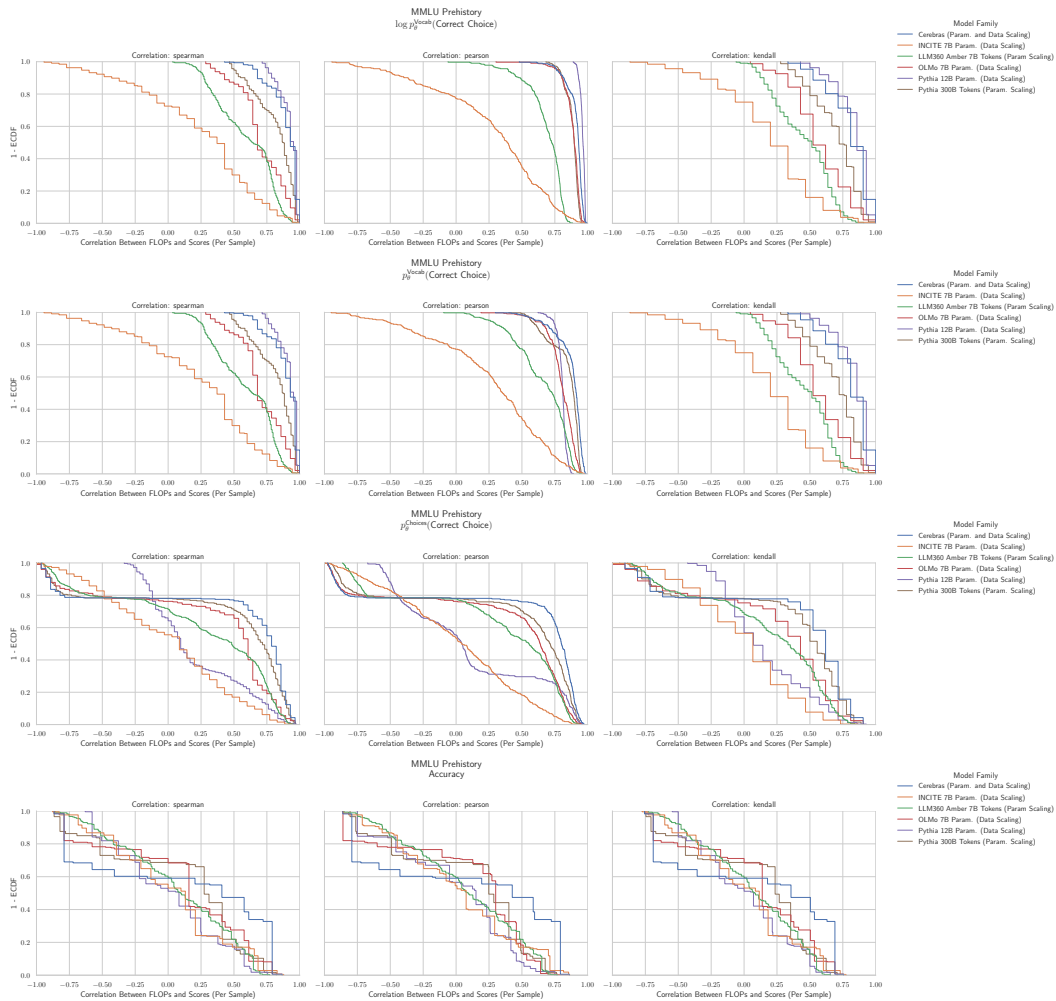
4052
40534054
4055
4056
4057
4058
4059

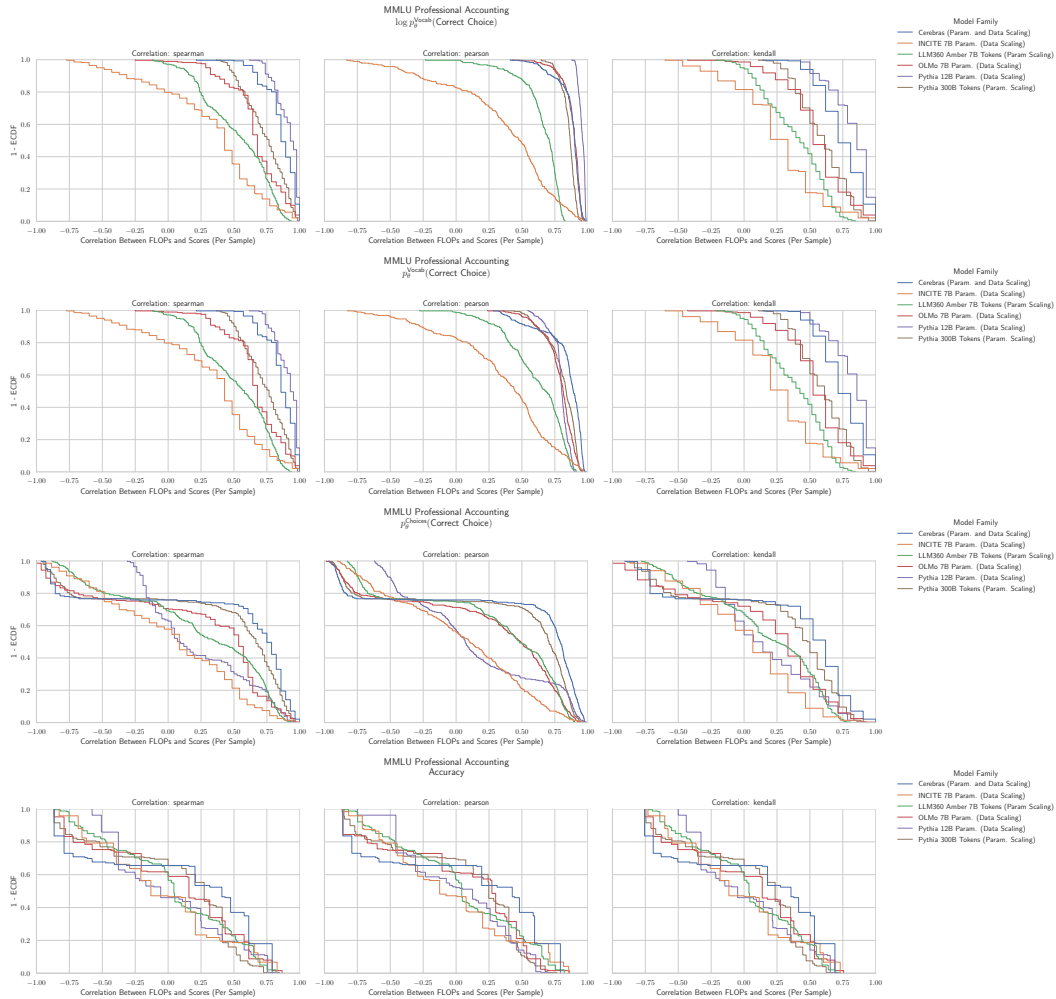
Figure 61: **MMLU Philosophy:** Downstream performance is computed via a sequence of transformations that deteriorate correlations between scores and pretraining compute.

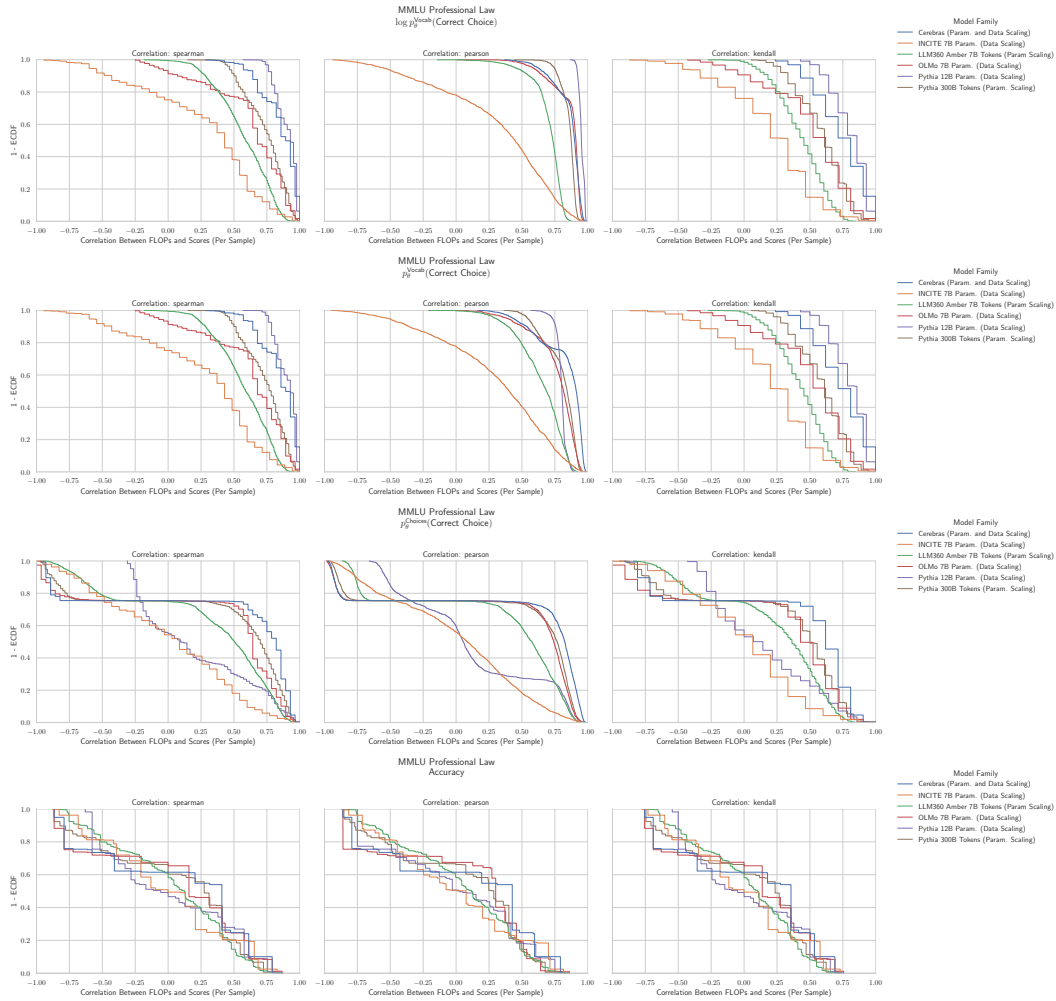
4060
40614062
4063
4064
4065
4066
40674068
40694070
4071
4072
4073
4074
40754076
40774078
4079
4080
4081
4082
4083

4084

4085
40864087
4088
4089
4090
4091
4092
4093
4094
4095
4096
4097
4098
4099
4100
4101
4102
4103

4104 G.53 NLP BENCHMARK: MMLU PREHISTORY HENDRYCKS ET AL. (2020)
41054139 Figure 62: MMLU Prehistory: Downstream performance is computed via a sequence of trans-
4140 formations that deteriorate correlations between scores and pretraining compute.
4141
4142
4143
4144
4145
4146
4147
4148
4149
4150
4151
4152
4153
4154
4155
4156
4157

4158 G.54 NLP BENCHMARK: MMLU PROFESSIONAL ACCOUNTING HENDRYCKS ET AL. (2020)
41594193 **Figure 63: MMLU Professional Accounting: Downstream performance is computed via a
4194 sequence of transformations that deteriorate correlations between scores and pretraining
4195 compute.**

4212 G.55 NLP BENCHMARK: MMLU PROFESSIONAL LAW HENDRYCKS ET AL. (2020)
42134247 **Figure 64: MMLU Professional Law: Downstream performance is computed via a sequence of
4248 transformations that deteriorate correlations between scores and pretraining compute.**
4249
4250
4251
4252
4253
4254
4255
4256
4257
4258
4259
4260
4261
4262
4263
4264
4265

4266
4267

G.56 NLP BENCHMARK: MMLU PROFESSIONAL MEDICINE HENDRYCKS ET AL. (2020)

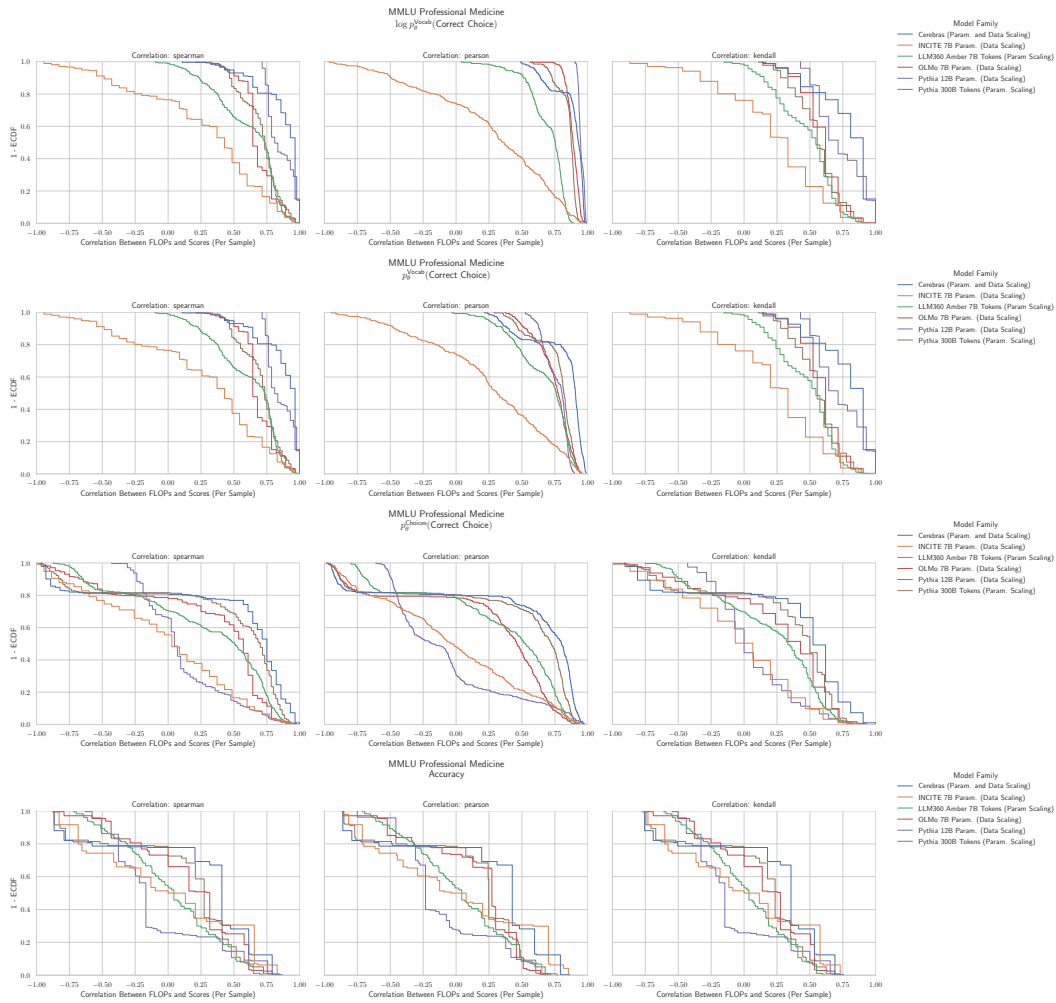
4268
4269

Figure 65: MMLU Professional Medicine: Downstream performance is computed via a sequence of transformations that deteriorate correlations between scores and pretraining compute.

4300

4301

4302

4303

4304

4305

4306

4307

4308

4309

4310

4311

4312

4313

4314

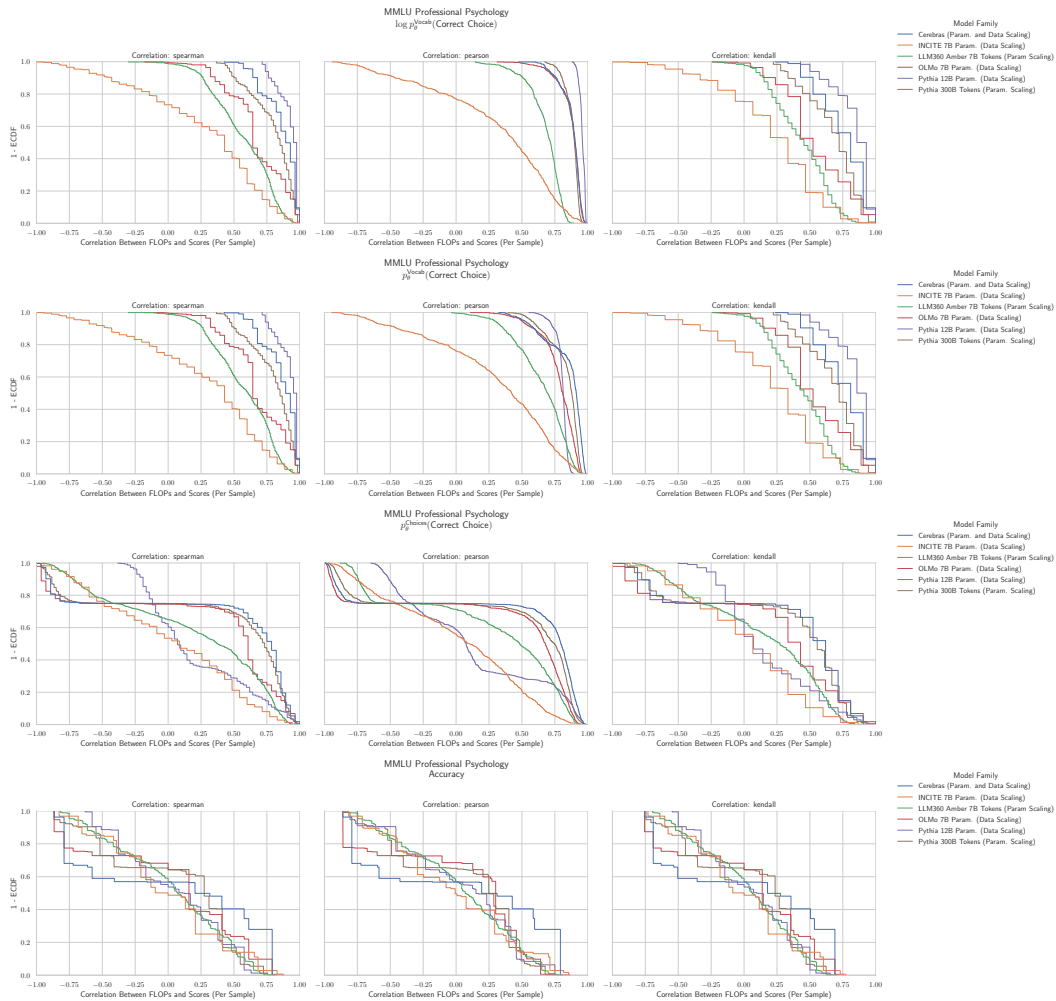
4315

4316

4317

4318

4319

4320 G.57 NLP BENCHMARK: MMLU PROFESSIONAL PSYCHOLOGY HENDRYCKS ET AL. (2020)
43214355 **Figure 66: MMLU Professional Psychology: Downstream performance is computed via a
4356 sequence of transformations that deteriorate correlations between scores and pretraining
4357 compute.**
4358
4359
4360
4361
4362
4363
4364
4365
4366
4367
4368
4369
4370
4371
4372
4373

4374
4375

G.58 NLP BENCHMARK: MMLU PUBLIC RELATIONS HENDRYCKS ET AL. (2020)

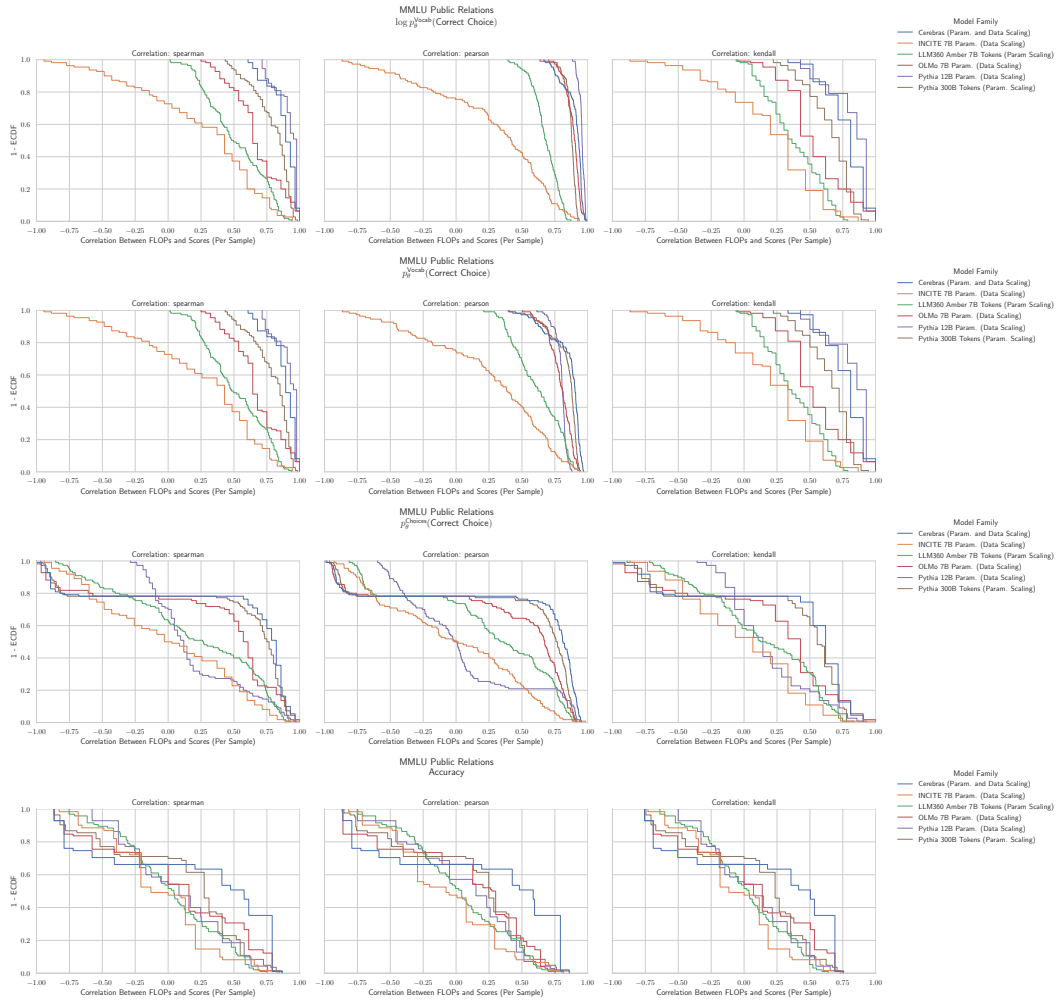
4376
4377

Figure 67: MMLU Public Relations: Downstream performance is computed via a sequence of transformations that deteriorate correlations between scores and pretraining compute.

4409
4410
4411
4412
4413
4414
4415
4416
4417
4418
4419
4420
4421
4422
4423
4424
4425
4426
4427

G.59 NLP BENCHMARK: MMLU SECURITY STUDIES HENDRYCKS ET AL. (2020)

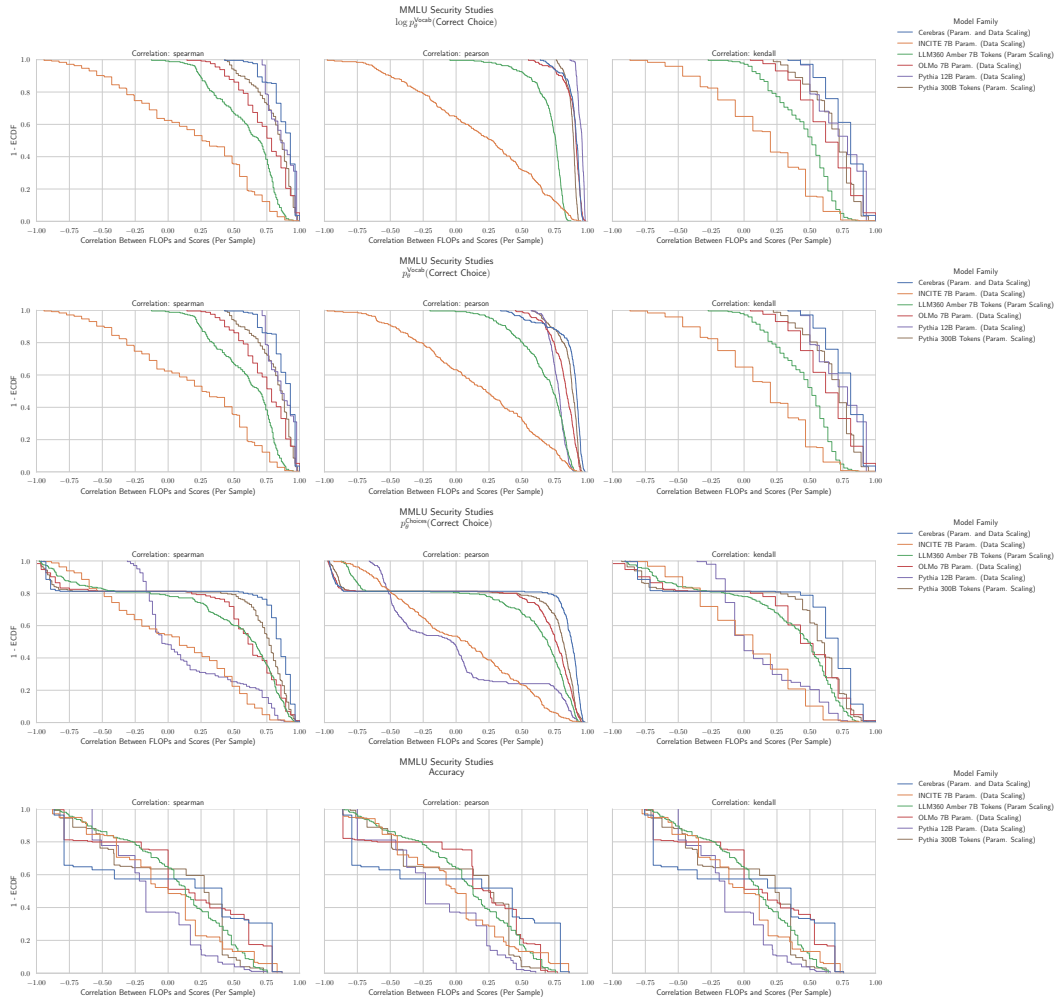


Figure 68: MMLU Security Studies: Downstream performance is computed via a sequence of transformations that deteriorate correlations between scores and pretraining compute.

4482
4483

G.60 NLP BENCHMARK: MMLU SOCIOLOGY HENDRYCKS ET AL. (2020)

4484

4485

4486

4487

4488

4489

4490

4491

4492

4493

4494

4495

4496

4497

4498

4499

4500

4501

4502

4503

4504

4505

4506

4507

4508

4509

4510

4511

4512

4513

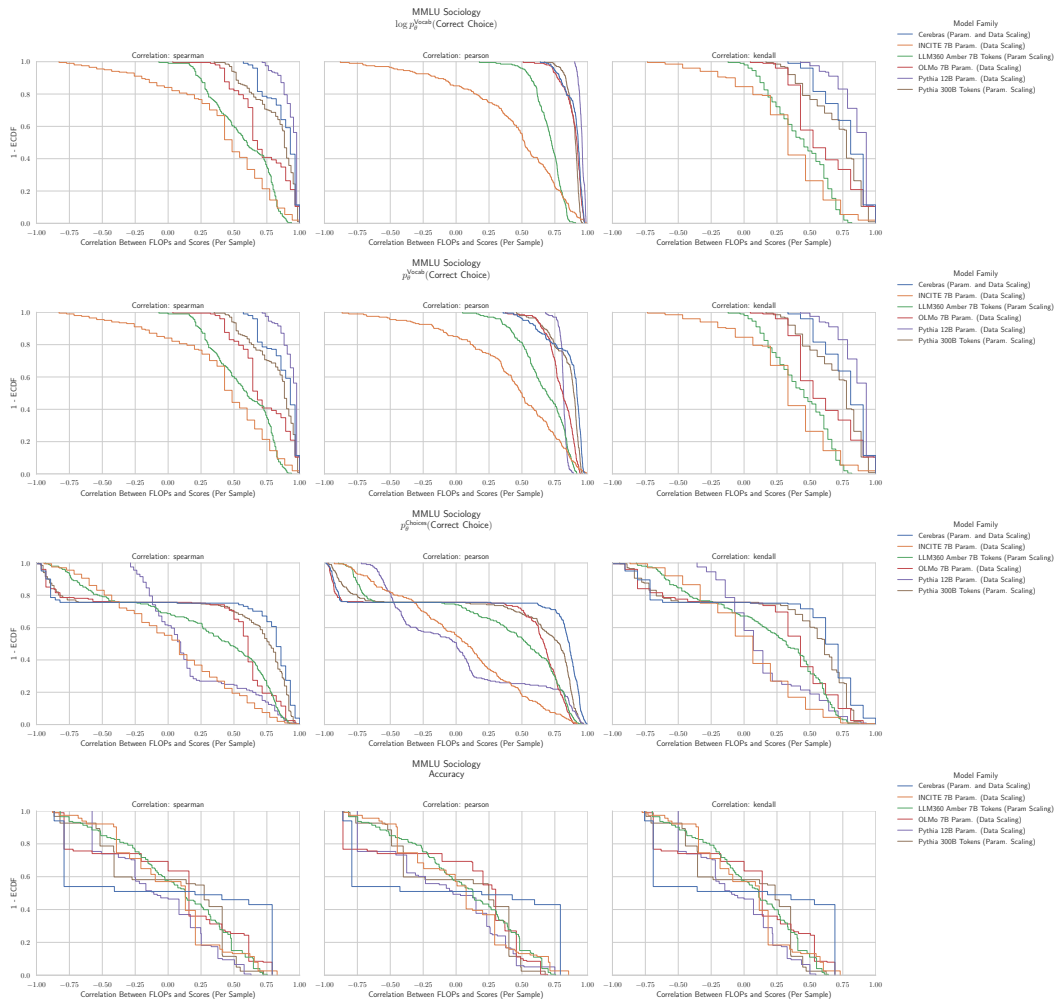
4514

4515

4516

4517

4518

Figure 69: **MMLU Sociology: Downstream performance is computed via a sequence of transformations that deteriorate correlations between scores and pretraining compute.**

4519

4520

4521

4522

4523

4524

4525

4526

4527

4528

4529

4530

4531

4532

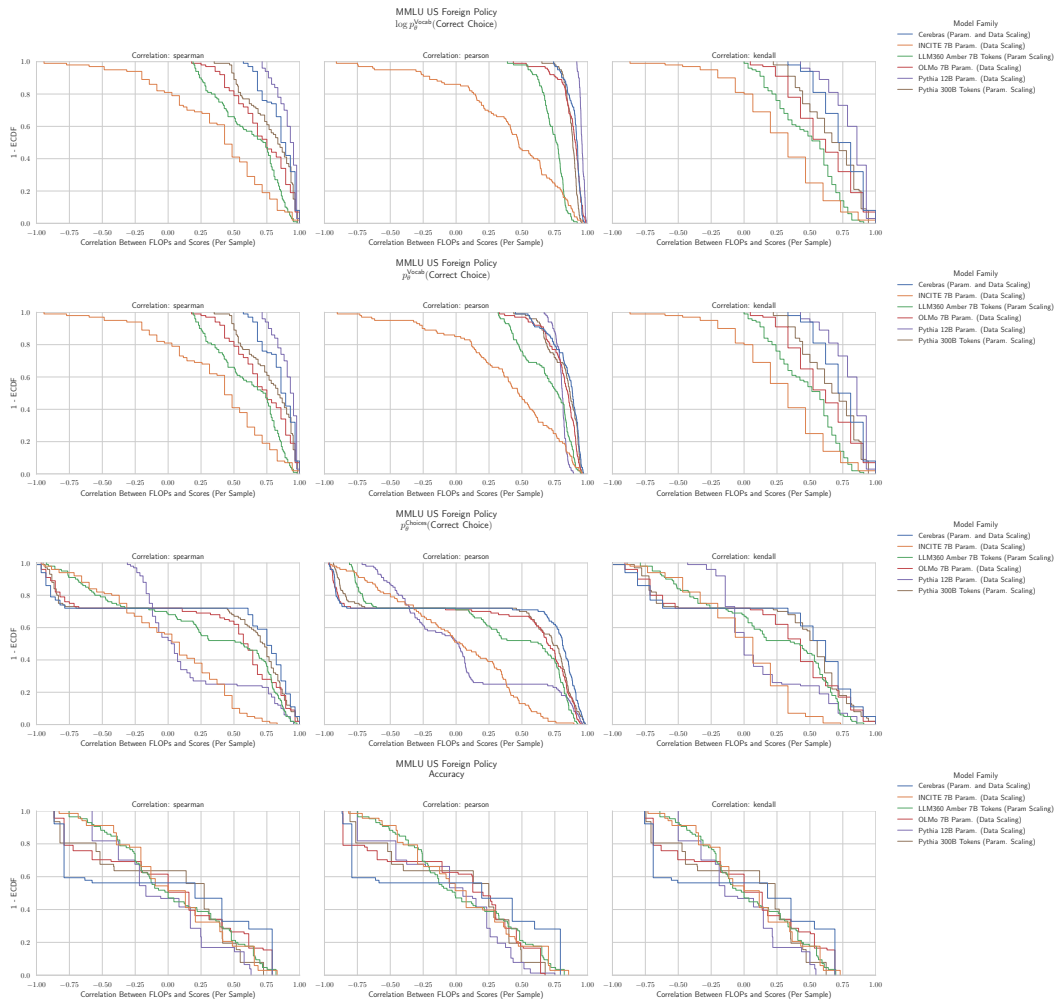
4533

4534

4535

4536
4537

G.61 NLP BENCHMARK: MMLU US FOREIGN POLICY HENDRYCKS ET AL. (2020)

4538
4539Figure 70: **MMLU US Foreign Policy: Downstream performance is computed via a sequence of transformations that deteriorate correlations between scores and pretraining compute.**

4570

4571

4572

4573

4574

4575

4576

4577

4578

4579

4580

4581

4582

4583

4584

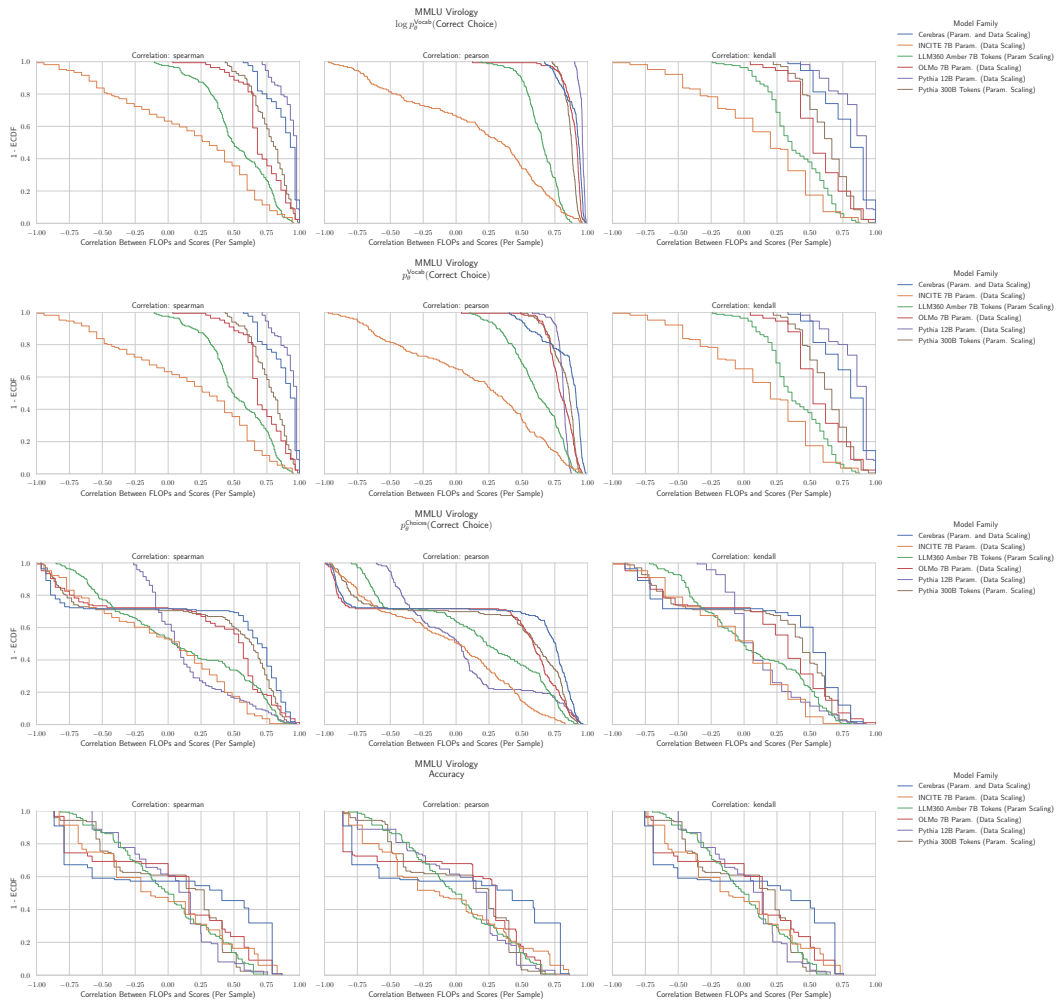
4585

4586

4587

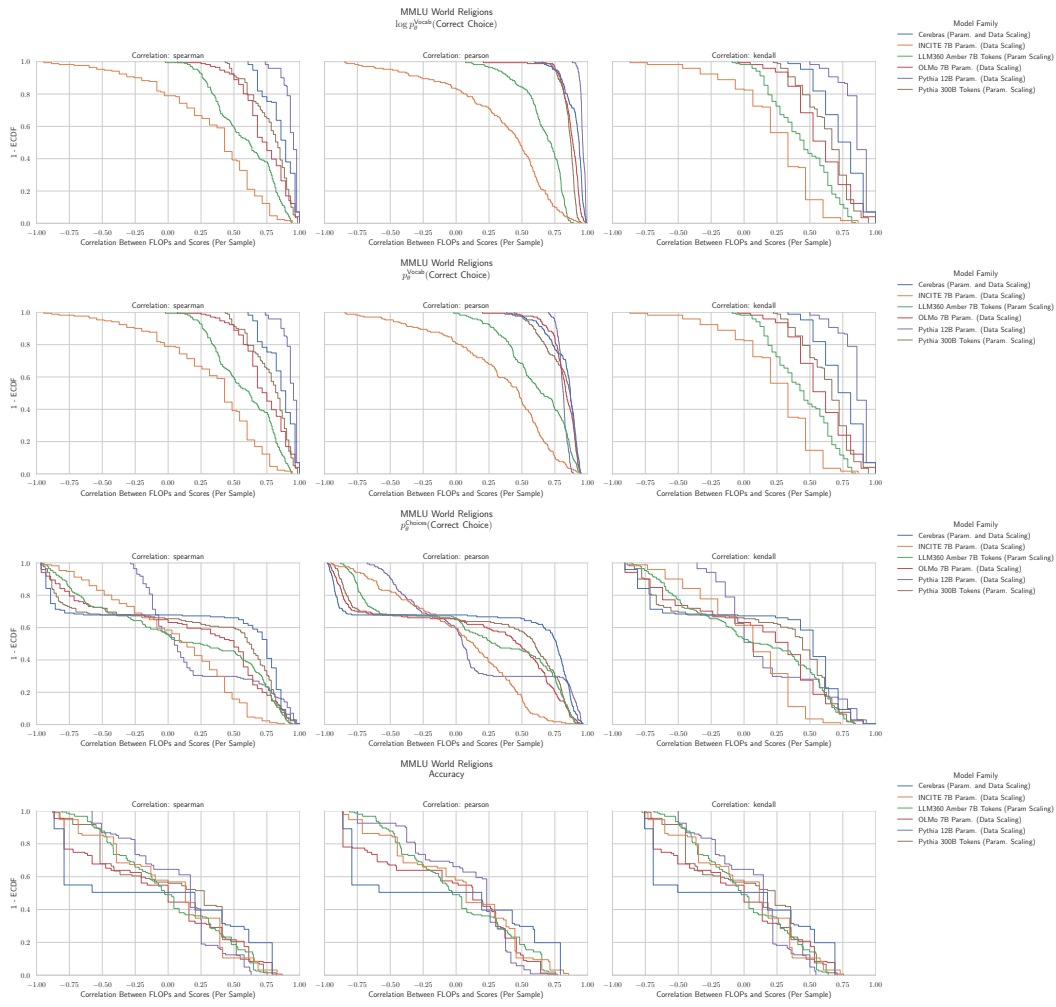
4588

4589

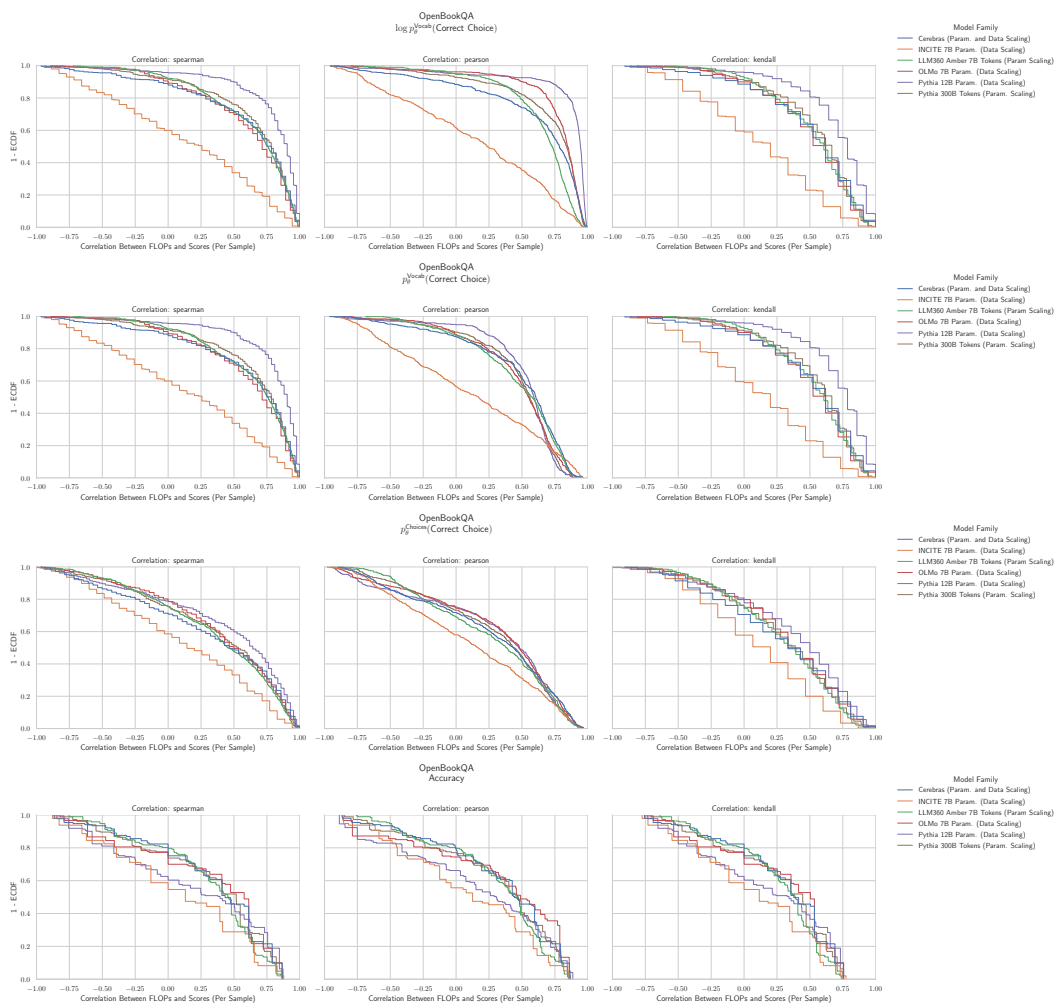
4590 G.62 NLP BENCHMARK: MMLU VIROLOGY HENDRYCKS ET AL. (2020)
45914625 **Figure 71: MMLU Virology: Downstream performance is computed via a sequence of transfor-
4626 mations that deteriorate correlations between scores and pretraining compute.**

4644
4645

G.63 NLP BENCHMARK: MMLU WORLD RELIGIONS HENDRYCKS ET AL. (2020)

4646
46474679
4680
Figure 72: MMLU World Religions: Downstream performance is computed via a sequence of
4681
4682
4683
4684
4685
4686
4687
4688
4689
4690
4691
4692
4693
4694
4695
4696
4697
transformations that deteriorate correlations between scores and pretraining compute.

4698 G.64 NLP BENCHMARK: OPENBOOKQA MIHAYLOV ET AL. (2018)
 4699



4733 **Figure 73: OpenBookQA: Downstream performance is computed via a sequence of transformations that deteriorate correlations between scores and pretraining compute.**
 4734

4735
 4736
 4737
 4738
 4739
 4740
 4741
 4742
 4743
 4744
 4745
 4746
 4747
 4748
 4749
 4750
 4751

G.65 NLP BENCHMARK: PIQA BISK ET AL. (2020)

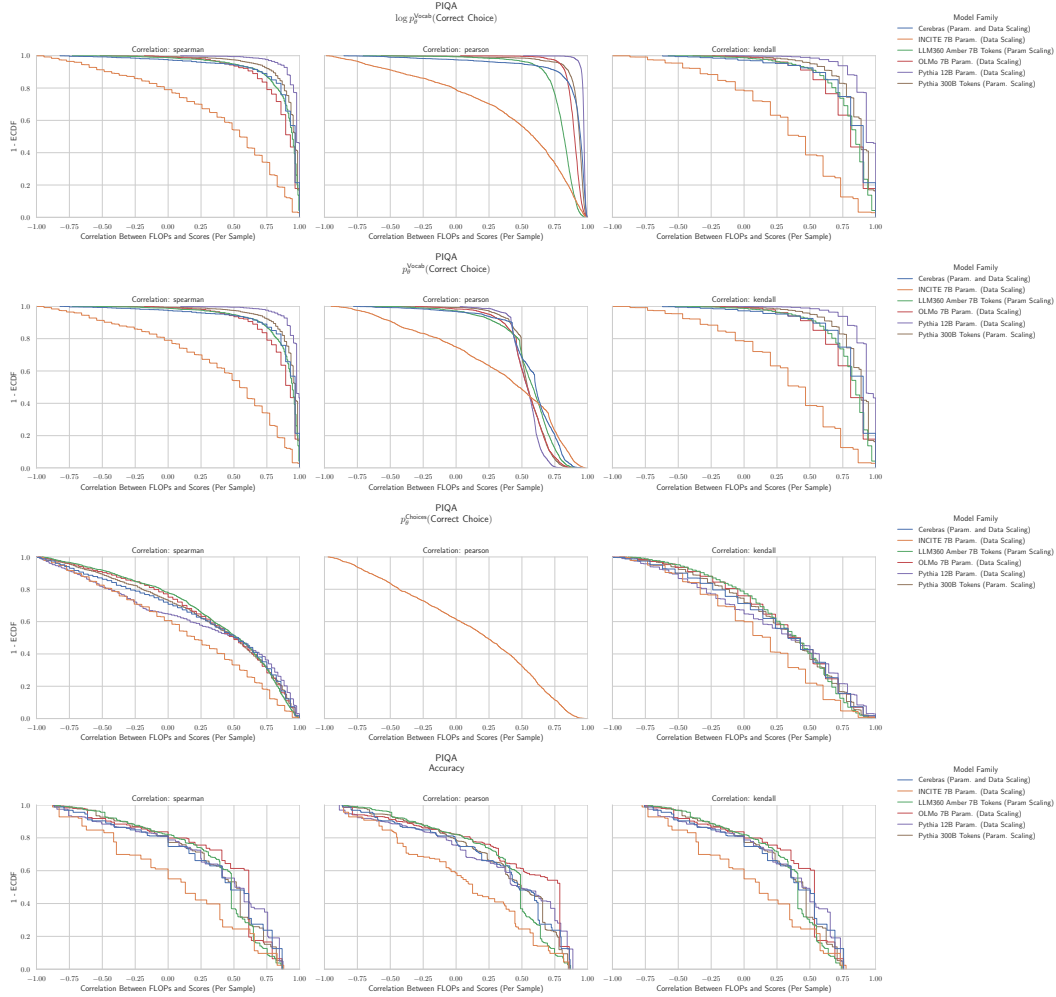
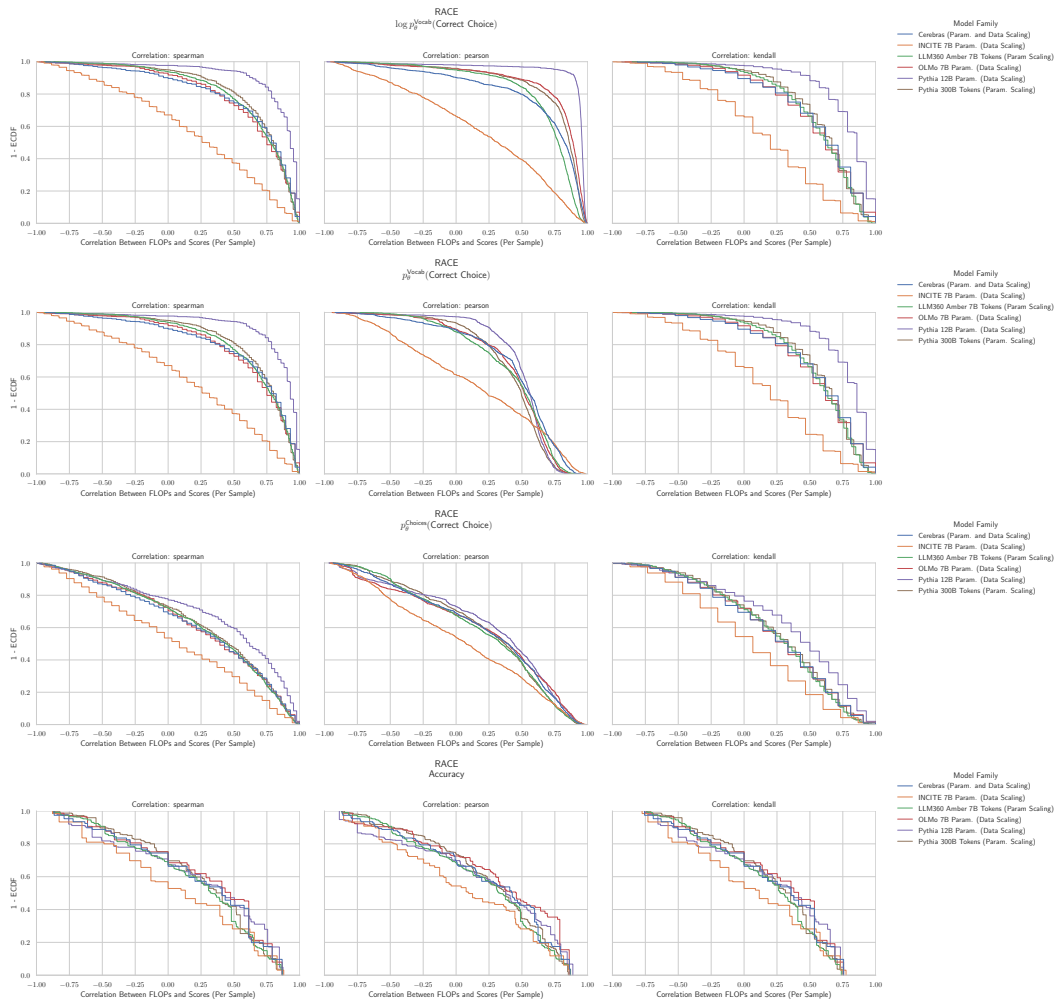
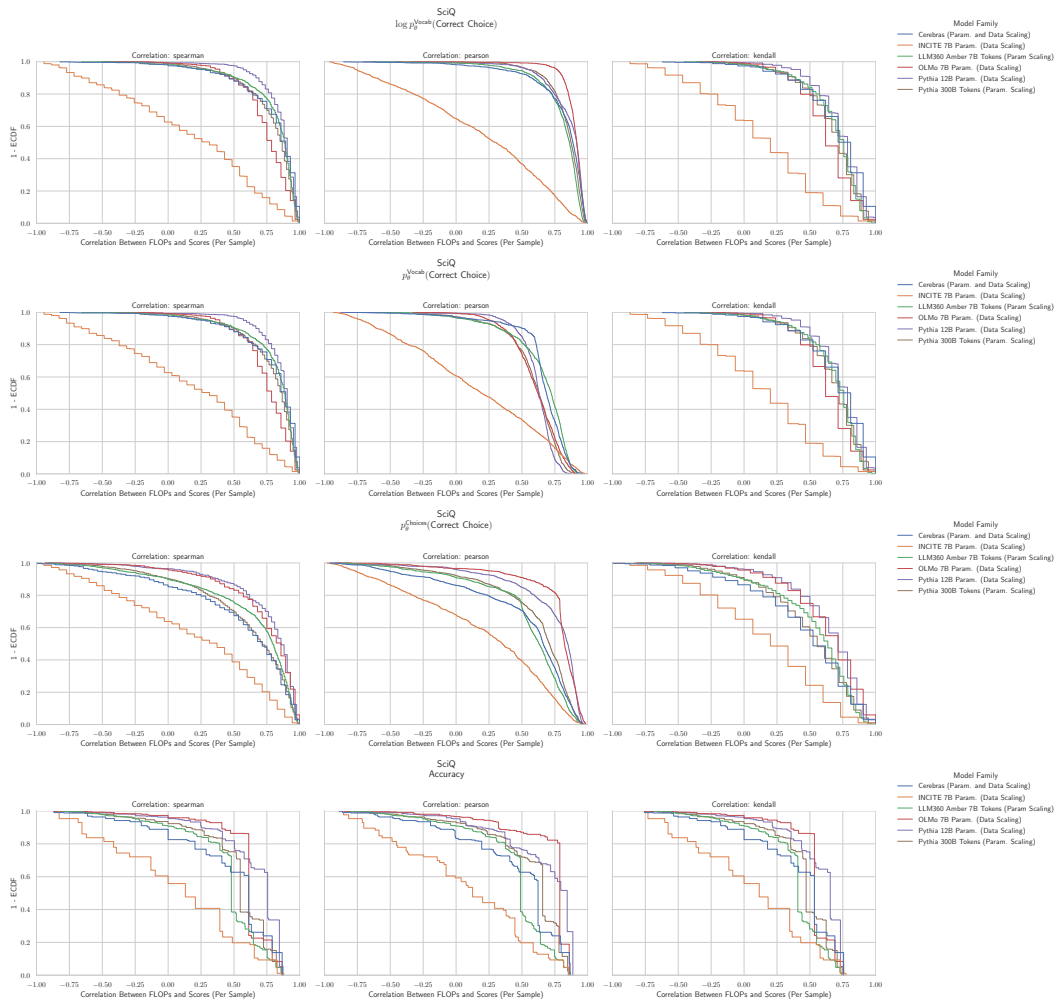
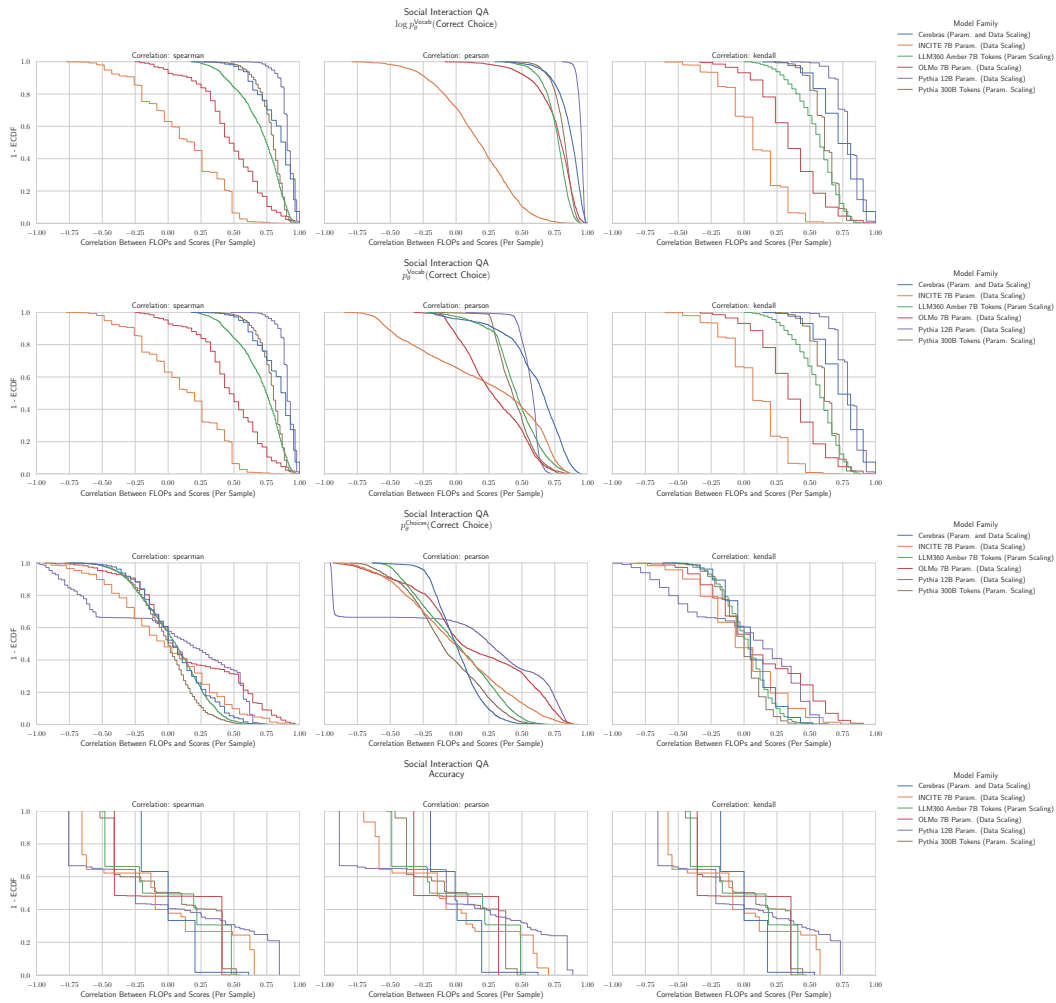


Figure 74: PIQA: Downstream performance is computed via a sequence of transformations that deteriorate correlations between scores and pretraining compute.

4806 G.66 NLP BENCHMARK: RACE LAI ET AL. (2017)
48074841 **Figure 75: RACE: Downstream performance is computed via a sequence of transformations
4842 that deteriorate correlations between scores and pretraining compute.**

4860 G.67 NLP BENCHMARK: SciQ WELBL ET AL. (2017)
48614895 **Figure 76: SciQ: Downstream performance is computed via a sequence of transformations that
4896 deteriorate correlations between scores and pretraining compute.**
4897
4898
4899
4900
4901
4902
4903
4904
4905
4906
4907
4908
4909
4910
4911
4912
4913

4914 G.68 NLP BENCHMARK: SOCIAL IQA SAP ET AL. (2019B)
4915
4916
4917
4918
4919
4920
4921
4922
4923
4924
4925
4926
4927
4928
4929
4930
4931
4932
4933
4934
4935
4936
4937
4938
4939
4940
4941
4942
4943
4944
4945
4946
4947
4948
4949
4950
4951
4952
4953
4954
4955
4956
4957
4958
4959
4960
4961
4962
4963
4964
4965
4966
4967

4949 **Figure 77: Social IQA: Downstream performance is computed via a sequence of transformations**
4950 **that deteriorate correlations between scores and pretraining compute.**

G.69 NLP BENCHMARK: WINOGRANDE KEISUKE ET AL. (2019)

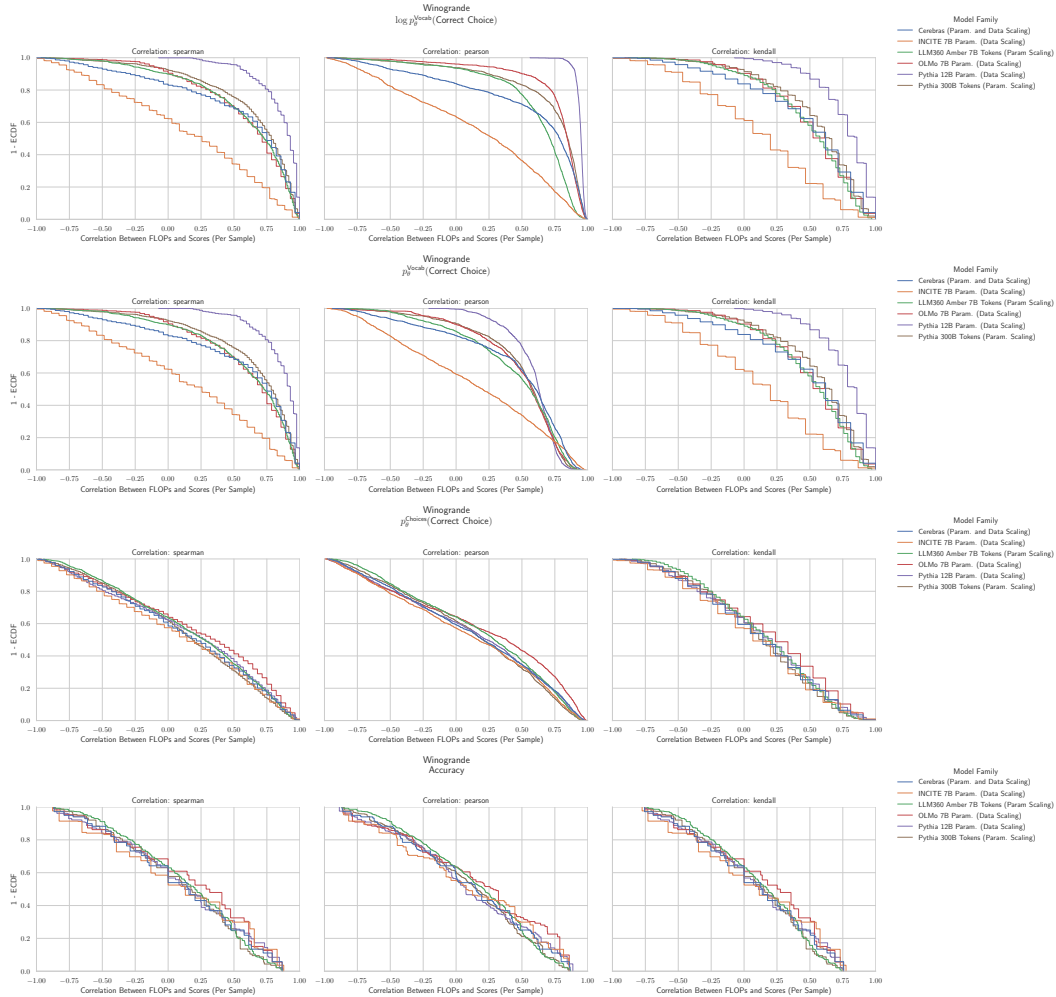
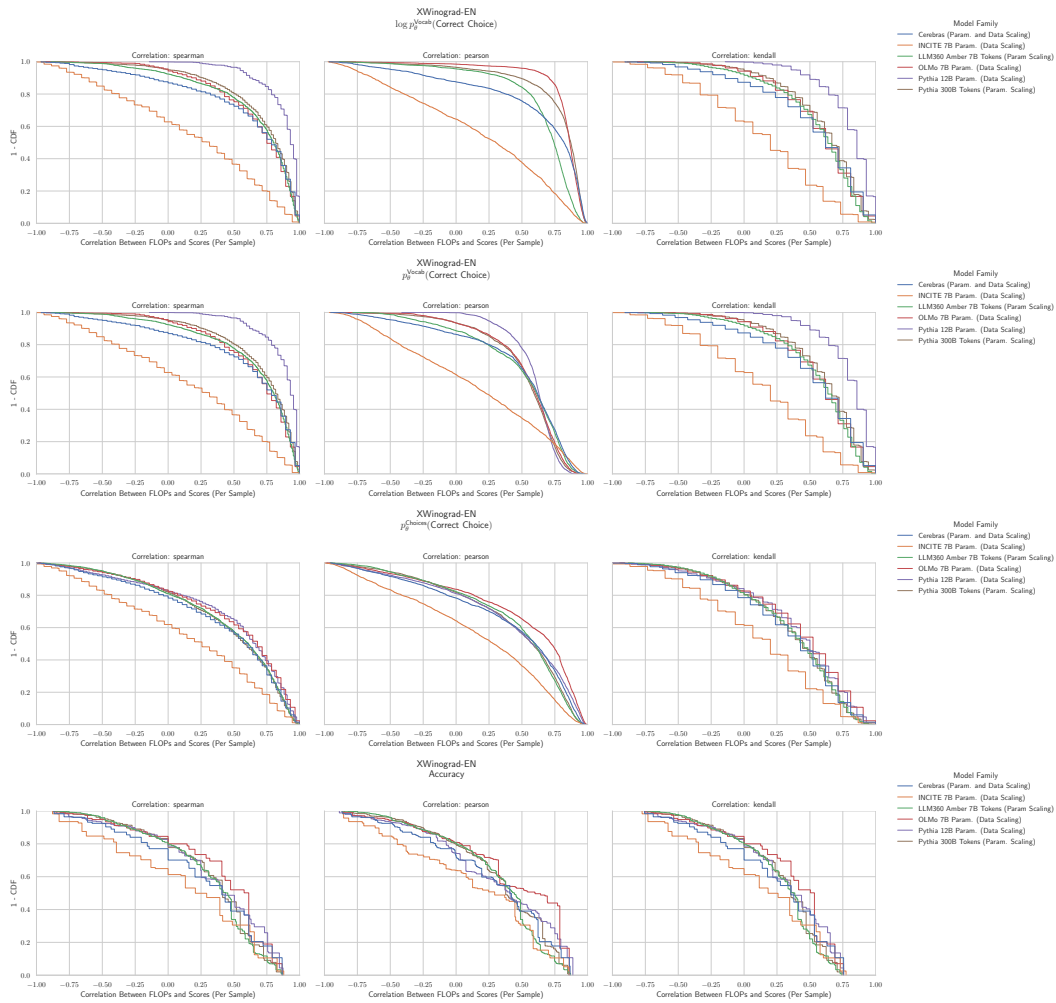


Figure 78: **Social IQA: Downstream performance is computed via a sequence of transformations that deteriorate correlations between scores and pretraining compute.**

5022 G.70 NLP BENCHMARK: XWINOGRAD ENGLISH MUENNIGHOFF ET AL. (2023)
50235057 Figure 79: **XWinograd English: Downstream performance is computed via a sequence of**
5058 **transformations that deteriorate correlations between scores and pretraining compute.**